December 2015

# The Mixing of a River into Coastal Waters at Two Beaches: Environmental Factors, E. Coli Contributions and Applications for Predictive Models

Adrian Jordan Koski
*University of Wisconsin-Milwaukee*

# THE MIXING OF A RIVER INTO COASTAL WATERS AT TWO BEACHES: ENVIRONMENTAL FACTORS, *E. COLI* CONTRIBUTIONS AND APPLICATIONS FOR PREDICTIVE MODELS

by

Adrian Koski

A Thesis Submitted in

Partial Fulfillment of the

Requirements of the Degree of

Master of Science

in Freshwater Sciences and Technology

at

The University of Wisconsin-Milwaukee

December, 2015

ABSTRACT

THE MIXING OF A RIVER INTO COASTAL WATERS AT TWO BEACHES: ENVIRONMENTAL FACTORS, *E. COLI* CONTRIBUTIONS AND APPLICATIONS FOR PREDICTIVE MODELS

by

Adrian Koski

The University of Wisconsin-Milwaukee, 2015
Under the Supervision of Professor Sandra McLellan

Beach closures and public health protection are confounded by analytical procedures that result in delays in notification of adverse water quality conditions and the lack of affordable analytical methods to identify pollutant sources. Attempts have been made to develop predictive frameworks using ancillary hydrometeorological data to statistically anticipate deteriorated water quality. Many urban coastal beaches are impacted by river runoff. In Kenosha Wisconsin, beach sanitary survey data from two beaches adjacent to the mouth of the Pike River were examined to ascertain whether simple river-lake mixing models identified river influence on coastal water quality and improved predictions of beach advisories.

Water samples (798 water samples) were collected from the Pike River (one location) and Lake Michigan beach locations to the north (three locations) and south (four locations) of the inflow during the summer months of 2012-2014. Specific conductivity was used as a conservative tracer for quantifying river-lake mixing. Mixing was dependent upon distance from the river mouth, river discharge, and wind and alongshore current directions ($p<0.05$). A two component mixing model quantified coastal *E. coli* concentrations when river waters were the dominant pollution source (n=9, $R^2$= 0.5773-0.9282), except near the mouth where

groundwater exfiltration confounded mixing calculations (n=8, $R^2$=0.1704). An ensemble model (predictive model which estimated river influence on coastal waters) more accurately predicted exceedances of water quality standards compared to traditional multiple linear regression models as measured by sensitivity (fraction of exceedances accurately predicted; 0.419 vs. 0.194), but with more false positives. Given the importance of external river borne sources of *E. coli* to coastal beaches, models and data which address riverine mixing under a variety of hydrometeorological conditions have the potential to improve predictions of water quality in nearby waters and therefore protect public health.

# TABLE OF CONTENTS

# LIST OF FIGURES

# LIST OF TABLES

# LIST OF ABBREVIATIONS

| | |
|---|---|
| ANOVA | Analysis of Variance |
| BAV | Beach Action Value |
| BEACH Act | Beach Environmental Assessment and Coastal Health Act |
| BIC | Bayesian Information Criteria |
| BSS | Beach Sanitary Survey |
| CFU/100 ml | Colony Forming Units per 100 Milliliters of Water |
| cm | Centimeters |
| E. *coli* | *Escherichia coli* |
| EMMM | End Member Mixing Model |
| FIB | Fecal Indicator Bacteria |
| GI | Gastrointestinal |
| GPS | Global Positioning System |
| km | Kilometer |
| m | Meter |
| $m^2$ | Square Meter |
| $m^3$ | Cubic Meter |
| ml | Milliliter |
| MLR | Multiple Linear Regression |
| MPN | Most Probable Number |
| MST | Microbial Source Tracking |
| NOAA | National Oceanic and Atmospheric Administration |
| NTU | Nephelometric Turbidity Units |
| $^oC$ | Degree Celsius |
| r | Pearson's Product Moment Correlation Coefficient |
| $R^2$ | Coefficient of Determination |
| RMSE | Root Mean Square Error |
| US EPA | United States Environmental Protection Agency |
| USGS | United States Geological Survey |
| VB | Virtual Beach |
| µm | Micrometer |
| µS | Micro-Siemens |
| ρ | Spearman's Rank Correlation Coefficient |

# ACKNOWLEDGEMENTS

I would like to acknowledge the members of my committee for their support, encouragement, and thoughtful comments through all phases of my graduate studies. In no particular order, Sandra McLellan's advice has helped to challenge and enrich my ideas. Julie Kinzelman has served as a mentor and has allowed me numerous opportunities for self-growth. Val Klump's wealth of knowledge has been illuminating and has helped me to link ideas in novel ways. Collectively, I am grateful for the time and effort the members of my committee spent to meet with me and read my drafts.

I am indebted to the members of the City of Racine Health Department Laboratory for their help collecting and analyzing water samples and allowing me to bounce ideas off of them. In particular, Stephan Kurdas, Joel Brunner, Sarah Wright, Jacob Jozefowski and Jennifer Creekmur deserve special mention. I would also like to thank the numerous student interns who assisted with data collection through the course of this study.

Most of all, I would like to thank my family, Eliza and Shari, for their patience and understanding throughout this journey. I would also like to thank my parents Wayne and Kitty (*in memoriam*) for instilling the value of education and persistence in me.

This work would not be possible without funding through the Great Lakes Restoration Initiative and support from the City of Racine.

# 1. Introduction/Background

Travel and tourism represents the United State's largest industry and beaches represent the top tourism destination (Houston, 2008). Unfortunately, water quality at many beaches is impaired. Excess risk of pathogen exposure is the number one reason for a water body to be placed on the 303(d) list of impaired waters in the United States (US EPA, 2011). Pathogens at bathing beaches can result in illnesses including gastroenteritis, respiratory infections, and skin infections amongst others (Craun et al, 2005; Seyfried et al, 1985). Public awareness has increased about water quality issues; however, there is little improvement. The percentage of beaches open the entire swimming season within the Great Lakes basin has remained nearly constant, with 73% in the United States and 49% of beaches in Canada in 100 percent compliance with regulatory standards from 1998 to 2007 (Environment Canada and US EPA, 2009). Nine percent of beaches in the US and 42% of beaches in Canada were designated as having impaired water quality for more than 10% of the available swim days from 2006 to 2007 (Environment Canada and US EPA, 2009). Differences in water quality impairment rates between the United States and Canada may be due to disparities in standards and may not reflect an actual difference in water quality. Due to the immense economic benefits of beaches and the threat poor water quality poses to public health, recreational water quality in the United States is regulated through the Environmental Protection Agency (US EPA).

## 1.1 BEACH Act

The Beach Environmental Assessment and Coastal Health (BEACH) Act was signed into federal law in 2000, as an amendment to the Clean Water Act, to inform users of bathing water quality (U.S.C. 114 STAT. 870). The BEACH Act requires states to adopt water quality standards

protective of public health for Great Lake and marine coastal waters used for swimming, bathing, surfing or other contact activities.

Water quality for bathing purposes is gauged using fecal indicator bacteria (FIB), specifically *Escherichia coli* (*E. coli*) and enterococci. *E. coli* is used exclusively in freshwater systems and enterococci may be used in either freshwater or marine systems. Revised recreational water quality criteria released by the United States Environmental Protection Agency in 2012 set beach action values (BAVs), concentrations of FIB at which the public is required to be notified of unsafe conditions (US EPA, 2012). BAVs were based upon gastrointestinal (GI) illness rates found in the National Epidemiological and Environmental Assessment of Recreational Water studies (US EPA, 2012). BAVs of 235 colony forming units per 100 milliliters of water (CFU/100 ml) *E. coli* and 70 CFU/100 ml enterococci for single samples are associated with 36 GI illnesses per 1,000 primary contact exposures.

## 1.2 Fecal Indicator Bacteria (*E. coli* and Enterococci)

Fecal indicator bacteria are present in the intestinal flora of warm blooded animals including humans. The presence of FIB such, as *E. coli* and enterococci, in water is used to signal recent fecal contamination and may denote the presence of pathogens associated with feces. Elevated concentrations of *E. coli* and enterococci in bathing waters have been shown to be associated with an increased prevalence of GI illnesses in exposed individuals (US EPA, 1986; Dufour, 1984; US EPA, 2012). The actual risk of illness depends on a variety of factors including the strength of an individual's immune system, the type of exposure, and the host origin of FIB, amongst other factors (Seyfried et al, 1985). Pathogen assessments are not directly used to determine water quality due to the prohibitive cost of testing, the elusiveness of pathogens in

aqueous environments and the lack of an agreed upon representative pathogenic indicator(s) (Field, 2008).

### 1.3 Drawbacks of using FIB in Bathing Waters

The direct detection of FIB does not indicate the host origin or method in which it was conveyed to recreational waters; this often results in the origin of FIB being attributed to unknown or unsubstantiated sources which in turn prevents the development of successful restoration strategies (Kovatch, 2006). Further, currently approved analytical (microbiological) methods require 18 to 24 hours to generate results. The time delay between sample collection and the availability of results does not represent the fluid nature of the aquatic environment and, therefore, is unable to effectively safeguard public health. Beach managers use the data obtained during monitoring to issue beach status updates using the persistence model (current beach status is based upon previous result). Most exceedances of bacteria recreational water quality standards, approximately 70% in marine waters and up to 96% in freshwater, only last one day (Leecaster and Weisberg, 2001; Nevers and Whitman, 2011); thus the persistence method fails to capture most exceedances. The delay between when water samples are collected and when results are available results in scenarios where patrons are exposed to potentially unsafe swimming conditions yet the beach remains open (Type II errors) and scenarios where water quality is acceptable, yet the beach is closed (Type I errors) (Frick et al, 2008). Delays in the issuance of untimely water quality updates have negative public health and economic consequences to local communities and businesses that rely on beach tourism (Rabinovici et al, 2004).

## 1.4 Sources and Sinks of FIB

FIB can enter aqueous environments from multiple host sources including humans and animals. Sediments, algal blooms and biofilms can serve as reservoirs of introduced FIB and studies indicate reproduction may occur within these media (Whitman et al, 2003; Byappanahalli et al, 2007; Englebert et al, 2008; Byappanahalli et al, 2009; Alm et al, 2003; Kinzelman et al, 2004; Beversdorf et al, 2007; Skinner et al, 2010). Once present, FIB may be distributed into coastal waters from its portal of entry through a variety of mechanisms including sewage overflows, stormwater infrastructure, direct runoff, tributaries or agitation in the case FIB from of sediments, algae and biofilms (Whitman and Nevers, 2003; Ishii et al, 2006; Kinzelman et al, 2004; Ge et al, 2010). The mechanism of delivery may be further classified as point sources (any single identifiable source from which pollutants are discharged such as pipes) or non-point source (from diffuse locations across the landscape).

FIB in water can be free floating or attached to suspended particles; this affects deactivation/disappearance rates. The decay rate of *E. coli* has been estimated to be two to four times slower attached to sestons compared to free floating (Garcia-Armisenet al, 2006; Wu et al, 2009); others have assumed no deactivation/decay when attached to sediments (Jamieson et al, 2005). This can create variability in FIB concentrations as meteorologic/hydrologic conditions which favor sedimentation/suspension can cause changes in bacterial survival rates and can serve as a mechanism which introduces/removes bacteria from the water column.

Several other mechanisms may remove bacteria from the water column, e.g. deactivation/decay and sedimentation (Schueler and Holland, 2000; Schillinger and Gannon,

1985). Methods of bacteria deactivation/decay vary based upon environmental conditions and include bacteriophage attacks, toxins produced by macrophytes, ultraviolet (UV) light exposure and natural cell death (Fujioka et al, 1981). It has been noted that sunlight, temperature, salinity and protozoa grazing can also influence the survival of FIB (Brauwere et al, 2014).

## 1.5 Dilution and Mixing

Although dilution does not serve as a removal mechanism for FIB, it can reduce concentrations. Therefore, the measurement of mixing may be an important determinant of final FIB concentration in an aquatic environment. The mixing/dilution of one water body into another have been measured via end member mixing models (EMMM) and the use of injected and natural tracers (Schemel et al, 2006; USGS 2007). End Member mixing models (two component) use mass balance equations for tracers and water to determine the fraction of water from each source. Schemel et al (2006) noted tracers for measuring mixing should be conservative in nature (non-reactive), such as salts or dissolved metals. Additionally, the concentration of tracers should be large enough to enable precise calculations.

## 1.6 Beach Sanitary Surveys and Microbiological Source Tracking

To help deduce the host origin and conveyance methods of FIB, the United States EPA piloted the use of beach sanitary surveys (BSSs) for marine and Great Lake beaches (US EPA, 2014). The BSS protocol is a standardized method for collecting information regarding beaches and associated watersheds. Examples of information collected include the number, type and location of wildlife, the accumulation of algae, the slope of the beach, the location and condition of bathrooms and daily meteorologic, hydrologic and physiochemical conditions. Relevant information about the watershed includes land use, the location(s) of stormwater

outfalls and septic tank use. The analysis and interpretation of this information may illuminate sources and conveyance mechanisms of FIB and meteorological/hydrologic conditions associated with exceedances of recreational water quality standards. The use of BSSs has been proven valuable and has been used to successfully guide mitigation strategies at Great Lake coastal beaches (Kinzelman and McLellan, 2009).

Numerous microbial source tracking (MST) methods have also been developed to further identify host origins of FIB (Field, 2008). Some techniques require extensive gene libraries and others isolate the origin of bacteria through the use of genetic primers (Field, 2008). Methods that rely on gene libraries or source identification through the use of species-specific bacteria focus on identifying the bacterial origin, not necessarily the mechanism by which FIB entered coastal waters. If multiple sources and/or delivery mechanisms exist, MST techniques may not provide discriminatory results. Therefore, additional information on the mechanism(s) which introduced FIB into waters is necessary to appropriately identify sources. MST methods are also time and labor intensive, therefore, they are not useful to the beach going public for daily decision making.

## 1.7 Near Real Time FIB Quantification

In order to address the time delay inherent to current analytical testing, multiple near real-time methods have been evaluated, including predictive models and rapid molecular analytical assays (i.e. quantitative real-time polymerase chain reaction or qPCR) (Dick and Field, 2004; Shannon et al, 2007; Nevers and Whitman, 2005). Models, for coastal water quality purposes, are mathematically based tools designed to determine FIB concentrations based upon readily measured variables. Results from these real-time methods/models can be used to

make management decisions or to inform laboratory-based testing. The use of models is more protective of public health while decreasing negative economic consequences by providing near real time results (Nevers and Whitman, 2005; Frick et al, 2008, Nevers et al, 2007). Models have been used in a variety of settings including rivers, beaches, lakes and catchments (Brauwere et al, 2014) and have been shown to be more accurate at informing the public of unsafe conditions than the persistence method (USGS, 2013). Models can be mechanistic, regression or based upon a hybrid of the two (an ensemble) in approach.

## 1.8 Mechanistic Models

Mechanistic models mathematically simulate FIB concentrations through mass balance equations based upon an understanding of external sources, conveyance and the disappearance/deactivation of FIB (Brauwere et al, 2014). These models are designed to characterize major processes within the watershed/coastal area. Equations describing these processes are based upon physical, chemical and/or biological parameters which can be readily measured or estimated such as FIB mortality, settling rates, solar insolation, bathymetry, salinity and others. Models may simulate multiple interactions depending upon complexity and may include sedimentation, re-suspension, dilution and variable disappearance rates for FIB caused by geospatial differences in salinity and solar insolation across study areas (including variably caused by suspended solids) (Brauwere et al, 2014). In addition to real-time water quality predictions, these models can be used to evaluate specific scenarios such as the direct effect of management actions and changes in source loading to aquatic environments (Coffey et al, 2010). Although useful for multiple purposes, this type of model tends to be

computationally complex and requires expertise which is not readily available to most beach managers.

## 1.9 Regression Based Models

Regression based models are created through direct empirical relationships between FIB concentrations and measurable parameters (Brauwere et al, 2014). Examples of parameters include meteorological, hydrological, physiochemical descriptors, land use and recently collected microbiological data (Nevers and Whitman, 2005; Nevers and Whitman, 2011; Brauwere et al, 2014). This type of modeling approach may use several methods to optimize performance including multiple linear regressions (MLRs), regression trees, partial least squares regressions, logistic regressions, and artificial neural networks (Brauwere et al, 2014). The general format of a MLR model is represented in equation 1, as described in Hellweger (2007). Where $C_e$ represents the predicted FIB concentration, $\beta_0$ is a constant, $\beta_1$ through $\beta_n$ are regression coefficients, $X_1$ through $X_n$ are independent variables and e is a residual error. Independent variables can be transformed using mathematical functions (e.g. log10) to improve model performance. The EPA has developed a tool, Virtual Beach (VB), to assist in the creation of regression models (US EPA, 2013).

$$Eq\ 1. \quad C_E = \beta_0 + \beta_1 X_1 + \beta_2 X_2 + \cdots + \beta_n X_n + e$$

Several drawbacks exist to using regression based models. Relevant explanatory variables may be extremely site specific; thus a model which is sufficient at one location may not be valid at others. This type of model is also unable to directly simulate processes which result in high concentrations of FIB. Thus, specific scenarios that may alter FIB concentrations such as changes in management actions or restoration activities cannot be evaluated. Further,

the mechanism which accounts for predicted bacteria concentrations is unclear. Additionally models that examine point sources (e.g. rivers, stormwater outflow) and coastal FIB concentrations have not linked together (Nevers and Whitman, 2005). At coastal areas that are a mixture of water from multiple sources (e.g. mixture of coastal water and point source), each water body may have different variables or relationships between variables that are explanatory for bacteria concentrations. Thus, trying to capture the bacteria concentration of a mixed water body in a single regression model may create error and result in a poor fit.

## 1.10 Ensemble Models

In order to optimize model fit, one study used a hybrid between a mechanistic and regression model known as an ensemble model (Hellweger, 2007). The basis for ensemble models are described in Thompson (1977):"two or more inaccurate, but independent predictions of the same future events may be combined in a very specific way to yield predictions that are, on the average, more accurate than either or any of them taken individually." For this model, the outputs of a regression and mechanistic based model were combined using equation 2, where $C_{ME}$, $C_{M1}$ and $C_{M2}$ are the FIB concentrations from the ensemble (models 1 and 2, respectively), and $a_{M1}$ and $a_{M2}$ are weighing coefficients (values of 0.5 respectively) (Hellweger, 2007). This model noted a lower root mean square error (RMSE) (190 CFU/100 ml) than either the mechanistic (370 CFU/100 ml) or regression (200 CFU/100 ml) based model in a river environment. Although this model had superior performance, as measured by RMSE, it also suffered from the same drawbacks of regression based models, e.g. there a lack of knowledge pertaining to the mechanistic basis for elevated levels of FIB.

$$\text{Eq 2.} \quad C_{ME} = a_{M1}C_{M1} + a_{M2}C_{M2}$$

## 2. Purpose of Study

An understanding of how point sources mix into coastal waters is required to determine sources of impairments at bathing beaches. This study seeks to identify conditions favorable to the mixing of the Pike River into Lake Michigan coastal waters, identify the associated impact of the river on coastal *E. coli* concentrations, and use this information to more accurately gauge water quality in real-time through predictive models. Specifically:

(1) This study evaluates the frequency and degree of mixing between the Pike River (serving as a point source) and coastal waters at two Great Lakes beaches (Alford and Pennoyer Park) in relation to alongshore current direction, flow volume, distance from the river, and wind direction (BSS variables). This information can be used when evaluating the health of recreational waters at coastal locations by ruling in/out point sources. Understanding the mixing of point sources with coastal waters under a variety of scenarios will provide information to make MST techniques more discriminative and aid in the identification of water quality impairments.

(2) This study also evaluates using an end member mixing model (two component mixing model) to determine *E. coli* contributions from a point source (Pike River) to Lake Michigan coastal waters. Equation 3 represents the proposed model. In equation 3, $C_{ec}$ represents the estimated FIB concentrations of coastal waters, W represents the mixing ratio, $C_r$ represents the actual FIB concentration of the river, and $C_c$ represents the estimated background concentration of FIB in unmixed areas. Reasonable fits between observed and

estimated FIB concentrations would aid in the evaluation of sources of contamination by providing estimates of the fecal bacteria contribution from the point sources to coastal waters.

$$Eq\ 3. \quad C_{ec} = W * C_R + (1 - W)C_C$$

(3) This study proposes a method to improve the performance of predictive models by linking point sources and coastal waters. Predictive models can be created for the Pike River and coastal areas, under the assumption of no river mixing. Actual coastal concentrations during mixing events can be calculated by combining these two models using the mixing ratio as a mechanistic link, i.e. an ensemble model. Coastal models predict the impact of non-point sources of *E. coli,* while the product of estimated Pike River *E. coli* concentration and the mixing ratio estimate the contributions from the river (equation 4). In equation 4, $C_p$ represents the predicted *E. coli* concentration of a mixed water body (river and coastal water), W represents the mixing coefficient and $C_{pR}$ and $C_{pc}$ represent MLR models which describe *E*. *coli* concentrations in the river and coastal areas (without mixing), respectively. By modeling the water bodies separately (source and coastal), the best explanatory variables corresponding to bacteria concentrations in each water body can be identified. If improved model performance is achieved compared to a traditional Virtual Beach MLR model, this modeling technique has the potential to better protect public health while limiting negative economic consequences associated with Type I errors.

$$Eq\ 4. \quad C_P = W * C_{pR} + (1 - W)C_{pC}$$

# 3. Methods

## 3.1 Study Site

The study area was located on the southwest shore of Lake Michigan in Kenosha, Wisconsin at the mouth of the Pike River (Figure 1). The location of the Pike River mouth, adjacent to two moderate priority Lake Michigan coastal beaches (Alford Park to the north and Pennoyer Park to the south), represents an ideal study area.

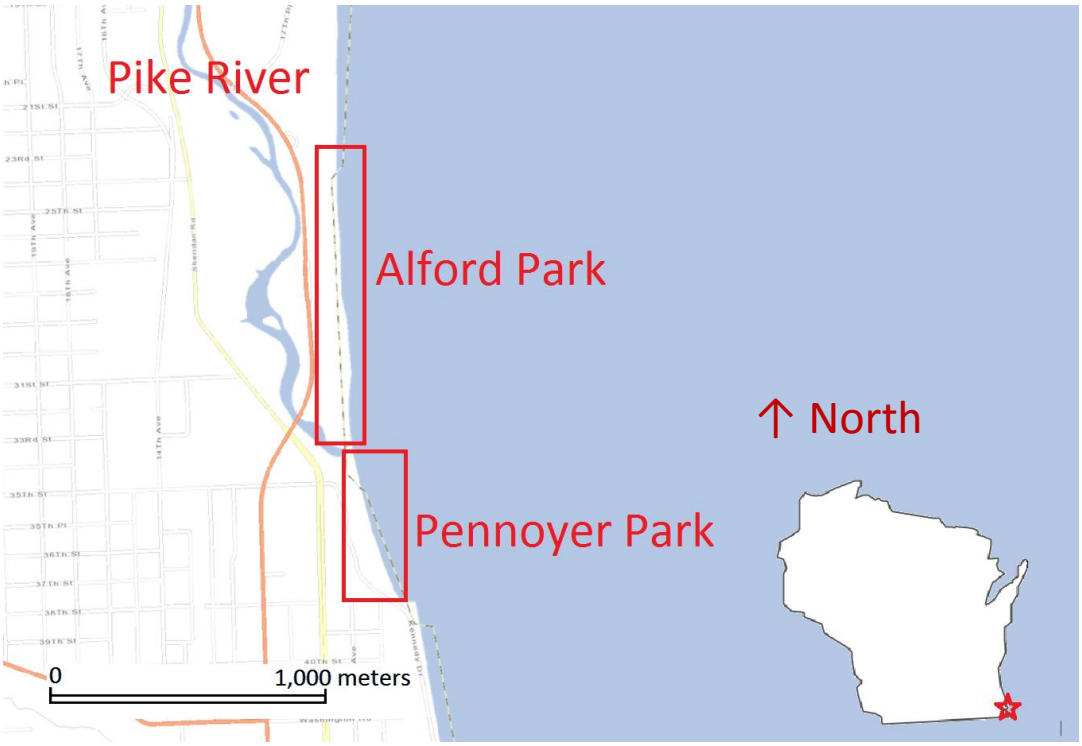


**Figure 1. Study Location-Pike River, Alford Park and Pennoyer Park in Kenosha, Wisconsin.**

The Pike River drains 132 square kilometers of eastern Kenosha and Racine Counties. Land use characteristics, the infill of wetlands and high amounts of impervious surfaces have led to flashy flow conditions where discharge volumes change rapidly due to rainfall and snowmelt. Effluent from this river has been demonstrated to possess consistently elevated *E.*

*coli* concentrations under high flow conditions and has been identified as a source of FIB to adjacent nearshore waters (Alford and Pennoyer Park) (Koski and Kinzelman, 2013).

Alford Park is approximately 1,100 meters long and is bound on the south end by the Pike River. The beach face is orientated along the north/south axis. The width of the beach varies from 16 meters on the north end to 65 meters on the south end. Water depths increase to 1.2 meters within a distance of 15 meters from the shoreline. Beyond the Pike River, there is one other point source, a stormwater outfall (drainage are =2,900 $m^2$) which discharges at the center of the beach. However, no dry weather discharge was noted from this outfall and flow lines in the sediments indicate the water infiltrates prior to reaching Lake Michigan following precipitation. Thus, non-point sources inherent to most beaches (e.g. direct bather contributions, wildlife, algal blooms and sediments) and the Pike River appear to have the greatest influence on FIB concentrations at this location.

Pennoyer Park is approximately 500 meters long and is bound on the north side by the Pike River and by shore armor to the south. The beach face is orientated along the north/south axis. The width of the beach varies from 71 meters on the north end to 96 meters on the south end. The depth of water reaches 1.2 meters within 10 meters of the shoreline. There is one stormwater outfall on the south end of the beach (drainage area= 115,000 $m^2$) and flow was noted to reach the lake following rainfall events. However, recent stormwater infrastructure improvements direct discharge into an infiltration basin, which lessens coastal water quality impacts. Beyond the aforementioned sources of FIB, non-point sources are likely to influence recreational water quality.

## 3.2 Field Methods

### 3.2.1 Water Sample Collection

Water samples were collected from seven locations across Alford and Pennoyer Park Beaches as well as from the mouth of the Pike River (PR) on 100 days between May and September, 2012-2014, to assess spatial and temporal variation (Table 1, Figure 2). Four sampling locations were located south of the Pike River mouth (Pennoyer Park) at distances of approximately 20 meters (P1), 130 meters (P2), 250 meters (P3) and 400 meters (P4). Three sampling locations were located to the north of the Pike River mouth (Alford Park) at distances of 130 meters (A1), 400 meters (A2) and 650 meters (A3). Sampling locations where selected to correspond with historical monitoring locations to facilitate comparisons with past data, if necessary.

**Table 1. GPS coordinates of sample locations.**

| GPS coordinates of sample locations | | |
|---|---|---|
| Sample Location | Latitude (°N) | Longitude (°E) |
| PR | 42.608110 | 87.819313 |
| A1 | 42.608019 | 87.818702 |
| A2 | 42.609990 | 87.818873 |
| A3 | 42.612234 | 87.818740 |
| P1 | 42.606479 | 87.818118 |
| P2 | 42.605622 | 87.817939 |
| P3 | 42.604708 | 87.817725 |
| P4 | 42.603533 | 87.817651 |


**Figure 2. Sampling Locations-Alford Park, Pennoyer Park and Pike River. Sample locations A1-A3 (Alford Park) are located to the north of the Pike River and locations P1- P4 (Pennoyer Park) are located to the south.**

Lake Michigan surface water samples were collected in sterile Whirl-Pak® (Nasco, Fort Atkinson, WI) bags from water of between 0.30 and 0.45 meters deep at coastal locations (knee high) from 0.15 meters below the water surface. Pike River surface water samples were collected from approximately half the depth of the water column. Steps in the sample collection process include: wading out to the proper depth of water, facing towards the direction of the longshore current, removing the perforated plastic strip from on top of the Whirl-Pak® bag, pulling the tabs located on the side of the bag to open, submerging the bag to the appropriate depth to collect the water sample, sealing the bag, and placing the sample on ice packs at 4 $^{o}$C until samples were returned to the laboratory for analysis. This process was repeated at all sampling locations.

3.2.2 Beach Sanitary Surveys

Beach Sanitary surveys were conducted in concert with sample collection to characterize and quantify hydrometeorological variables and field conditions. Parameters collected and described included: wind speed, wind direction, current speed, current direction, cloud cover, air temperature, precipitation, river discharge volume, longshore current direction, estimated wave height, water temperature and water clarity.

*Wind Speed and direction* was determined using an anemometer operated and maintained by the National Weather Service Central Region located 2 km south of the beach (http://www.ndbc.noaa.gov/station_page.php?station=knsw3) at an elevation of 19.5 meters above lake level. Data was obtained for the closest ten minute interval in which samples were collected.

*Current speed* and *direction* were obtained from model results provided by the Great Lakes Coastal Forecast System Nowcast 2D model (http://data.glos.us/glcfs/) at Latitude: 42.59671, Longitude: -87.8069. Model results were obtained for the closest hour samples were collected. Estimated wave heights (referred to as modeled wave heights) were also collected from this system.

*Cloud cover* was visually estimated using the amount of sky covered by non-transparent clouds. This description mirrors the scale the National Oceanic and Atmospheric Administration (NOAA) uses. Cloud cover was classified as sunny (0 to 1/8$^{th}$ cloud coverage), mostly sunny (1/8$^{th}$ to 1/4$^{th}$ cloud coverage), partly sunny (1/4 to ½ cloud coverage), mostly cloudy (1/2 to 7/8$^{th}$ cloud coverage) and cloudy (7/8$^{th}$ to total coverage).

*Air temperature* was determined using a calibrated Kestrel® 4000 Pocket Weather Meter (Boothwyn, Pennsylvania) in the shade or in the shadow of the technician's body if shade was not available to prevent temperature readings from being directly influenced by solar radiation.

*Precipitation* amounts for the 24 hours prior to sampling were obtained from a weather station located at the Kenosha Regional Airport 8.5 km to the southwest of the study site (http://www.weather.gov/data/obhistory/KENW.html).

*River discharge volume* at the time of sample collection was approximated using a United States Geological Survey (USGS) gauging station (Station 04087257) located approximately 14 km upstream from the mouth of the Pike River (http://waterdata.usgs.gov/wi/nwis/uv?site_no=04087257).

*Longshore current direction* was determined by visually examining the direction in which waves traveled parallel to the shoreline. If this method was indeterminate, a floatable object was tossed into the water beyond the breaker zone and the direction the object travels parallel to the shoreline was recorded.

*Wave height* was determined by visual estimation (Field Estimated Wave Height). Wave height, measured from crest to through, was estimated by taking the average wave height of ten waves.

*Water Temperature* was determined at the time of sample collection using a calibrated alcohol thermometer placed in the water adjacent to the sample location. After equilibrating, the temperature was recorded to the nearest 0.1 $^{o}$C.

*Water clarity* was visually estimated in water 0.30-0.45 meters deep. Water clarity was described as clear, slightly turbid, turbid or opaque. Clear water corresponded with conditions when field technicians could clearly see their feet in knee deep water without any disturbance. Slightly turbid water was defined as when a technician had difficulty seeing their feet but could make out their ankles. Turbid was defined as when a technician had trouble seeing their ankles, but can clearly see their mid calf. Opaque water was defined as when a technician could not clearly see their mid calf. All approximations were made in the shadow of the technician to control for solar isolation altering estimates.

## 3.3 Laboratory Methods

### 3.3.1 *E. coli*

*E. coli* concentrations were determined within six hours of sample collection, using Colilert-18® (IDEXX Laboratories, Westbrook, ME) (Standard Methods, 2005). Colilert-18® uses enzyme substrate for the simultaneous detection of total coliforms and *E. coli*. In brief, water samples were diluted with sterile water to a total volume of 100 ml (e.g. 10 ml of sample + 90ml of sterile water) in a sterile vessel. Colilert-18® reagent was added to the vessel containing the sample and mechanically agitated to promote the dissolution of the reagent. The solution was transferred into a Quanti-Tray® 2000 (IDEXX Laboratories, Westbrook, ME) and sealed using a Quanti-Tray sealer (IDEXX Laboratories, Westbrook, ME). Samples were incubated at 35 $^{o}$C for 18 hours per manufactures instructions (IDEXX, 2013). Following incubation, samples were placed under a 366 nm light and the number of small and large cells that fluoresced were counted. The number of cells that fluoresced was compared to a manufacturer's provided most probable number (MPN) table to determine the *E. coli* concentration of the diluted sample, expressed as MPN/100 ml. This value was multiplied by the corresponding dilution factor used (e.g. 1:10) to determine the *E. coli* concentration of the sample.

### 3.3.2 Specific Conductivity

Specific conductivity, a unit of conductivity temperature corrected to 25$^{o}$C, was measured using either an Oakton 400 or Oakton 510 (Vernon Hills, IL) conductivity meter. The meter was calibrated at least monthly, according to manufacturer's recommendations, using NIST traceable 10, 100, 1413 and 12,880 micro-Siemens (µS) standards (manufactured by/on

behalf of: Fisher Scientific, Pittsburg, PA and Forestry Suppliers, Jackson, MS). The accuracy of calibrations were also verified daily by evaluating secondary standards; if secondary standards deviated by more than 1% from the actual value, the unit was recalibrated. Prior to analysis, the conductivity probe was rinsed with deionized water (0.2 μm final filtration) (~10 μS) to remove any contamination from previous samples and dried using lint free Kimwipes™ (Kimberly-Clark, Neenah, WI). An aliquot of water was transferred into a sample cup following bacterial analysis. The probe was lowered into the solution and allowed to equilibrate until a static value was obtained, generally within 10 seconds and the value was recorded. The probe and calibration cup was rinsed thoroughly with deionized water, dried and the next sample was processed.

### 3.3.3 Turbidity

The turbidity of water samples was determined within 24 hours of sample collection following bacterial analysis. Turbidity was reported as Nephelometric Turbidity Units (NTU) using a HF Scientific Inc. (Fort Myers, FL) Micro 100 Turbidimeter. The turbidimeter was calibrated at least once every 30 days according to the manufactures instructions using 0, 10 and 1000 NTU primary AMCOCLear Standards manufactured by GFS Chemicals Inc (Powel, OH).

Once daily, after allowing the turbidimeter to warm up for at least 30 minutes, the calibration of the equipment was verified using sealed secondary standards (AMCOClear) of 0, 10 and 1000 NTU. If values deviated by more than 10%, the equipment was recalibrated using primary standards. Following calibration, samples were gently mixed and small aliquots were used to rinse a scratch free cuvette three times. After the third rinse, the cuvette was filled with sample (approximately 25 ml) and capped. The sides of the cuvette was cleaned with ethyl alcohol to remove any debris or oils that may interfere with measurements and thoroughly

dried using lint free wipes (Kimwipes™). The cuvette was placed into the turbidimeter and allowed to equilibrate (approximately 10 seconds). The cuvette was slowly rotated 360$^{o}$ (indexed) and the lowest displayed value was recorded.

## 3.4 Data Analysis

### 3.4.1 Mixing Ratio

Specific conductivity values have been used as surrogates for dissolved tracers (Schemel et al, 2006; Matsubayashi et al, 1993). The mixing ratio, the volumetric fraction of river water present in coastal waters, was calculated using specific conductivity as a tracer according to equation 5. In equation 5, W represents the volumetric fraction of water from the Pike River present in coastal waters, $K_1$ represents the specific conductivity of the Pike River, $K_2$ represents the background specific conductivity value and $M_z$ represents the specific conductivity value in mixed areas. The specific conductivity of the river ($K_1$) was treated as the actual value determined from grab samples. The specific conductivity of the mixed zone ($M_z$) was represented as the actual value for each sampling location. A dynamic value, described below, was chosen to represent $K_2$ due to factors causing variability in specific conductivity values close to the shoreline.

A dynamic specific conductivity value was chosen due to daily variability in specific conductivity values. Open lake specific conductivity values are fairly constant due to the large residence time of water within Lake Michigan. However, the sampling locations were near the shoreline (<15 m) where localized groundwater exfiltration can cause variability in measured values. Groundwater specific conductivity levels are elevated relative to surface waters due to the dissolution and interaction with minerals. For example, conductivity levels in groundwater

below Hamilton Harbor in Ontario were noted to be two to three times higher than adjacent surface water values (Harvey et al, 1997). Additionally, total dissolved solid measurements, which are proportional to conductivity levels, were noted to be higher by a factor of up to five within groundwater compared to surface waters 20 km to the south of the beach (Visocky, 1977). The water table adjacent to beaches (>2m aquifer depth) rises and fall proportionally with lake levels (Crowe and Meek, 2009; Visocky, 1977). As such, seiches, storm surges and other short term factors which affect lake levels will result in the exfiltration of groundwater into the lake. Past research at Pennoyer Park indicated the gradient of the groundwater table was relatively flat. However, the gradient varied and at times was observed to be at a direction where the lake would recharge the local aquifer (Skalbeck et al, 2010). Changes in the gradient of the groundwater table causes the exfiltration of water with elevated specific conductivity values into coastal water which necessitates the use of a dynamic background conductivity level near the shoreline.

The specific conductivity of the unmixed zone ($K_2$) was estimated by calculating the median conductivity at Alford and Pennoyer Park for each day samples collection occurred. The lower of the two median values (from Alford or Pennoyer Park) was chosen to represent the background conductivity for each date. This was justified based upon visual observations. When plumes were visible, they generally moved in one direction parallel to the shoreline, either north or south. By taking the median specific conductivity values on the side of the river with lower values, as opposed to taking the lowest value, variations in background values are corrected. Mean and median differences between chosen background values and the lowest measured value on each day were 4.2 and 2.5 µS, respectively. Mixing ratios less than 0.01

were treated as a value of zero for statistical analysis and modeling; this value was chosen based upon the accuracy of the conductivity meter (1% error). Precise measurements cannot be obtained for lower values.

$$Eq\ 5. \qquad W = \frac{M_z - K_2}{K_1 - K_2}$$

3.4.2 End Member Mixing Model Construct

End Member mixing models were created to quantify the *E. coli* contribution of the Pike River to coastal waters. End member mixing models were constructed using equation 3, one for each coastal location. W x $C_R$ was defined as the portion of *E. coli* derived from the river and (1-W) x $C_c$ was defined as the portion of the *E. coli* from non-river related sources. Creating end member mixing models required defining the mixing ratio, using equation 5, the *E. coli* concentration of the river ($C_R$), and the background *E. coli* concentration ($C_c$). In practice, dates were examined where contributions from non-river sources could be treated as negligible (i.e. $C_c$ could be treated as zero); for example when *E. coli* concentrations at coastal locations were an order of magnitude higher on one side of the river compared to the other. These conditions indicate the river was the major driver of elevated *E. coli* concentrations. Outliers were defined as 1) samples that had mixing rations equal to zero, or 2) dates when coastal *E. coli* concentrations were an order of magnitude higher than river concentrations, indicating other sources were responsible for the elevated counts.

Alternatively, equation 3 was manipulated to calculate $C_c$, an estimate of beach bacteria concentrations in the absence of river contributions (Equation 6). In equation 6, $C_o$ represents measured coastal *E. coli* concentrations.

$$Eq\ 6. \qquad C_c = \frac{C_o - (W * C_R)}{1 - W}$$

3.4.3 Multiple Linear Regression Model Construct

Predictive models were created to compare the performance of traditional Virtual Beach MLR models to ensemble models, models which link the Pike River and coastal waters. Two types of predictive models were created; traditional VB MLR models and MLR models that were components of ensemble models (Table 2) (i.e. sub-ensemble models which represent the contributions from non-point sources). Models were created for each sampling location and are referred to as location specific models. Location specific models were created for each sampling location. Additionally, models with data combined across multiple locations were created and were referred to as composite models. Composite models were created for locations north of the river (A1-A3) and south of the river (P2-P4). Sample compositing was justified based upon similar *E. coli* concentrations across beach transects.

Data was split into training (75% of data) and verification sets (remaining 25% of data) using a random number generator. MLR models for the purpose of creating an ensemble model used a subset of training data that was identified to have mixing ratios less than 0.01 (e.g. limited mixing occurring) to identify non-point sources of *E. coli* impacting coastal waters. All other MLR models (e.g. model for the river and traditional VB MLR models) used all available training data.

**Table 2. Description of predictive *E. coli* MLR models.**

| List of *E. coli* predictive MLR models |
|---|
| **Traditional VB MLR Models** |
| Predictive model for location A3 (n=75) |
| Predictive model for location A2 (n=75) |
| Predictive model for location A1 (n=75) |
| Predictive model for location P1 (n=73) |
| Predictive model for location P2 (n=75) |
| Predictive model for location P3 (n=75) |
| Predictive model for location P4 (n=75) |
| Predictive model for the Pike River (used to create ensemble models) |
| Composite predictive model for locations A1-A3 (n=225) |
| Composite predictive model for locations P2-P4 (n=225) |
| **Sub-Ensemble Models** |
| Predictive model with data removed when mixing was occurring at location A3 (n=55) |
| Predictive model with data removed when mixing was occurring at location A2 (n=59) |
| Predictive model with data removed when mixing was occurring at location A1 (n=50) |
| Predictive model with data removed when mixing was occurring at location P1 (n=16) |
| Predictive model with data removed when mixing was occurring at location P2 (n=27) |
| Predictive model with data removed when mixing was occurring at location P3 (n=31) |
| Predictive model with data removed when mixing was occurring at location P4 (n=32) |
| Predictive model with data removed when mixing was occurring for locations A1-A3 (n=164) (composite) |
| Predictive model with data removed when mixing was occurring for locations P2-P4 (n=90) (composite) |

*E. coli* concentrations were log (base 10) transformed to achieve assumptions of normality. Descriptive parameters were assigned ordinal values. Water clarity corresponding to clear was assigned a value of 1, 2 for slightly turbid, 3 for turbid and 4 for opaque. Cloud coverage corresponding to cloudy was assigned a value of 1, 2 for mostly cloudy, 3 for partly sunny, 4 for mostly sunny and 5 for sunny. Wind speed/direction and current speed/directions were converted into components perpendicular and parallel to the shoreline.

MLR models were created in Virtual Beach 3.0 (US EPA, 2013) to identify empirical relationships between explanatory variables (sanitary survey data, specific conductivity,

turbidity and river discharge) and *E. coli* concentrations. Potential explanatory variables for *E. coli* concentrations were transformed using built in Virtual Beach 3.0 functions: log base 10, square, square root, $x^{-1/2}$ or no transformation. Transformed parameters with the best fit between log transformed *E. coli* data (measured using Pearson's Coefficient) were selected for the model build. All possible combinations of MLR models were generated for each model run based upon input variables, and the model with the lowest Bayesian Information Criteria (BIC) was chosen to provide parsimony and avoid overfitting data.

### 3.4.4 Ensemble Model Construct

Ensemble models (n=7) were created for each coastal location using the MLR model for the river, the mixing ratio on each respective date and the sub-ensemble model created for each sample location under assumptions of no mixing by combing the models according to equation 4.

### 3.4.5 Statistical Analysis

Statistical analysis was performed using Sigma Plot 12.03 (Systat Software Inc., San Jose, Ca). Results were considered significant if p values were less than 0.05 ($\alpha$=0.05). Prior to analysis, a Shapiro-Wilk test was performed to test for normality and equal variance. Comparison tests were chosen based upon the distribution of the data, either Kruskal-Wallis test (ANOVA on ranks; data that failed normality or equal variance tests) or one-way analysis of variance (ANOVA; normally distributed data with equal variance). If significant differences were found amongst the population, post hoc test (Dunn's or Tukey post hoc) were used to determine where differences occurred. To test for statistical dependence, Pearson's product

moment correlation coefficients (r) (normally distributed data) or Spearman's rank correlation coefficients (ρ, rho) (for non-parametric data) were calculated. For box-whisker plots, the lower whisker represents the minimum value, the lower part of the box represents the 25$^{th}$ percentile, the center line represents the median, the top of the box represents the 75$^{th}$ percentile and the top of the whisker represents the maximum value.

Model fits were evaluated by calculating coefficients of determination ($R^2$). Model fit for the ensemble and conventional MLR models were also evaluated by calculating RMSE, sensitivity and specificity based upon their ability to predict the appropriate public notification using a BAV of 235 MPN/100 ml *E. coli*. Sensitivity was defined as the fraction of exceedances accurately predicted. Specificity was defined as the fraction of non-exceedances accurately predicted. Type I errors were created when models predicted *E. coli* concentrations above the BAV when actual *E. coli* concentrations were less (false positive). Type II errors were generated when actual *E. coli* concentrations were above the BAV and models failed to predict values above the BAV (false negative).

# 4. Results

## 4.1 *E. coli*

In total, 698 water samples were collected on 100 days from Alford and Pennoyer Park during May, June, July and August of 2012, 2013 and 2014. Associated *E. coli* concentrations from coastal locations ranged from below the limit of detection (<10 MPN/100 ml) to 19,862 MPN/100 ml (Table 3). The geometric mean *E. coli* concentrations ranged from 42 to 75 MPN/100 ml at coastal locations with 15 to 31 percent of samples exceeding BAVs (>235 MPN/100 ml *E. coli*), location dependent.

**Table 3. Summary of *E. coli* (MPN/100ml) data by sample location (2012-2014).**

| *E. coli* concentrations (MPN/100ml) and % exceedances of BAVs by sample location | | | | | | | | |
|---|---|---|---|---|---|---|---|---|
| Sample location | A3 | A2 | A1 | PR | P1 | P2 | P3 | P4 |
| Number of Samples (n) | 100 | 100 | 100 | 100 | 98 | 100 | 100 | 100 |
| Minimum | <10 | <10 | <10 | <10 | <10 | <10 | <10 | <10 |
| Maximum | 8,164 | 4,611 | 19,862 | 24,192 | 6,131 | 6,867 | 8,664 | 5,475 |
| Geometric mean | 42 | 52 | 52 | 320 | 62 | 69 | 75 | 68 |
| Exceedances (>235) (%) | 15 | 16 | 17 | 46 | 23.5 | 26 | 31 | 30 |

An additional 100 water samples were collected from the mouth of the Pike River on the same dates. *E. coli* concentrations from the Pike River ranged from below the limit of detection to 24,192 MPN/100 ml, with a geometric mean value of 320 MPN/100 ml (arithmetic mean= 2,328 MPN/100 ml). Forty-six percent of samples from the Pike River had *E. coli* concentrations that exceeded the BAV. Pike River *E. coli* values were analyzed to determine factors effecting concentration. There was a significant positive correlation between log transformed river discharge volumes and log transformed Pike River *E. coli* concentrations (n=100, r=0.603, $p<0.05$) (Figure 3). Discharge volumes were further grouped into wet (>0.00 cm precipitation within 24 hours prior to sampling) and dry weather events. A Mann Whitney test indicated

significantly higher discharge volumes following precipitation ($p<0.05$) (Figure 4). Therefore, Pike River discharge volumes and *E. coli* concentrations increase following precipitation events.

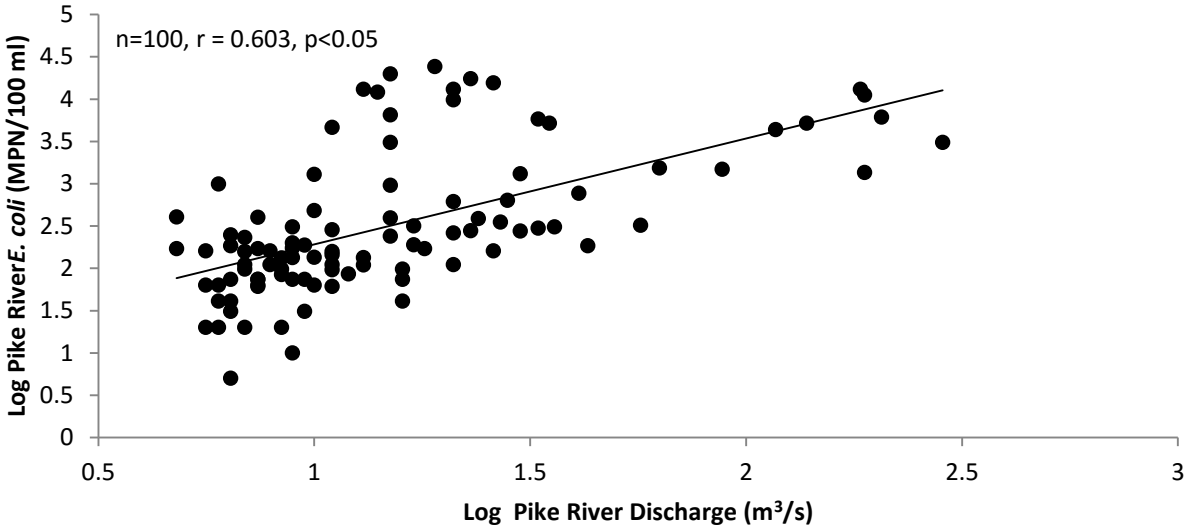


**Figure 3. Comparison between log transformed Pike River *E. coli* concentrations (MPN/100ml) and discharge volumes ($m^3/s$).**

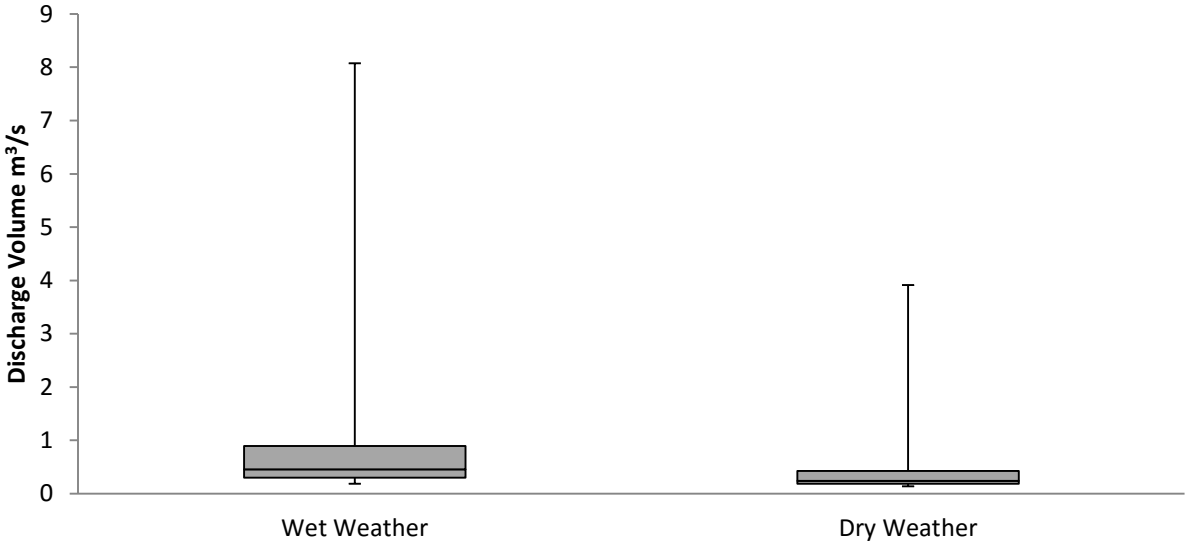


**Figure 4. Pike River discharge ($m^3/s$) under wet and dry weather conditions prior to sampling events (>0.00 cm precipitation in the 24 hours prior to sampling constitutes a wet weather event). Significantly higher discharge volumes associated with wet weather events (Wet weather: n=47, median=0.453 $m^3/s$; Dry weather: n=53, median=0.238 $m^3/s$) ($p<0.05$, Mann Whitney Test).**

Log transformed *E.* coli concentrations from coastal locations and the Pike River were grouped by sample location. A Shapiro-Wilk test was performed indicating the data was not normally distributed ($p<0.05$). A One Way Analysis Variance on Ranks (ANOVA on Ranks) was performed to determine if *E. coli* concentrations differed significantly by sampling location. Results from the ANOVA on Ranks indicated differences amongst the population ($p<0.05$) and a Dunn's post hoc test indicated significantly higher *E. coli* concentrations from Pike River samples compared to all coastal locations ($p<0.05$); no other differences were noted. Results indicate the river has the potential to serve as a source of *E. coli* contamination to coastal locations.

## 4.2 Specific Conductivity

Specific conductivity values from samples collected from Alford and Pennoyer Park ranged from 275 to 789 µS (median of 312 to 326 µS). Pike River values ranged from 415 to 1108 µS (median of 730 µS) (Table 4). Background specific conductivity levels, $K_2$, were determined on each day for the purpose of calculating mixing ratios (see section 3.4.1). $K_2$ values ranged from 280 to 351 µS with a median value of 310 µS.

**Table 4. Summary of specific conductivity (µS) by sampling location. Significantly higher specific conductivity values associated with the Pike River compared to coastal locations (p<0.05; ANOVA on Ranks).**

| Specific conductivity (µS) by sampling location | | | | | | | | |
|---|---|---|---|---|---|---|---|---|
| Sampling location | A3 | A2 | A1 | PR | P1 | P2 | P3 | P4 |
| Number of Samples (n) | 100 | 100 | 100 | 100 | 98 | 100 | 100 | 100 |
| Minimum | 281 | 279 | 278 | 415 | 283 | 277 | 275 | 280 |
| 10th Percentile | 295 | 293 | 296 | 538 | 306 | 302 | 300 | 299 |
| 25th Percentile | 304 | 304 | 306 | 613 | 313 | 311 | 309 | 308 |
| 50th Percentile (Median) | 312 | 313 | 314 | 730 | 326 | 322 | 320 | 318 |
| 75th Percentile | 326 | 328 | 338 | 856 | 376 | 374 | 338 | 337 |
| 90th Percentile | 354 | 353 | 369 | 945 | 510 | 458 | 423 | 389 |
| Maximum | 435 | 514 | 517 | 1108 | 727 | 789 | 680 | 543 |

Specific conductivity values were grouped by sampling location and a Shapiro-Wilk test was performed indicating the data was not normally distributed ($p<0.05$). An ANOVA on Ranks was performed to determine whether specific conductivity differed by sampling location. Results from the ANOVA on Ranks indicated differences amongst the population ($p<0.05$) and a Dunn's post hoc test indicated significantly higher specific conductivity values in samples from the Pike River compared to all coastal locations ($p<0.05$). This indicates the mixing of the river into coastal waters will imprint elevated specific conductivity levels. These elevated values can be used to quality the ratio of river water present in coastal waters.

### 4.2.1 Accuracy - Sources Mixing of Error

Several factors can influence the accuracy of mixing calculations. It was assumed specific conductivity levels were constant across the study area on each date, with the exception of changes caused by river mixing. During the study period, there were a sub-set of days when a sandbar formed across the mouth of the river, preventing discharge. The accuracy of mixing ratios was evaluated on this subset of dates, i.e. when river discharge did not occur.

Mean specific conductivity varied on this subset of dates: 308, 307, 307, 328, 318, 310 and 310 µS at locations A3, A2, A1, P1, P2, P3 and P4 respectively. Significant differences were present between sampling locations P1 and A2 and A3 ($p<0.05$; ANOVA with Tukey post hoc test). Although visual observations indicated direct mixing did not occur, i.e. the sand bar was blocking the river's mouth; the calculations indicate that the elevated specific conductivity were due to mixing. Therefore the assumption that specific conductivity levels are similar across all sampling locations, except for days with river contributions, may be invalid close to the river's mouth.

### 4.2.2 Precision – Sources of Mixing Error

Mixing calculations also assume a large difference in tracer levels/concentrations between the source and receiving body. Specific conductivity levels in samples from the Pike River were grouped by the amount of precipitation received in the 24 hours prior to sampling. Events with 0.00 cm of rain were considered dry weather events, the remainder were considered wet weather events. A Shapiro-Wilk test was performed indicating the data was normally distributed with equal variance ($p>0.05$). Lower specific conductivity levels in the river discharge were associated with wet weather events (wet weather: mean=694 µS, $\sigma$=146, vs. dry weather: mean= 776 µS, $\sigma$=157) ($p<0.05$, T-test). Mixing ratios were measured as the difference between coastal and river conductivity levels. Therefore, the precision of calculated mixing ratios is reduced following precipitation events (i.e. river and coastal specific conductivity values are more similar).

## 4.3 Mixing Ratios

Calculated mixing ratios were analyzed to determine factors associated with the blending of river water into coastal locations. Factors evaluated include spatial variation, longshore current direction, wind direction and volume of river discharge.

### 4.3.1 Spatial Variability

Between 35 (35%) and 69 (70%) samples per location had a mixing ratio above 0.01 (Table 5). There was a greater frequency of mixing events at Pennoyer Park (50 – 69 samples depending upon sampling location) compared to Alford Park (29 – 41 samples depending upon sampling location). Mixing ratios were grouped by locations north (Alford Park) and south (Pennoyer Park) of the river's mouth. A Shapiro-Wilk was performed indicating the data was not normally distributed ($p<0.05$). An ANOVA on Ranks was performed to determine if mixing ratios differed based upon their position relative to the river's mouth ($p<0.05$). There were significantly higher mixing ratios at locations south of the river ($25^{th}$ percentile= 0.00, median=0.02, $75^{th}$ percentile=0.12) compared to locations to the north ($25^{th}$ percentile= 0.00, median=0.00, $75^{th}$ percentile=0.02) ($p<0.05$, Dunn's post hoc test). Although the magnitude and frequency of mixing was greater at Pennoyer Park, environmental variables which are hypothesized to influence the direction of mixing (wind and longshore current direction) were not predictive of mixing occurring more frequently to the south of the river (Table 6).

**Table 5. Summary of mixing ratios. Mixing ratios less than 0.01 treated as 0.00.**

| Mixing ratio by sampling location | | | | | | | |
|---|---|---|---|---|---|---|---|
| Location | A3 | A2 | A1 | P1 | P2 | P3 | P4 |
| Number of Samples (n) | 100 | 100 | 100 | 98 | 100 | 100 | 100 |
| Number of samples with mixing (>0.01) | 35 | 29 | 41 | 69 | 57 | 50 | 51 |
| Minimum | 0.000 | 0.000 | 0.000 | 0.000 | 0.000 | 0.000 | 0.000 |
| $10^{th}$ percentile | 0.000 | 0.000 | 0.000 | 0.000 | 0.000 | 0.000 | 0.000 |
| $25^{th}$ percentile | 0.000 | 0.000 | 0.000 | 0.000 | 0.000 | 0.000 | 0.000 |
| Median | 0.000 | 0.000 | 0.000 | 0.047 | 0.016 | 0.005 | 0.010 |
| $75^{th}$ percentile | 0.022 | 0.018 | 0.043 | 0.142 | 0.165 | 0.098 | 0.062 |
| $90^{th}$ percentile | 0.124 | 0.111 | 0.176 | 0.350 | 0.327 | 0.254 | 0.181 |
| Maximum | 0.315 | 0.292 | 0.374 | 0.918 | 0.898 | 0.862 | 0.482 |
| Average | 0.030 | 0.028 | 0.045 | 0.125 | 0.101 | 0.078 | 0.055 |

**Table 6. Summary of longshore current and wind direction at the time of sample collection.**

| Longshore current and wind direction at the time of sample collection | | |
|---|---|---|
| Longshore Current Direction | Alford and Pennoyer Park (n) | |
| North | 51 | |
| South | 49 | |
| Wind direction | Alford Park (n) | Pennoyer Park (n) |
| North | 18 | 18 |
| Northeast | 14 | 10 |
| East | 4 | 5 |
| Southeast | 7 | 6 |
| South | 19 | 20 |
| Southwest | 14 | 16 |
| West | 16 | 13 |
| Northwest | 8 | 12 |

The mixing of the river into coastal waters was evaluated with the respect to the distance from the river to sampling sites. The median (Pennoyer Park only), $75^{th}$ percentile, $90^{th}$ percentile and maximum mixing ratios at each location were compared to the distance from the sampling location to the river's mouth (Figures 5 and 6). At Pennoyer Park, the mixing ratio decreased successively with increasing distance from the river's mouth. There was a large

decrease in the maximum ratio at distances of 400 meters from the river's mouth compared to closer locations (0.86-0.91 vs. 0.48). However, r values between mixing ratios and the distance between sampling locations were below the threshold required to indicate significant linear trends ($p>0.05$), with the exception of the 90$^{th}$ percentile ($p<0.05$) (Median ratio, r= -0.787; 75$^{th}$ percentile ratio, r= -0.884; 90$^{th}$ percentile ratio, r= -0.988; maximum ratio, r= -0.876).

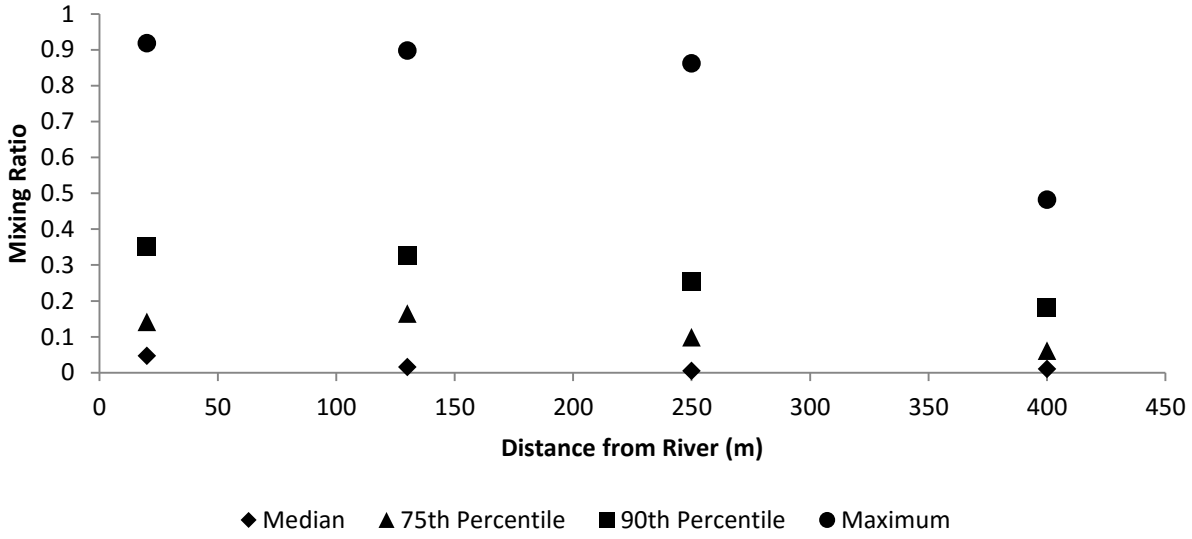


**Figure 5. Mixing ratios at Pennoyer Park sampling locations in comparison to distance from river's mouth. Pearson's product moment correlation coefficients were not significant ($p>0.05$) except for the 90$^{th}$ percentile ($p<0.05$) (median ratio, r= -0.787; 75$^{th}$ percentile ratio, r= -0.884; 90$^{th}$ percentile ratio, r= -0.988; maximum ratio, r= -0.876).**

Similar trends were observed with sampling locations at Alford Park; 75$^{th}$ percentile, 90$^{th}$ percentile and maximum mixing ratios were lower at location A3 compared to A1. However, 75$^{th}$ percentile, 90$^{th}$ percentile and maximum mixing ratios were greater at location A3 compared to A2. Similar to Pennoyer Park, r values did not indicate a significant linear trend at Alford Park (75$^{th}$ percentile, r= -0.796; 90$^{th}$ percentile, r= -0.769; maximum, r= -0.714). At both beaches, the mixing generally decreased with increasing distance from the river's mouth; however, trends were not linear.

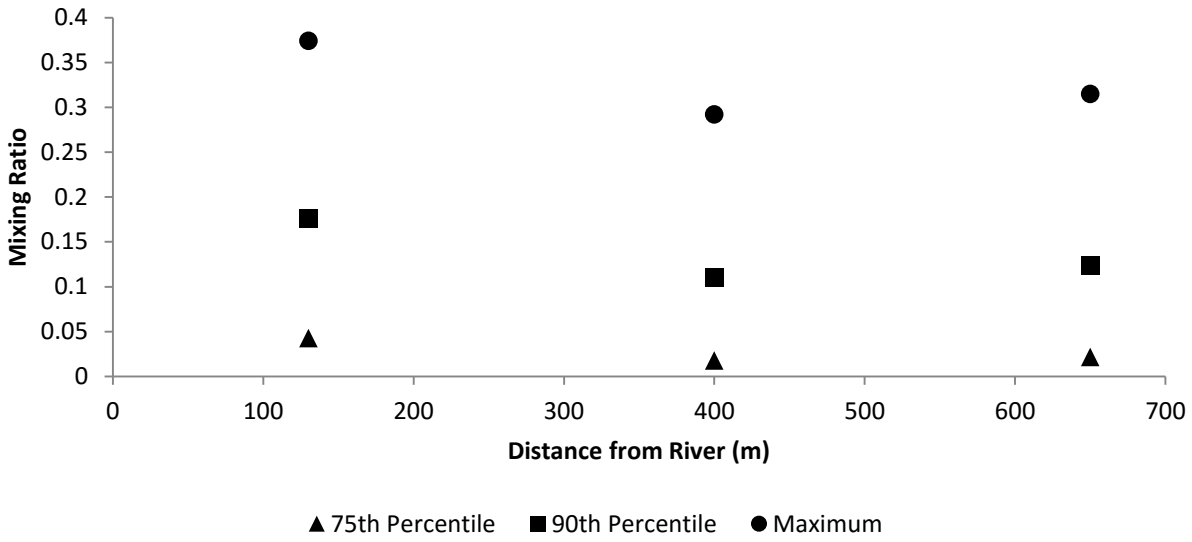


**Figure 6. Mixing Ratio at Alford Park in comparison to distance from river's mouth. Pearson's product moment correlation coefficients were not significant ($p<0.05$) ($75^{th}$ percentile, $r= -0.796$; $90^{th}$ percentile, $r= -0.769$; maximum, $r= -0.714$).**

4.3.2 Longshore Current Direction

Longshore current directions were compared to mixing ratios to determine its influence on the directionality of river mixing. Longshore current directions were observed to be north on 51 days and south on 49 days. Mixing ratios were combined based upon their location relative to the river's mouth (Alford Park = North, Pennoyer Park = South) and grouped by the longshore current direction. A Shapiro-Wilk test was performed indicating the data was not normally distributed ($p<0.05$). A Mann-Whitney Rank Sum test was performed and results implied higher mixing ratios at Alford Park with northern longshore currents and at Pennoyer Park with southern longshore currents compared to the alternative direction ($p<0.05$). The mixing ratios at each sampling location were further evaluated using a Mann-Whitney Rank Sum test. Significantly higher mixing ratios were associated with northern longshore currents compared to southern ones at locations A1, A2 and A3 ($p<0.05$) (Figure 7).

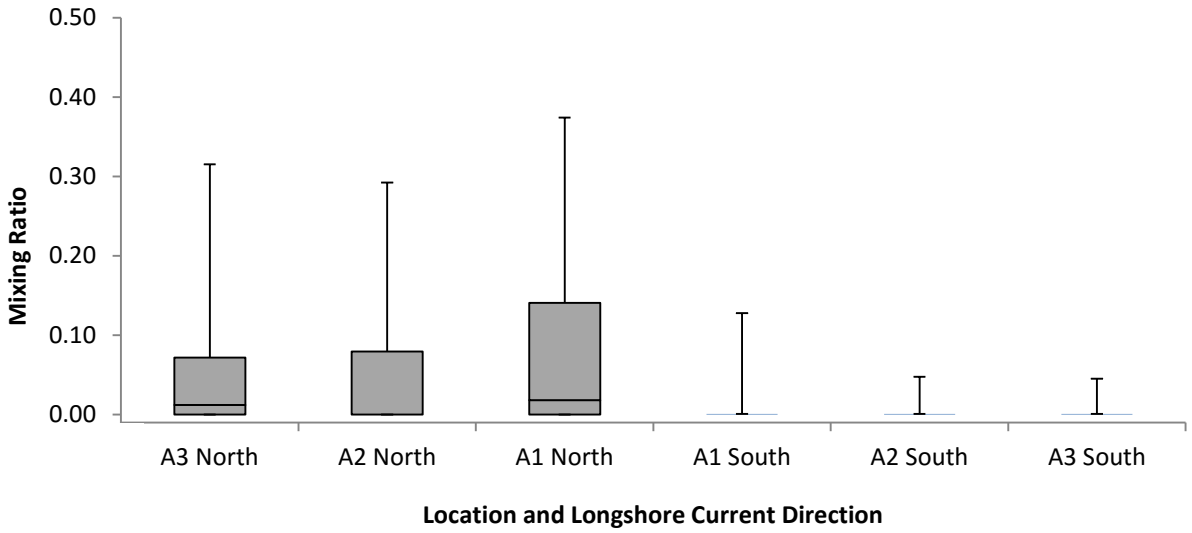


**Figure 7. Mixing ratio compared to longshore current direction at Alford Park. Significant differences present between mixing ratios at location A3-northern current (median= 0.0121, 75$^{th}$ percentile= 0.0766) and A3-southern current (median= 0.000, 75$^{th}$ percentile= 0.000), A2-northern current (median= 0.000, 75$^{th}$ percentile= 0.0965) and A2-southern current (median= 0.000, 75$^{th}$ percentile= 0.000), and A1-northern current (median= 0.0184, 75$^{th}$ percentile= 0.141) and A1-southern current (median= 0.000, 75$^{th}$ percentile= 0.000) ($p<0.05$, Mann-Whitney Test).**

Conversely, significantly higher mixing ratios were associated with southern longshore currents at locations P2, P3 and P4 ($p<0.05$) (Figure 8); no differences were noted at location P1 ($p=0.109$). The direction of the longshore current had a significant influence on river mixing at each beach and all locations except P1. Mixing generally followed the direction of the longshore current.

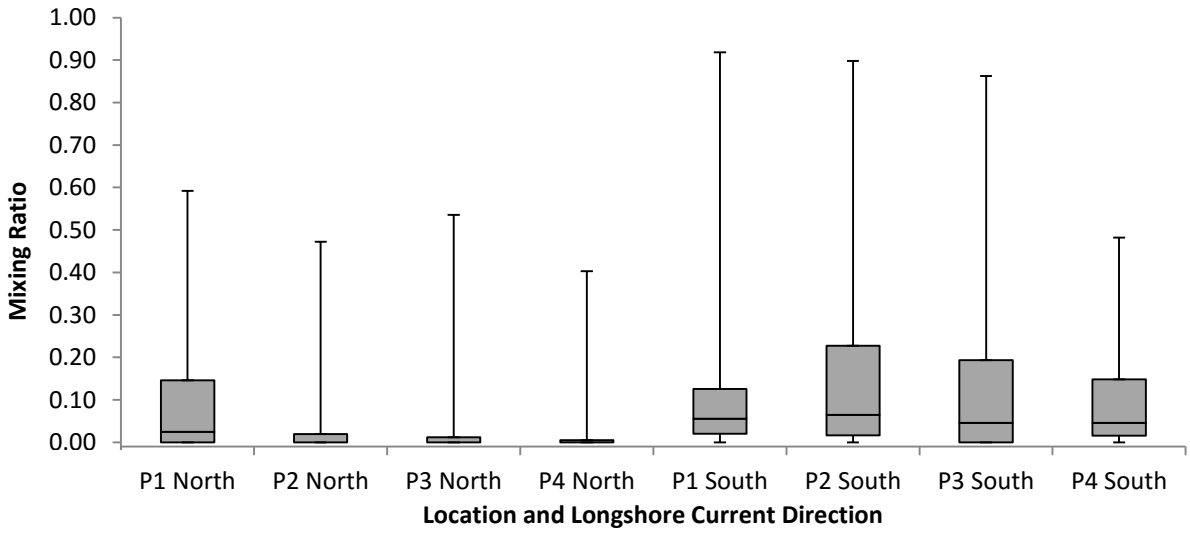


**Figure 8. Mixing ratio compared to longshore current direction at Pennoyer Park. Significant differences present between mixing ratios at location P2-northern current (median= 0.000, 75$^{th}$ percentile= 0.023) and P2-southern current (median= 0.064, 75$^{th}$ percentile= 0.234), P3-northern current (median= 0.000, 75$^{th}$ percentile= 0.012) and P3-southern current (median= 0.046, 75$^{th}$ percentile= 0.194), and P4-northern current (median= 0.000, 75$^{th}$ percentile= 0.010) and P4-southern current (median= 0.046, 75$^{th}$ percentile= 0.151) ($p<0.05$, Mann-Whitney Test). No differences noted between mixing ratios for locations P1 (northern current: median= 0.024, 75$^{th}$ percentile= 0.153; southern current: median= 0.056, 75$^{th}$ percentile= 0.172) ($p<0.05$ Mann-Whitney Test).**

### 4.3.3 Wind Direction

There were slight variations in wind direction between samples collected at Alford Park and those collected from Pennoyer Park due to differences in sample collection time (Alford Park=8:54am; Pennoyer Park=9:20am) (Figure 9). Although wind directions were similar, there were several more dates with northwest (12 vs. 8) and southwest (16 vs. 14) winds at Pennoyer Park compared to Alford Park. At Alford Park, there were several more dates with northeast (14 vs. 10) and west (16 vs. 13) winds compared to Pennoyer Park. Overall, the wind direction in order of most frequent to least frequent direction was: south, north, southwest, west, northeast, northwest, southeast and east.

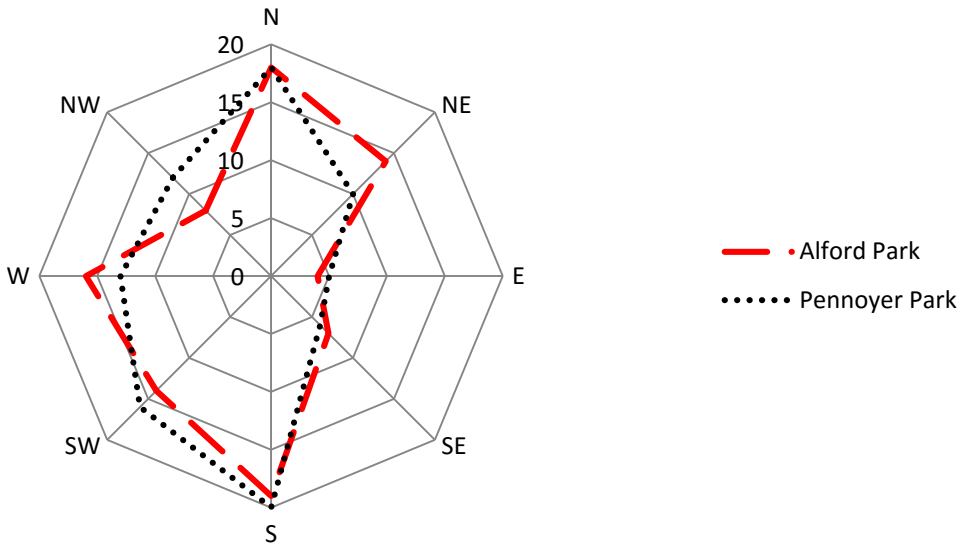


**Figure 9. Number of dates with each wind directions at Alford and Pennoyer Park. Radial axis represents the number of dates with each wind direction.**

Mixing ratios were compared to wind directions to determine its influence on the direction of river mixing. Mixing ratios were grouped at locations north of the river (Alford Park) by the cardinal and intercardinal wind direction at the time of sample collection. A Shapiro-Wilk test was performed indicating the data was not normally distributed ($p<0.05$). An ANOVA on ranks test ($p<0.05$) and Dunn's post-hoc test was performed indicating significantly higher mixing ratios with south compared to west, northwest, north, northeast, east and southeast wind directions ($p<0.05$) (Figure 10).

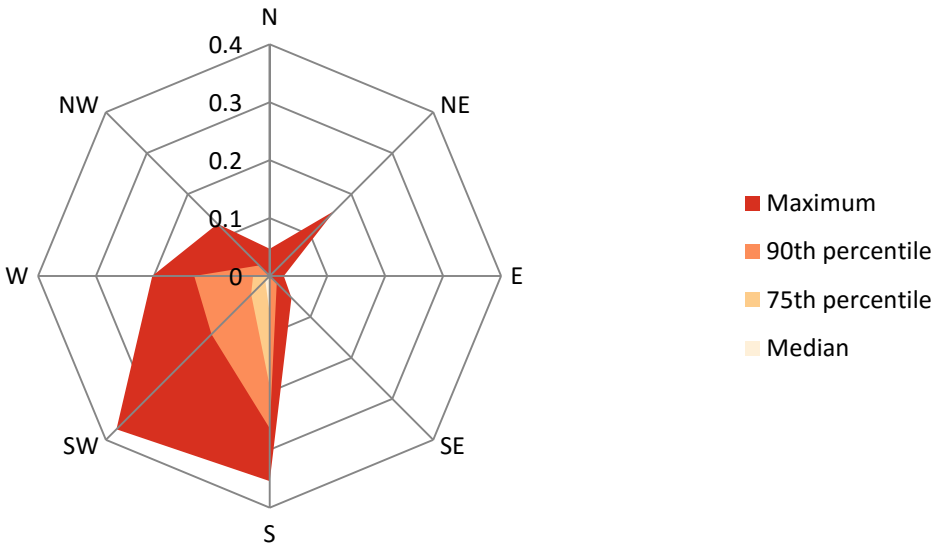


**Figure 10. Mixing ratios at Alford Park compared to wind direction. Significantly higher mixing ratios were associated with south compared to west, northwest, north, northeast, east and southeast wind directions ($p<0.05$; ANOVA on ranks, $p<0.05$)**

Similarly, mixing ratios were grouped at locations south of the river (Pennoyer Park) by the cardinal and inter-cardinal wind direction at the time of sample collection. A Shapiro-Wilk test was performed indicating the data was not normally distributed ($p<0.05$). An ANOVA on ranks test was performed indicating differences amongst the population ($p<0.05$). A Dunn's post hoc test determined significantly higher mixing ratios with northwest, north, northeast, east, southeast, and south compared to southwest winds ($p<0.05$) (Figure 11). Additionally, higher mixing ratios were associated with north and northeast compared to west winds ($p<0.05$).

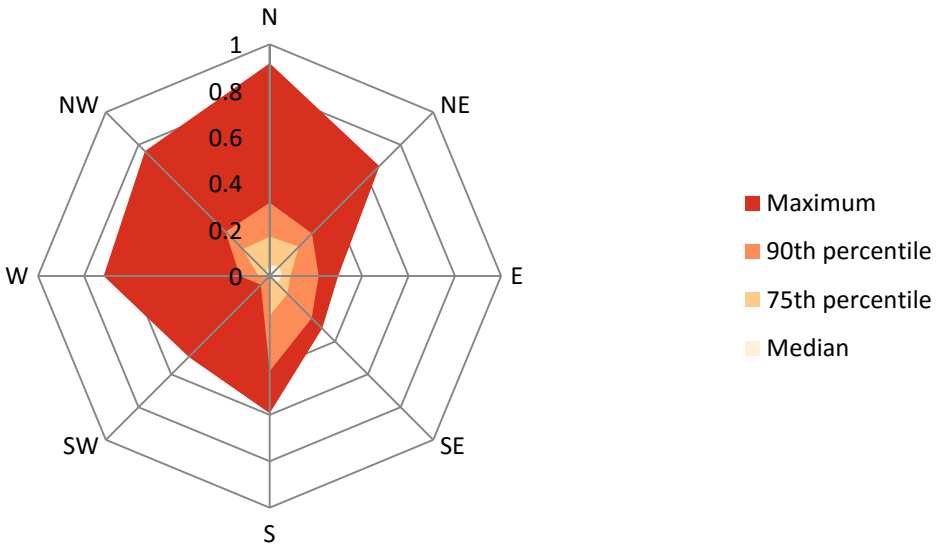


**Figure 11. Mixing ratios at Pennoyer Park compared to wind direction. Significantly higher mixing ratios were associated with northwest, north, northeast, east, southeast, and south compared to southwest winds ($p<0.05$); higher mixing ratios were associated with north and northeast compared to west winds ($p<0.05$; ANOVA on rank).**

Wind direction influenced the directionality of river mixing. Mixing was more prevalent with south winds at locations to the north of river (Alford Park). At locations to the south of the river (Pennoyer Park), mixing was less prevalent with southwest and west winds. During the course of the study, there were more instances of wind direction favoring river mixing towards Pennoyer Park rather than Alford Park.

### 4.3.4 River Discharge

River discharge volumes were compared to mixing ratios at each sampling location (Table 7). River discharge volumes ranged from 0.14 to 8.08 cubic meters per second with a median discharge volume of 0.31 cubic meters per second. There were significant positive correlations between mixing ratios and discharge volumes at locations P1, P2, P3 and P4 on all sampling dates ($p<0.05$).

**Table 7. Spearman correlations (rho) between mixing ratio and discharge volume overall and binned by longshore current direction. Bolded values are significant.**

| Correlation between discharge volume overall and binned by longshore current direction | | | | | | | | | |
|---|---|---|---|---|---|---|---|---|---|
| Location | Northern Longshore Current | | | Southern Longshore Current | | | Overall | | |
| | n | ρ (rho) | p | n | ρ (rho) | p | n | ρ (rho) | p |
| A3 | 51 | 0.107 | 0.453 | 49 | -0.217 | 0.134 | 100 | 0.042 | 0.677 |
| A2 | 51 | 0.155 | 0.276 | 49 | -0.0134 | 0.927 | 100 | 0.052 | 0.606 |
| A1 | 51 | 0.267 | 0.058 | 49 | 0.186 | 0.199 | 100 | 0.169 | 0.093 |
| P1 | **50** | **0.362** | **0.009** | 48 | 0.118 | 0.419 | ***98*** | ***0.251*** | ***0.012*** |
| P2 | 51 | 0.231 | 0.102 | **49** | **0.528** | **<0.001** | ***100*** | ***0.354*** | ***<0.001*** |
| P3 | 51 | 0.212 | 0.134 | **49** | **0.522** | **<0.001** | ***100*** | ***0.331*** | ***0.001*** |
| P4 | 51 | 0.194 | 0.172 | **49** | **0.534** | **<0.001** | ***100*** | ***0.318*** | ***0.001*** |

River discharge volumes were grouped based upon longshore current direction at the time of sample collection to control for factors influencing the direction of river mixing. Data was not normally distributed (Shapiro-Wilk, $p<0.05$). Higher discharge volumes were associated with northern compared to southern longshore current directions (Mann-Whitney Test, $p<0.05$) (Figure 12). When examining dates with northern longshore currents, significant correlations were present between river discharge volume and mixing ratios at location P1 ($p<0.05$). With southern longshore currents, there were significant positive correlations between mixing ratios and discharge volumes at locations P2, P3 and P4 ($p<0.05$). No correlations were noted at Alford Park locations ($p>0.05$).

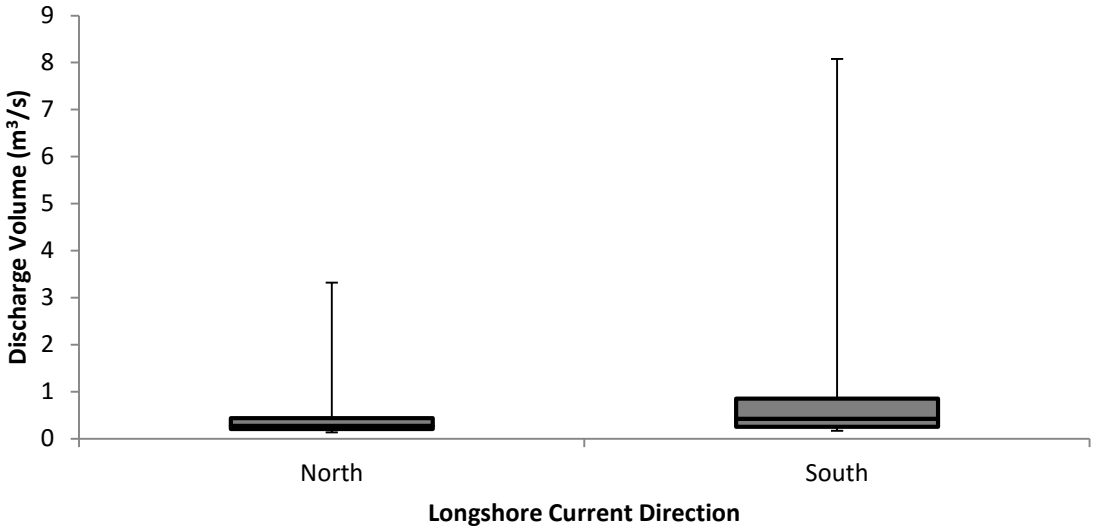


**Figure 12. Pike River discharge volume compared to longshore current direction. Significantly higher discharge volumes were associated with southern, compared to northern longshore current directions ($p<0.05$; Mann-Whitney Test).**

Higher river discharge volumes increased mixing at all locations to the south of the beach, but not at northern locations. Discharge volumes were smaller with northern longshore currents. Correlations between discharge volumes and mixing ratios were also observed at locations P2, P3, and P4 when binning the data by a southern longshore current direction. Mixing occurred close the river's mouth (P1) independent of discharge volumes when a southern longshore current was present. However, elevated discharge volumes increased river mixing at location P1 when a northern longshore current was present.

## 4.4 End Member Mixing Models

End member mixing models were created to provide an estimate of river *E. coli* contributions to coastal waters.

4.4.1 Evaluation of End Member Mixing Models (EMMM)

A subset of data (n=10 days) was evaluated when there was an order of magnitude difference in geometric mean *E. coli* concentration between Pennoyer Park and Alford Park, indicating the river was likely contributing to the differences in bacteria concentrations. These conditions allowed background *E. coli* concentrations within the EMMM to be treated as zero. All dates with a magnitude higher geometric mean *E. coli* concentration were associated with Pennoyer Park. Outliers were removed from the data set prior to analysis. Four outliers (one at each sampling location; P1-P4) were associated with a single date when coastal *E. coli* concentrations at Pennoyer Park were elevated (geometric mean=1,296MPN/100 ml) and river *E. coli* concentrations were low (41 MPN/100 ml) and could not explain elevated coastal bacteria levels. One other outlier was associated with sampling location P1. On this date, the mixing ratio was zero indicating no contribution from the river at location P1, while measured *E. coli* concentrations were 109 MPN/100 ml. Concentrations at Alford Park (unmixed zone) ranged from 41 to 86 MPN/100 ml and concentrations at Pennoyer Park ranged from 573 to 1850 MPN/100 ml on this date (excluding P1).

Within this subset (described above), *E. coli* contributions from the river to coastal areas were estimated and compared to observed concentrations (Figure 13). Overall, estimated *E. coli* contributions correlated significantly with observed concentrations ($p<0.05$, $R^2=0.5486$, n=34). At locations P2 (n=9, $R^2=0.8002$) and P3 (n=9, $R^2=0.9282$) model fit was excellent and the slope of the regression with the y-intercept set to zero approximated a 1:1 fit (1.014 and 1.009 at locations P2 and P3 respectively). The amount of variation in coastal *E. coli*

concentrations explained by the model at location P4 was lower (n=9, $R^2$=0.5773) than P2 and P3 However, the slope also approximated a 1:1 fit (1.034). Model fit was extremely low at location P1 in comparison to other locations, (n=8, $R^2$=0.1704). Additionally, the slope of the line which best fit the data was below 1.0 (0.892) indicated the model generally predicted higher *E. coli* contributions than measured. End member mixing models (EMMM) were able to accurately estimate coastal *E. coli* concentrations on this subset of data with the exception of the location closest to river's mouth (P1).

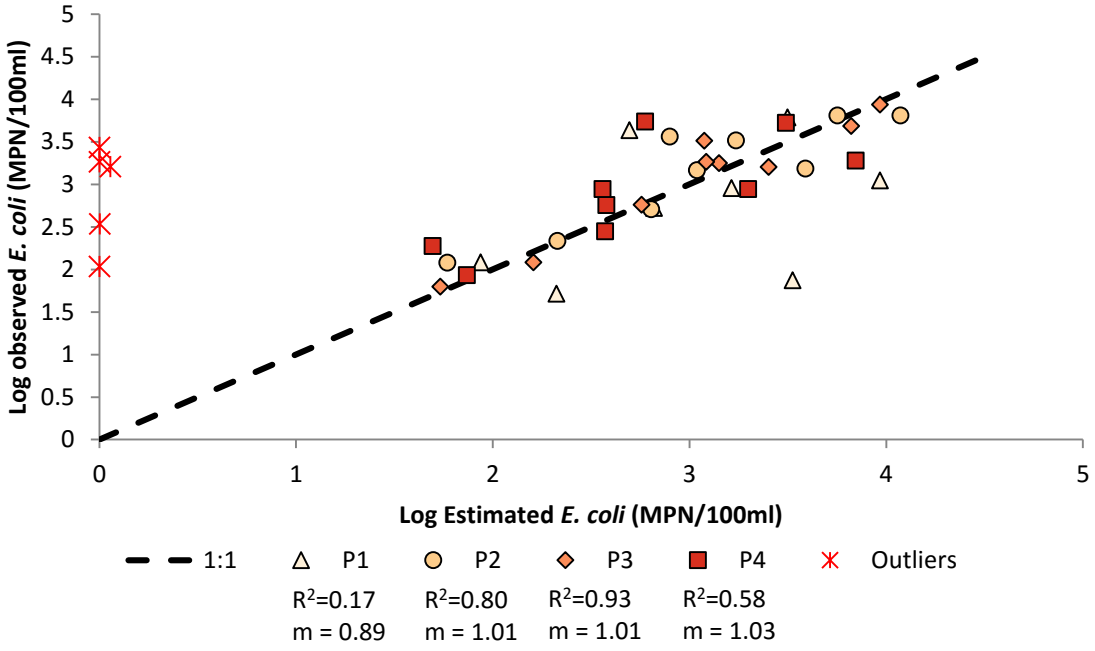


**Figure 13. Comparison between observed and predicted *E. coli* concentrations at coastal locations using an end member mixing model under conditions when the Pike River is suspected as the major source of *E. coli* contamination. Five outliers associated with dates/locations when no mixing was occurring or when Pike River *E. coli* concentrations were low and could not explain elevated coastal concentrations. Eight, nine, nine and nine samples were associated with locations P1, P2, P3 and P4 respectively.**

4.4.2 Estimated *E. coli* Contribution of the Pike River to Coastal Waters

Estimated *E. coli* contributions from the Pike River to coastal waters were calculated as the product of the mixing ratio and *E. coli* concentration of the river (Figures 14-20). Estimated *E. coli* contributions from the river to coastal locations ranged from zero to 11,829 MPN/100 ml (Table 8). In all instances, mixing ratios were below 1.00 and estimated *E. coli* contributions to coastal locations were below the concentration of the river.

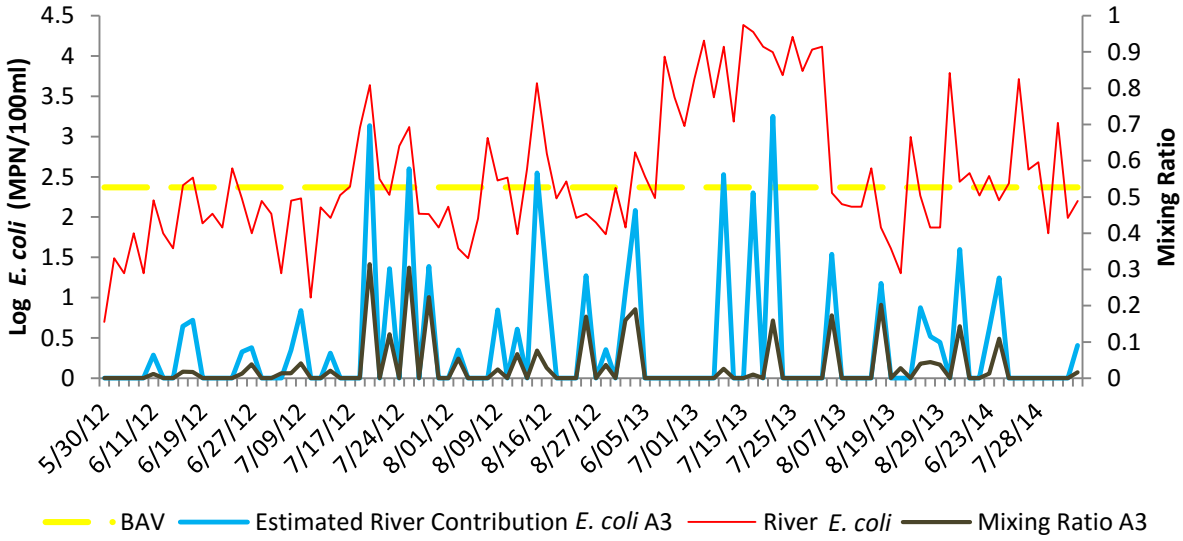


**Figure 14. Estimated contributions of *E. coli* from the Pike River to location A3 (n=100). *E. coli* contributions from the Pike River to coastal locations were estimated as the product of the mixing ratio and actual river *E. coli* concentrations.**

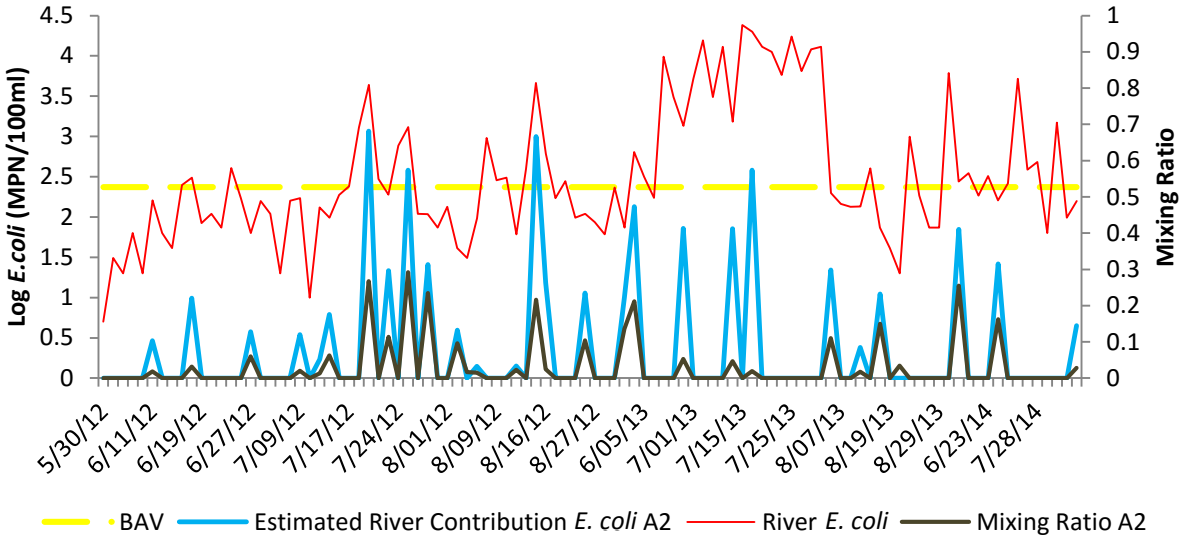


**Figure 15. Estimated contributions of *E. coli* from the Pike River to location A2 (n=100). *E. coli* contributions from the Pike River to coastal locations were estimated as the product of the mixing ratio and actual river *E. coli* concentrations.**

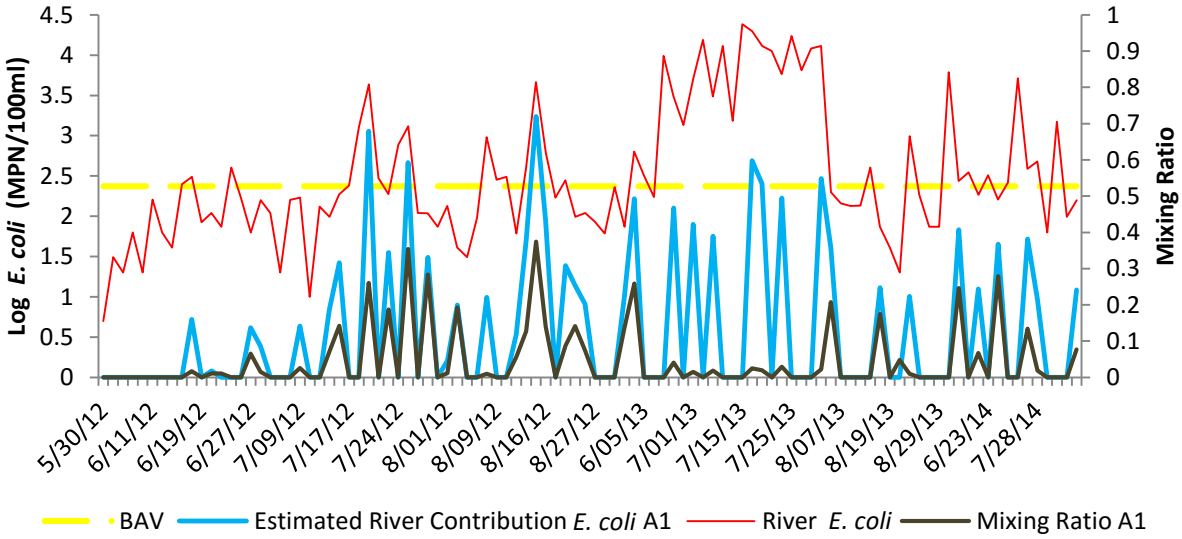


**Figure 16. Estimated contributions of *E. coli* from the Pike River to location A1 (n=100). *E. coli* contributions from the Pike River to coastal locations were estimated as the product of the mixing ratio and actual river *E. coli* concentrations.**

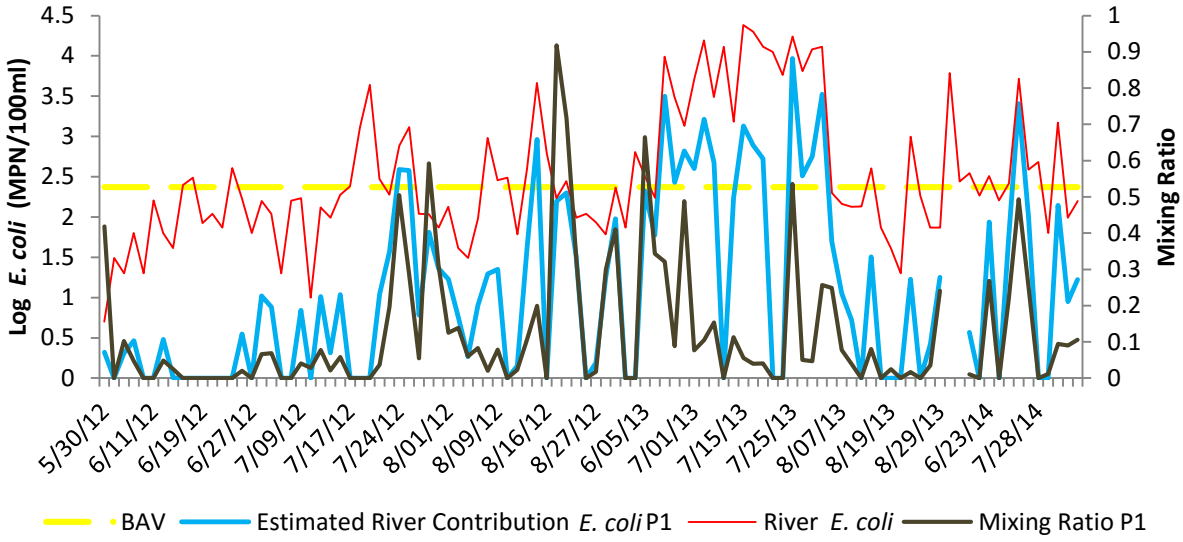


**Figure 17. Estimated contributions of *E. coli* from the Pike River to location P1 (n=98). *E. coli* contributions from the Pike River to coastal locations were estimated as the product of the mixing ratio and actual river *E. coli* concentrations.**

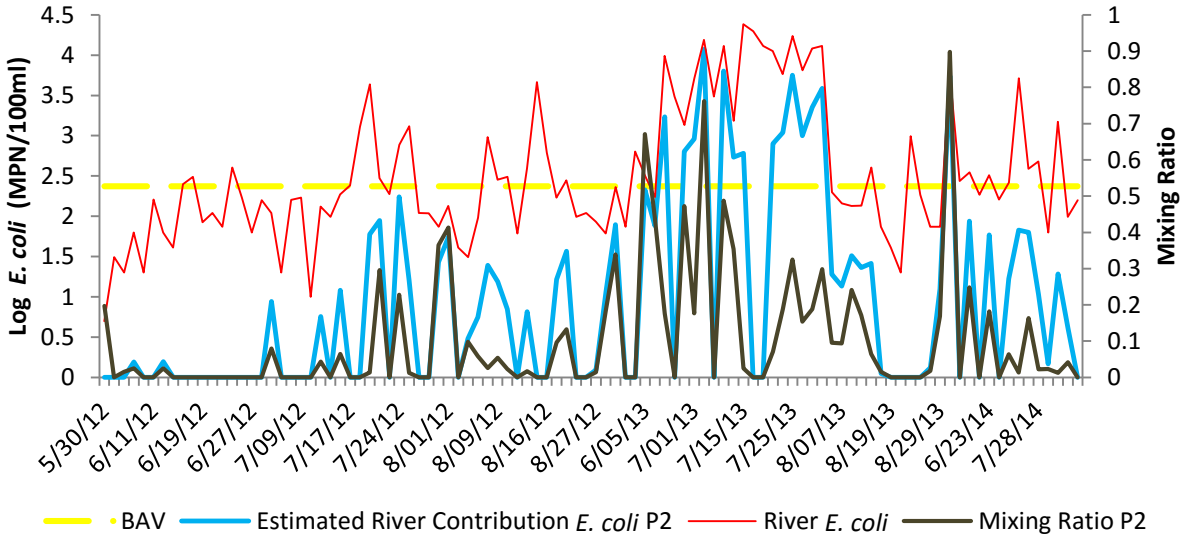


**Figure 18. Estimated contributions of *E. coli* from the Pike River to location P2 (n=100). *E. coli* contributions from the Pike River to coastal locations were estimated as the product of the mixing ratio and actual river *E. coli* concentrations.**

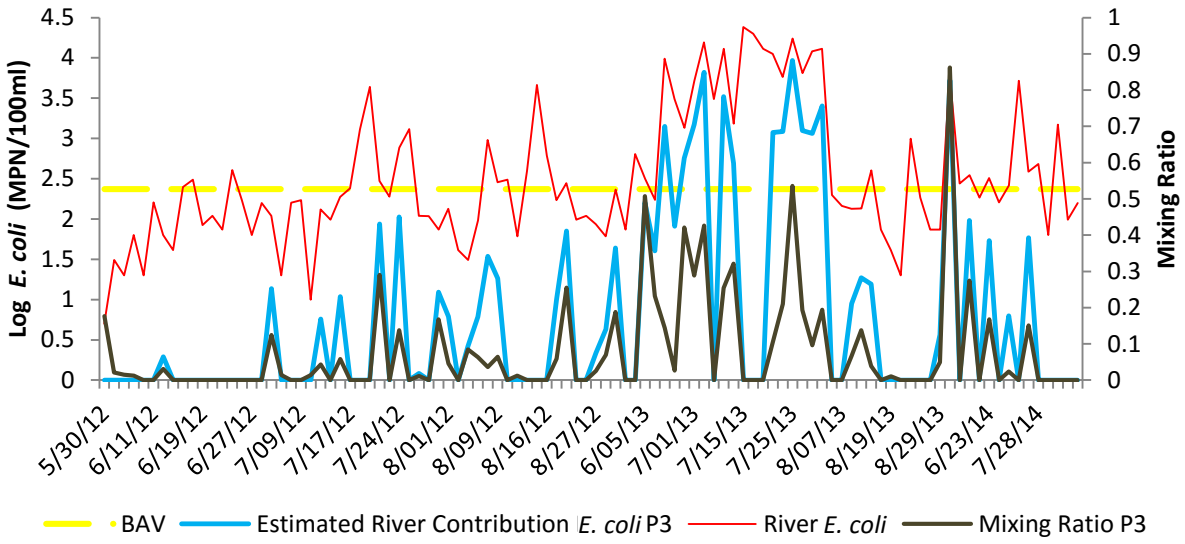


**Figure 19. Estimated contributions of *E. coli* from the Pike River to location P3 (n=100). *E. coli* contributions from the Pike River to coastal locations were estimated as the product of the mixing ratio and actual river *E. coli* concentrations.**

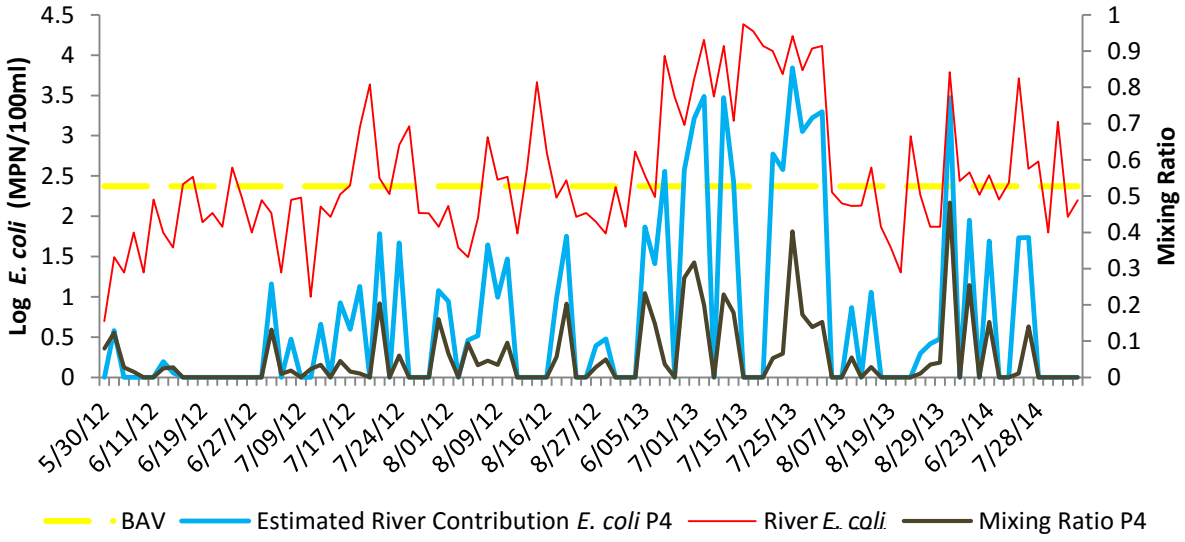


**Figure 20. Estimated contributions of *E. coli* from the Pike River to location P4 (n=100). *E. coli* contributions from the Pike River to coastal locations were estimated as the product of the mixing ratio and actual river *E. coli* concentrations.**

**Table 8. Summary of Pike River *E. coli* (MPN/100 ml) contributions to costal locations. Pike river *E. coli* contribution to coastal locations estimated as the product of the mixing ratio and Pike River *E. coli* concentration.**

| Estimated *E. coli* contributions (MPN/100ml) from the Pike River to coastal locations | | | | | | | |
|---|---|---|---|---|---|---|---|
| Location | A3 | A2 | A1 | P1 | P2 | P3 | P4 |
| Median | 0 | 0 | 0 | 7 | 2 | 0 | 0 |
| 75th Percentile | 3 | 1 | 11 | 81 | 42 | 18 | 14 |
| 90th Percentile | 23 | 22 | 80 | 539 | 805 | 1,157 | 372 |
| Maximum | 1,784 | 1,163 | 1,725 | 9,283 | 11,829 | 9,283 | 6,980 |

Estimated *E. coli* contributions from the Pike River were grouped by sample location. A Shapiro-Wilk test was performed indicating the data was not normally distributed ($p<0.05$). An ANOVA on Ranks was performed to determine whether estimated *E. coli* contributions differed by sampling location. Results from the ANOVA on Ranks indicated differences amongst the population ($p<0.05$). A Dunn's post hoc test determined higher contributions at location P1 compared to A1, A2 and A3 ($p<0.05$). Additionally, higher contributions from the river were estimated to occur at location P2 compared to A2 ($p<0.05$).

Measured coastal *E. coli* concentrations were compared to estimated contributions from the Pike River at each sampling location (Figures 21-27). $R^2$ values between estimated contributions from the Pike River and actual coastal *E. coli* concentrations were 0.1018, 0.0771, 0.0549, 0.1386, 0.4194, 0.4106 and 0.4370 at locations A3, A2, A1, P1, P2, P3 and P4 respectively. Correlations between estimated Pike River *E. coli* contributions and actual coastal *E. coli* concentrations were greater than direct correlations between specific conductivity and coastal *E. coli* concentrations at all sampling locations (See Appendix A). Correlations between estimated contributions from the Pike River and actual coastal *E. coli* concentrations indicate river *E. coli* contributions explain more of the variation in coastal *E. coli* concentrations at

Pennoyer Park than Alford Park. However, there were several cases at each sampling location when estimated *E. coli* contributions from the Pike River to coastal waters were above actual values. However, no estimates were greater than an order of magnitude higher than actual.

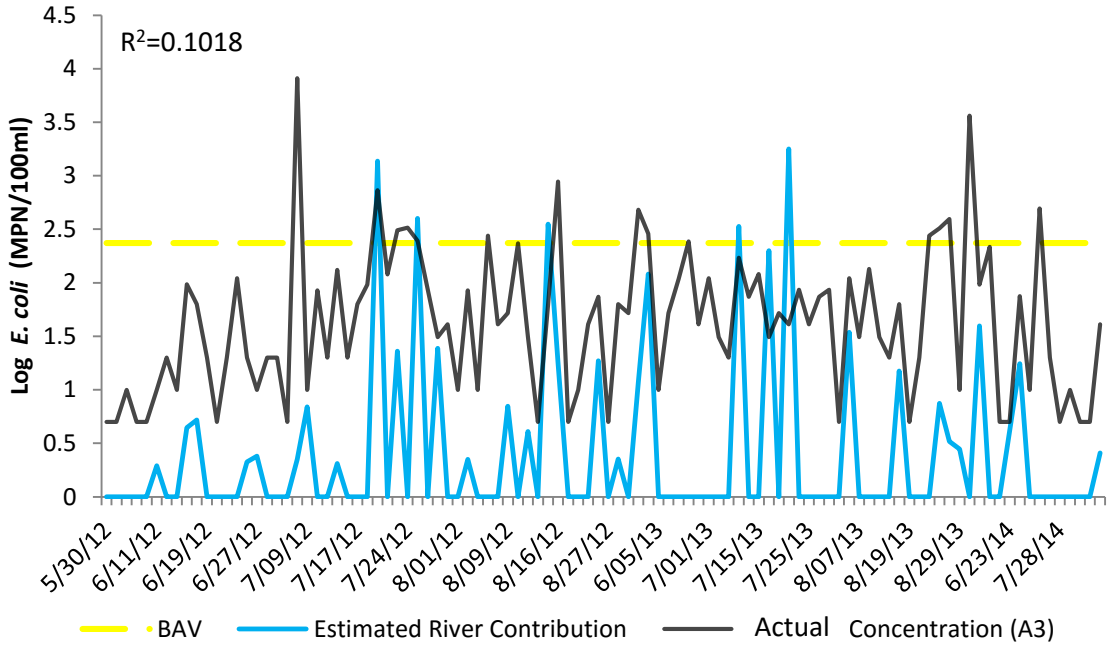


**Figure 21. Comparison between estimated *E. coli* contributions from the Pike River and actual concentrations at location A3 (n=100). River *E. coli* contributions to costal locations were estimated as the product of the mixing ratio and actual river *E. coli* concentrations.**

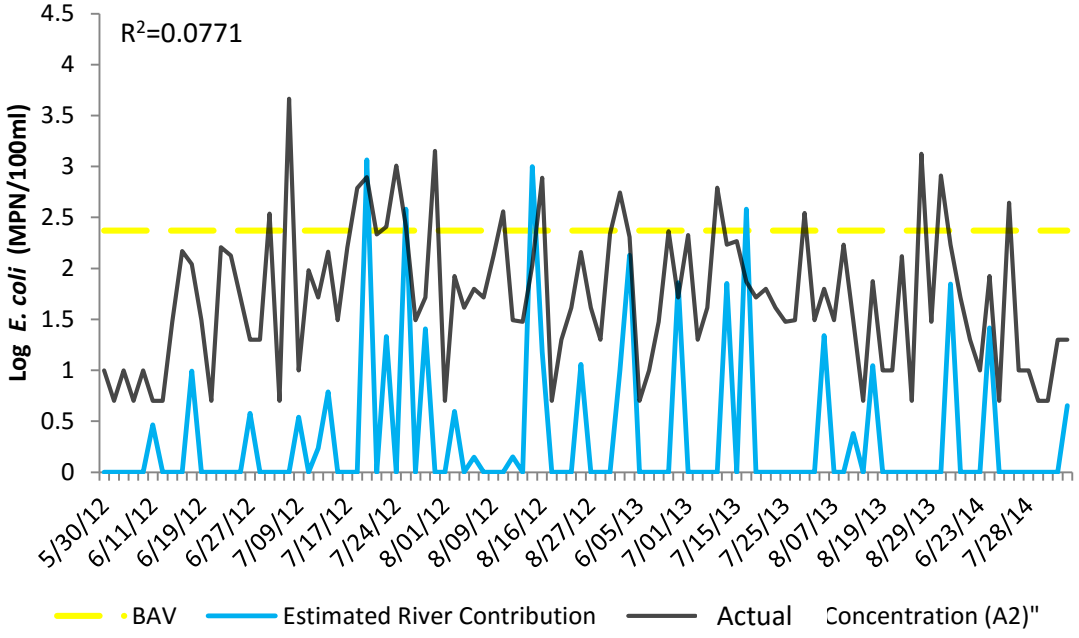


**Figure 22. Comparison between estimated *E. coli* contributions from the Pike River and actual concentrations at location A2 (n=100). River *E. coli* contributions to costal locations were estimated as the product of the mixing ratio and actual river *E. coli* concentrations.**

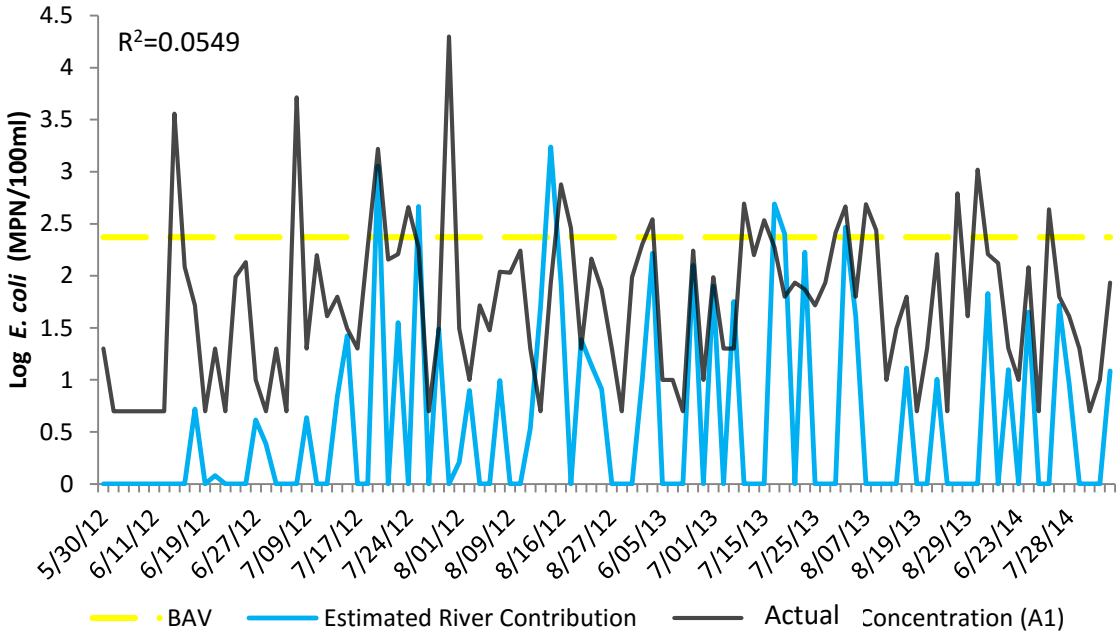


**Figure 23. Comparison between estimated *E. coli* contributions from the Pike River and actual concentrations at location A1 (n=100). River *E. coli* contributions to costal locations were estimated as the product of the mixing ratio and actual river *E. coli* concentrations.**

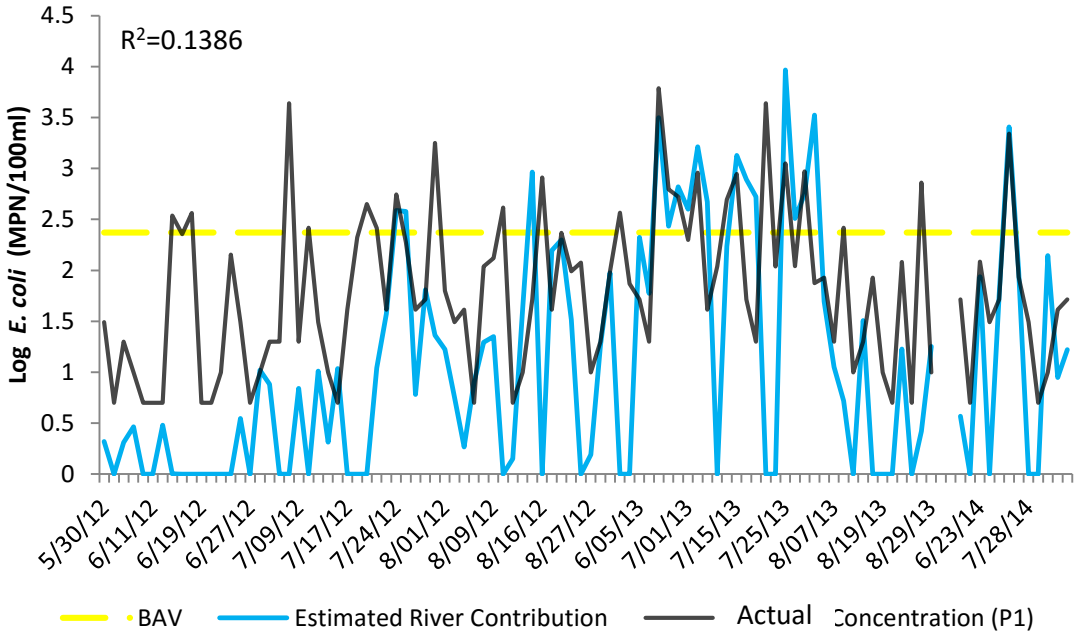


**Figure 24. Comparison between estimated *E. coli* contributions from the Pike River and actual concentrations at location P1 (n=98). River *E. coli* contributions to costal locations were estimated as the product of the mixing ratio and actual river *E. coli* concentrations.**

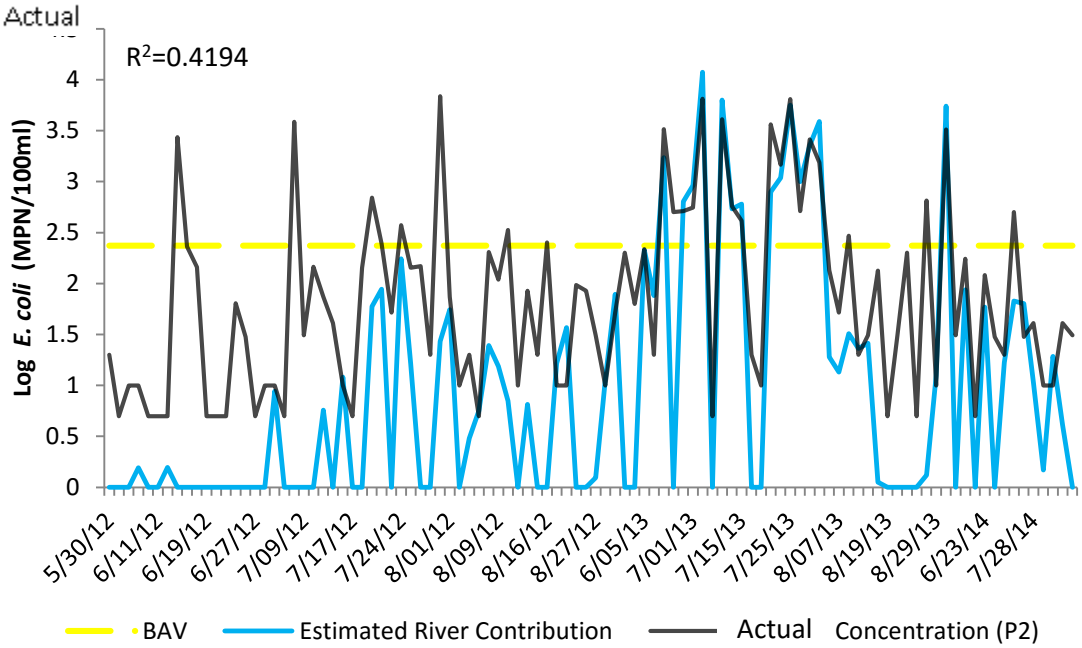


**Figure 25. Comparison between estimated *E. coli* contributions from the Pike River and actual concentrations at location P2 (n=100). River *E. coli* contributions to costal locations were estimated as the product of the mixing ratio and actual river *E. coli* concentrations.**

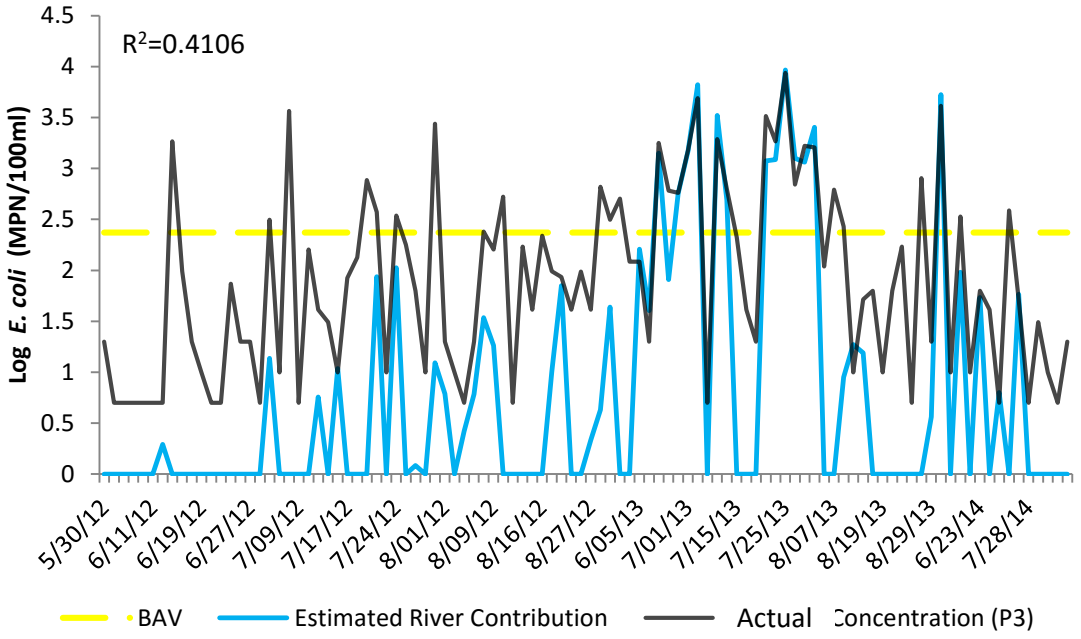


**Figure 26. Comparison between estimated *E. coli* contributions from the Pike River and actual concentrations at location P3 (n=100). River *E. coli* contributions to costal locations were estimated as the product of the mixing ratio and actual river *E. coli* concentrations.**

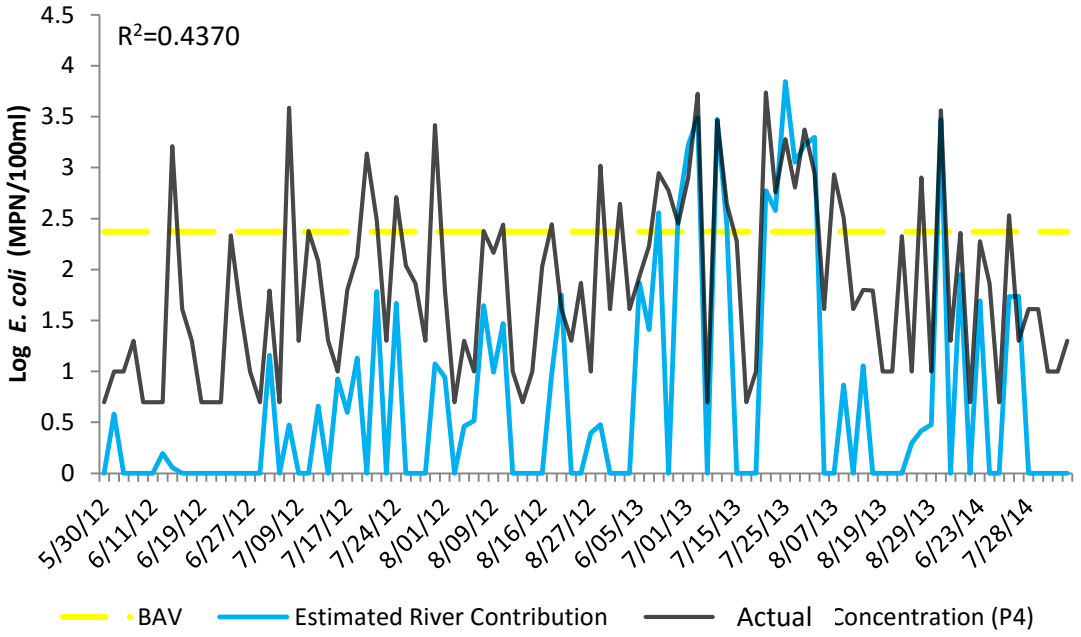


**Figure 27. Comparison between estimated *E. coli* contributions from the Pike River and actual concentrations at location P4 (n=100). River *E. coli* contributions to costal locations were estimated as the product of the mixing ratio and actual river *E. coli* concentrations.**

### 4.4.3 Exceedances of BAVs Attributed to the Pike River

The number of *E. coli* BAVs exceedances associated with the Pike River was estimated at each sample location by removing the estimated *E. coli* contribution of the Pike River from the observed concentrations and then correcting for the river's dilution effect (Equation 6) (Table 9). Two or three exceedances of *E. coli* standards were associated with the Pike River at Alford Park, sampling location dependent, and between six and 11 were associated with Pennoyer Park. Most of the exceedances of BAVs were associated with wet weather events. Overall, it was estimated the Pike River was responsible for between 12 and 15 percent of exceedances of BAVs at Alford Park and between 26 and 42 percent at Pennoyer Park.

**Table 9. *E. coli* BAV exceedances (*E. coli* >235 MPN/100ml) associated with the Pike River. Exceedances of BAV calculated by removing estimated *E. coli* concentrations from the Pike River from coastal locations (See equation 6).**

| Estimated BAV exceedances caused by Pike River *E. coli* contributions | | | | | | | |
|---|---|---|---|---|---|---|---|
| Location | A3 | A2 | A1 | P1 | P2 | P3 | P4 |
| Number of Exceedances (>235 MPN/100ml *E. coli*) | 15 | 16 | 17 | 23 | 26 | 31 | 30 |
| Estimated exceedances caused by river | 3 | 3 | 2 | 6 | 11 | 10 | 9 |
| Estimated wet weather exceedances caused by river (rainfall >0.00 cm) | 3 | 2 | 2 | 3 | 7 | 5 | 4 |
| Estimated exceedances without river influence | 12 | 13 | 15 | 17 | 15 | 21 | 21 |
| Percent exceedances related to river | 20% | 19% | 12% | 26% | 42% | 32% | 30% |

## 4.5 Predictive Models

Predictive *E. coli* models were created to determine the model performance of ensemble models, which accounts for Pike River *E. coli* contributions, in comparison to

traditional VB MLR models, which do not explicitly model point source contributions. Additional visualizations and statistics on model performance are located in Appendix B.

### 4.5.1 Traditional VB MLR Models

Traditional VB MLR predictive *E. coli* models were created using Virtual Beach 3.0 (US EPA, 2013) for each sampling location, including the Pike River, using all training set data (75% of data) (Table 10). Common model variables included river discharge volume, wave height, current velocity vectors, water clarity, turbidity, air temperature and mixing ratios. Models were optimized for lowest BIC to provide parsimony and avoid over fitting data. Associated $R^2$ and RMSE values between modeled and observed log transformed *E. coli* concentrations ranged from 0.162 to 0.620 and 0.499 and 0.730 respectively using training set data.

**Table 10. Traditional VB MLR model description and summary statistics for training set.**

| Traditional VB MLR model description and summary statistics for training set data | | | | |
|---|---|---|---|---|
| Location | Traditional VB Model Equation | n | $R^2$ | RMSE |
| A3 | 0.109712 + 0.000787724 x (Air Temp)$^2$ + 0.518479 x Log(Turbidity) + 0.492249 x Log(River Discharge) | 75 | 0.324 | 0.551 |
| A2 | 0.840957+ 0.0830368 x (Wave Intensity)$^2$ + 0.042491 x (Current Velocity North)$^{-1/2}$ + 0.522497 x Log(River Discharge) | 75 | 0.252 | 0.603 |
| A1 | 1.14182e + 1.3732 x (Field Estimated Wave Height)$^2$ | 75 | 0.162 | 0.730 |
| P1 | -0.839038 - 0.322747 x Rainfall Amount + 1.10281 x (Water Clarity)$^{1/2}$ + 0.989892 x Log (River Discharge) | 73 | 0.500 | 0.578 |
| P2 | 0.721452 - 0.706055 x (GLCFS Wave Height)$^{1/2}$ + 0.320953 x (Water Clarity) + 0.933066 x Log(Turbidity) | 75 | 0.564 | 0.636 |
| P3 | 0.591458 + 1.30403 x (Mixing Ratio)$^{1/2}$ - 0.0524481 x (GLCFS Wave Height)$^2$ + 0.497522 x (Clarity) | 75 | 0.499 | 0.673 |
| P4 | 0.506573 + 1.50591 x (Mixing Ratio)1/2 + 1.18794 x (Field Estimated Wave Height)$^{1/2}$ - 0.764307 x [GLCFS Wave Height]$^{1/2}$ + 0.479075 x (Clarity) | 75 | 0.620 | 0.578 |
| Pike River | 4.08672 - 5.56256 x (River Discharge)$^{-1/2}$ | 75 | 0.409 | 0.681 |
| A1-A3 Composite | 0.0635857 – 0.442639 x (Rainfall)$^{1/2}$ - 213.335 x (Current Velocity East)$^2$ + 0.334406 x Log(Coastal Turbidity) + 0.40035 x Log (Pike Discharge) + 0.00546898 x (Pike Turbidity)+ 0.00166763 (Pike Water Temp)$^2$ | 225 | 0.339 | 0.587 |
| P2-P4 Composite | 0.218114 + 0.733196 x (Mixing Ratio)$^{1/2}$ + 0.000699667 x (Air Temp)$^2$ -0.317264 (Rainfall)$^{1/2}$ – 1.62202 x (Current Velocity East)$^{1/2}$ – 0.906949 x (GLCFS Wave Height)$^{1/4}$ +0.386537 x (Clarity) + 0.3404 x log (Turbidity) + 0.604707 x Log(Pike Discharge) | 225 | 0.616 | 0.584 |

4.5.2 Sub-Ensemble Models

Sub-ensemble models were created for each coastal location using the same training set data when the mixing ratio was equal to zero (Table 11). These models were combined with

modeled Pike River *E. coli* concentration to create ensemble models using equation 4. Associated $R^2$ and RMSE values between modeled and actual log transformed *E. coli* concentrations ranged from 0.301 to 0.757 and 0.432 and 0.741 respectively using training set data. Common model variables included river discharge volume, longshore current direction, wave height, wave intensity, current velocity vectors, wind velocity vectors, water clarity, and air temperature.

**Table 11. Sub-ensemble MLR model description and summary statistics for training set.**

| Sub-ensemble MLR model description and summary statistics for training set data | | | | |
|---|---|---|---|---|
| Location | Sub-Ensemble Model Equation | n | $R^2$ | RMSE |
| A3 | -0.126859 + 0.546052 x (Longshore Current Direction) - 0.217015 x (Rainfall Amount) + 0.00864766 x (Wind Speed North)$^{1/2}$ + 0.0940627 x (Wave Intensity)$^2$ + 95.5112 x Log(Current Velocity North) + 0.920896 x Log(River Discharge) | 55 | 0.585 | 0.432 |
| A2 | 1.10956 + 0.103089 x (Wave Intensity)$^2$ + 0.0544718 x (Current Velocity East)$^{-1/2}$ + 0.0586274 x (River Discharge)$^{1/2}$ | 59 | 0.301 | 0.635 |
| A1 | 0.314699 + 0.00156576 x (Air Temp)$^2$ + 1.53392 x (Field Estimated Wave Height)$^{1/2}$ - 612.413 x (Current Velocity East)$^2$ | 50 | 0.357 | 0.741 |
| P1 | 0.39142 + 0.00124674 x (Air Temp)$^2$ + 0.679469 x (Clarity) - 2.69691 x (River Discharge)$^{-1/2}$ | 16 | 0.757 | 0.464 |
| P2 | 1.47442 - 8.40296 x (Air Temp)$^{-1/2}$ - 0.445846 x (Wave Intensity) - 4.55137 x (Current Velocity East)$^{1/2}$ + 0.888624 x (Current Velocity North)$^{1/2}$ + 1.88215 x (Clarity)$^{1/2}$ | 27 | 0.749 | 0.465 |
| P3 | 0.67356 - 2.55171 x (Current Velocity East)$^{1/2}$ - 0.0744804 x (GLCFS Wave Height)$^2$ + 0.828889 x (Clarity)$^{1/2}$ | 31 | 0.341 | 0.711 |
| P4 | 0.915946 - 0.292551 x (Wind Velocity North)$^{-1/2}$ - 10.4271 x (Current Velocity East) + 0.0934215 x (Clarity)$^2$ | 32 | 0.539 | 0.442 |
| A1-A3 Composite | -0.269677 - 0.486821 x (Rainfall Amount)$^2$ -276.75 x (Current Velocity East)$^2$ + 0.354208 x Log(Coastal Turbidity)+ 0.292203 x (River Discharge)$^{1/4}$ + 0.00611664 x (Pike Turbidity) + 0.00200401 x (Pike Water Temp) | 164 | 0.386 | 0.609 |
| P2-P4 Composite | 0.875454 - 0.826865 x (Cloud Cover)$^{-1/2}$ – 0.110025 x (Wave Intensity) - 4.50461 x (Current Velocity East)$^{1/2}$ + 0.5029 x (Current Velocity North)$^{1/4}$ + 0.294084 x (GLCFS Wave Height)$^{-1/2}$ + 0.483947 x (Clarity) +0.000133193 x (Pike Turbidity)$^2$ | 90 | 0.548 | 0.539 |

### 4.5.3 Predictive Model Performance

Verification data (remaining 25% of the dataset) was used to evaluate model performance (Figures 28-36; Table 12-13). There was a significant correlation between predicted Pike River *E. coli* concentrations and actual concentrations ($n=25$, $R^2=0.3274$, $p<0.05$). For verification data, mixing events were more frequent at locations A3, A2, A1 and P1 compared to the remaining locations. Additionally, exceedances of *E. coli* standards were most frequent at A3, A2 and P1 compared to the remaining sample locations. Estimated Pike River *E. coli* contributions (actual Pike River *E. coli* concentration multiplied by mixing ratio) were compared to coastal *E. coli* concentrations for this subset of data. $R^2$ values were 0.4084, 0.4465, 0.6314, 0.1035, 0.3625, 0.2184 and 0.3126 at locations A3, A2, A1, P1, P2, P3 and P4 respectively. This indicates that the Pike River explained a greater amount of variation in coastal *E. coli* concentration at Alford Park sampling locations compared to Pennoyer Park for the training set data. Using the entire data set, mixing occurred more frequently at Pennoyer Park than Alford Park (see section 4.3.1).

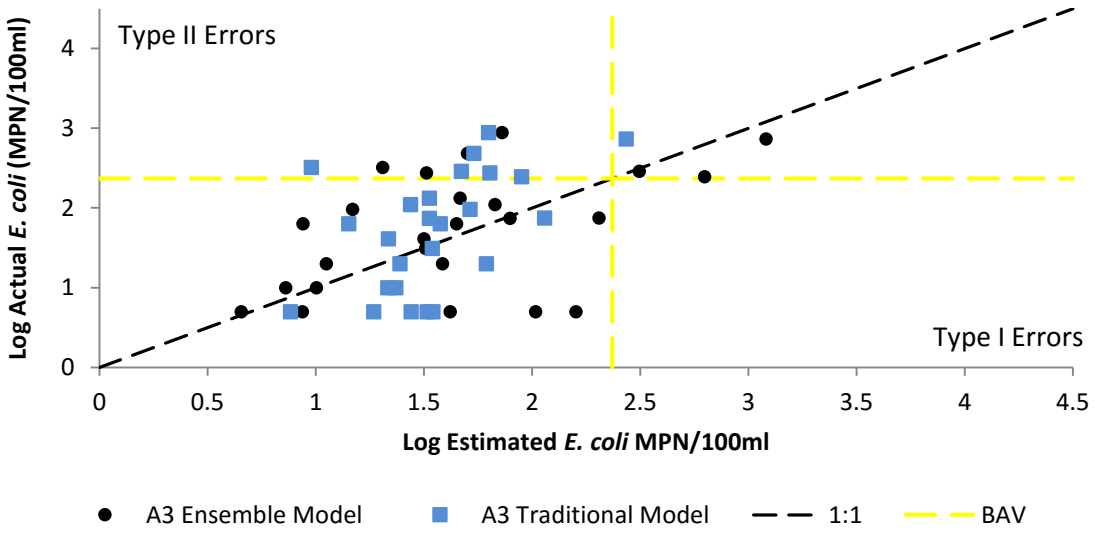


**Figure 28. Ensemble and traditional VB MLR location specific models compared to actual verification set *E. coli* data at location A3 (n=25). Data in upper right quadrant, upper left quadrant, lower left quadrant and lower right quadrant represent accurate predictions of exceedances, Type II errors, accurate predictions of non-exceedances and Type I errors, respectively.**

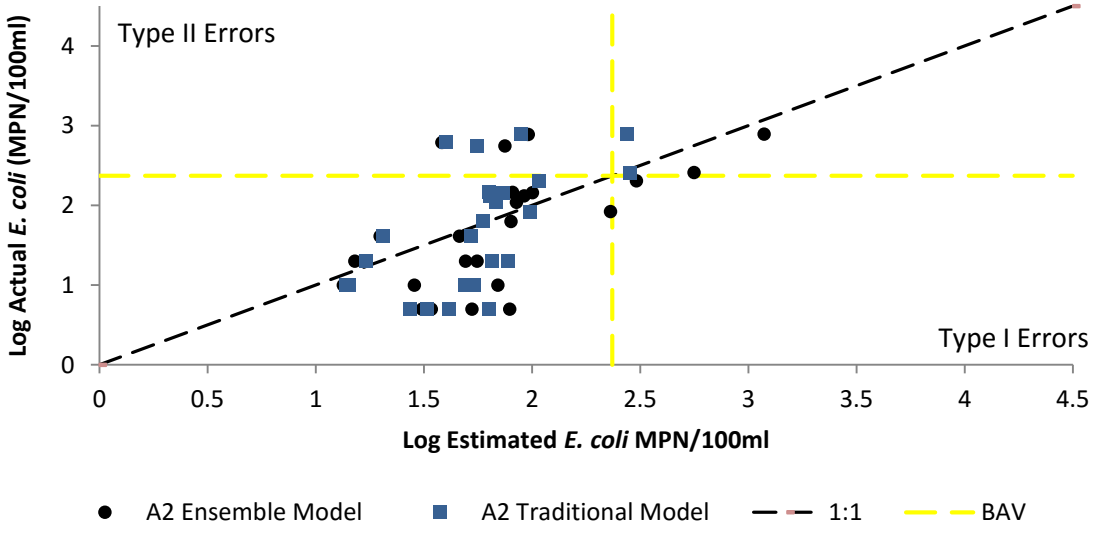


**Figure 29. Ensemble and traditional VB MLR location specific models compared to actual verification set *E. coli* data at location A2 (n=25). Data in upper right quadrant, upper left quadrant, lower left quadrant and lower right quadrant represent accurate predictions of exceedances, Type II errors, accurate predictions of non-exceedances and Type I errors, respectively.**

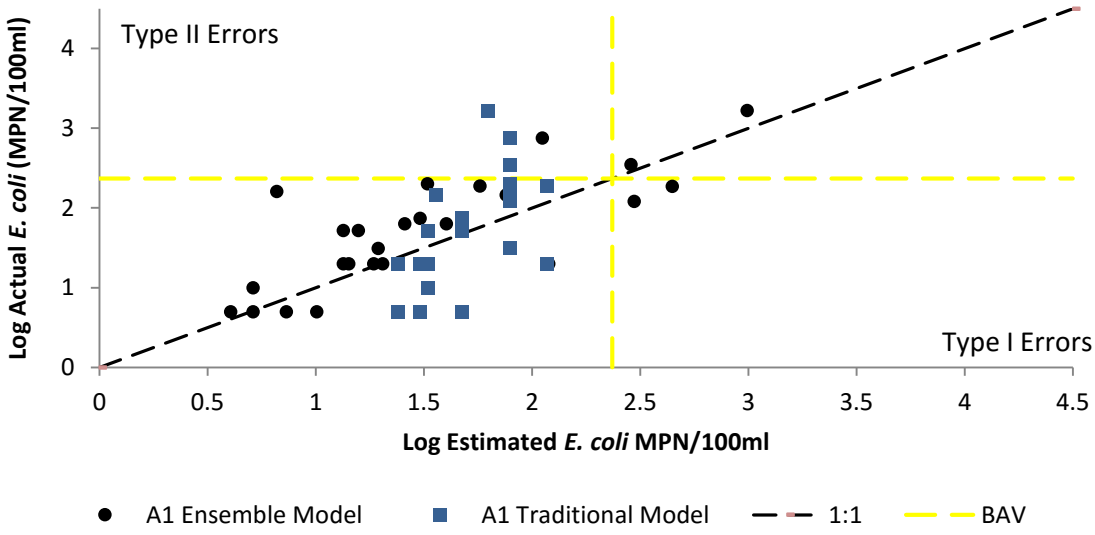


**Figure 30. Ensemble and traditional VB MLR location specific models compared to actual verification set *E. coli* data at location A1 (n=25). Data in upper right quadrant, upper left quadrant, lower left quadrant and lower right quadrant represent accurate predictions of exceedances, Type II errors, accurate predictions of non-exceedances and Type I errors, respectively.**

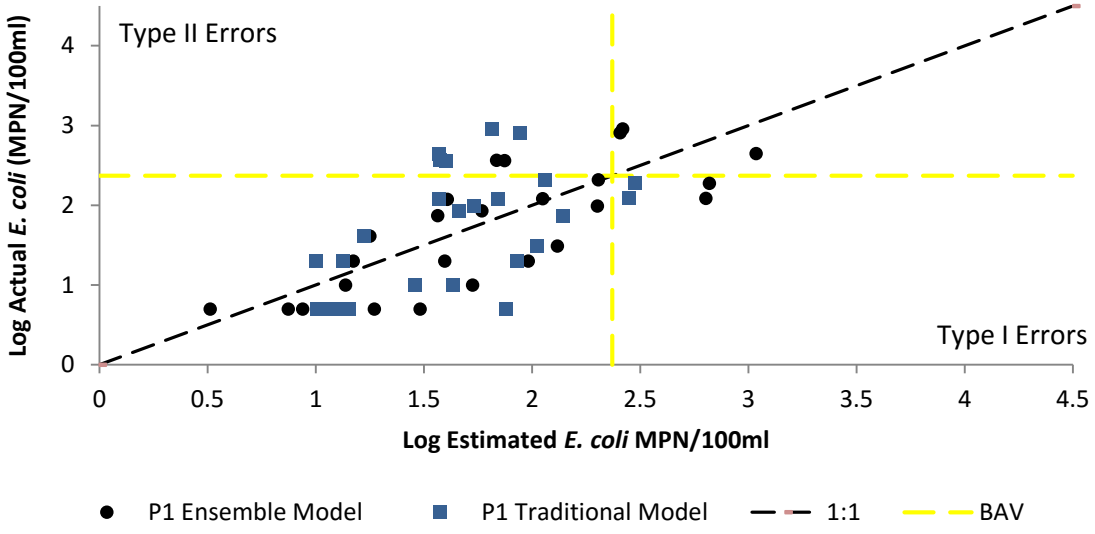


**Figure 31. Ensemble and traditional VB MLR location specific models compared to actual verification set *E. coli* data at location P1 (n=25). Data in upper right quadrant, upper left quadrant, lower left quadrant and lower right quadrant represent accurate predictions of exceedances, Type II errors, accurate predictions of non-exceedances and Type I errors, respectively.**

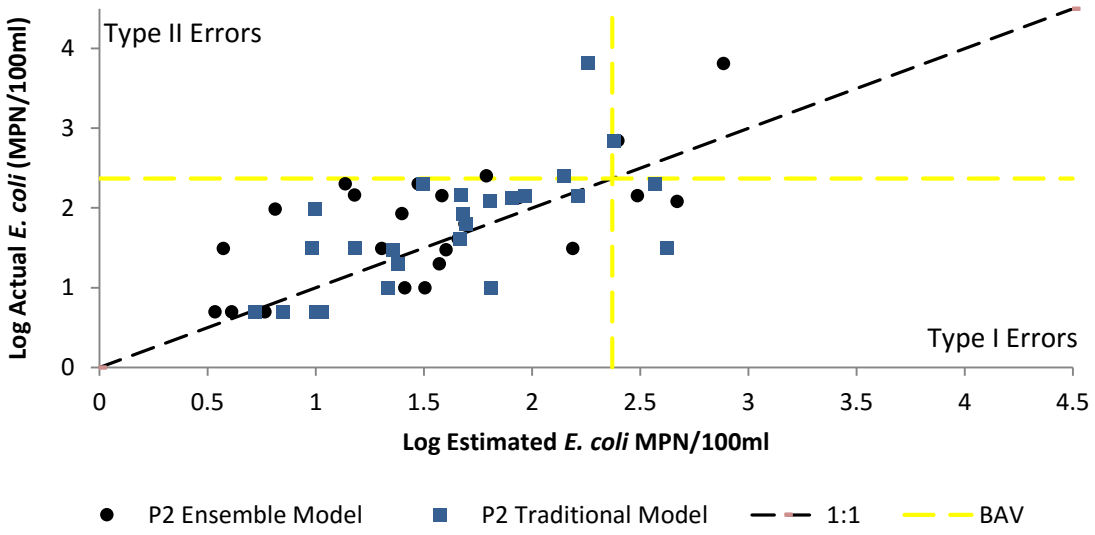


**Figure 32. Ensemble and traditional VB MLR location specific models compared to actual verification set *E. coli* data at location P2 (n=25). Data in upper right quadrant, upper left quadrant, lower left quadrant and lower right quadrant represent accurate predictions of exceedances, Type II errors, accurate predictions of non-exceedances and Type I errors, respectively.**

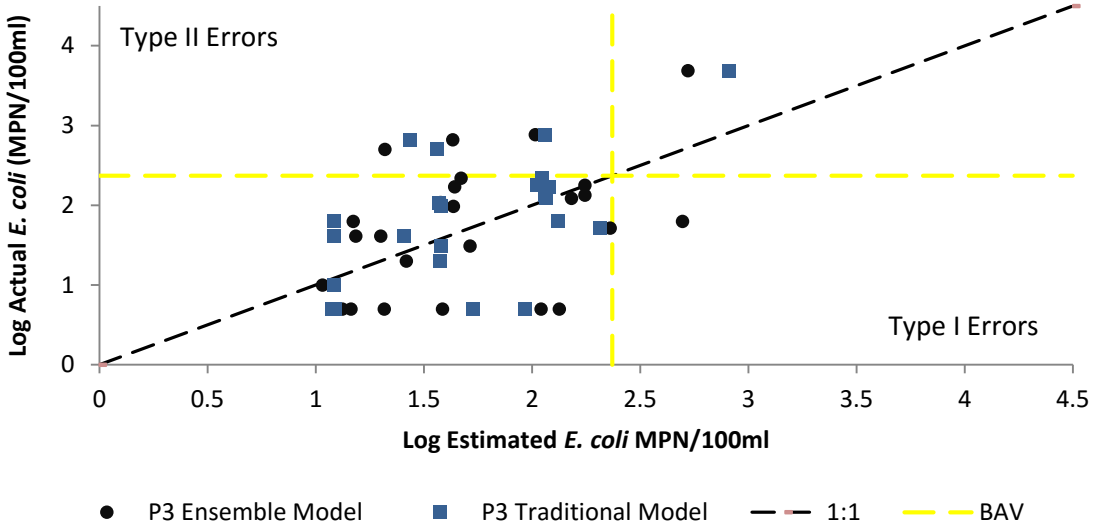


**Figure 33. Ensemble and traditional VB MLR location specific models compared to actual verification set *E. coli* data at location P3 (n=25). Data in upper right quadrant, upper left quadrant, lower left quadrant and lower right quadrant represent accurate predictions of exceedances, Type II errors, accurate predictions of non-exceedances and Type I errors, respectively.**

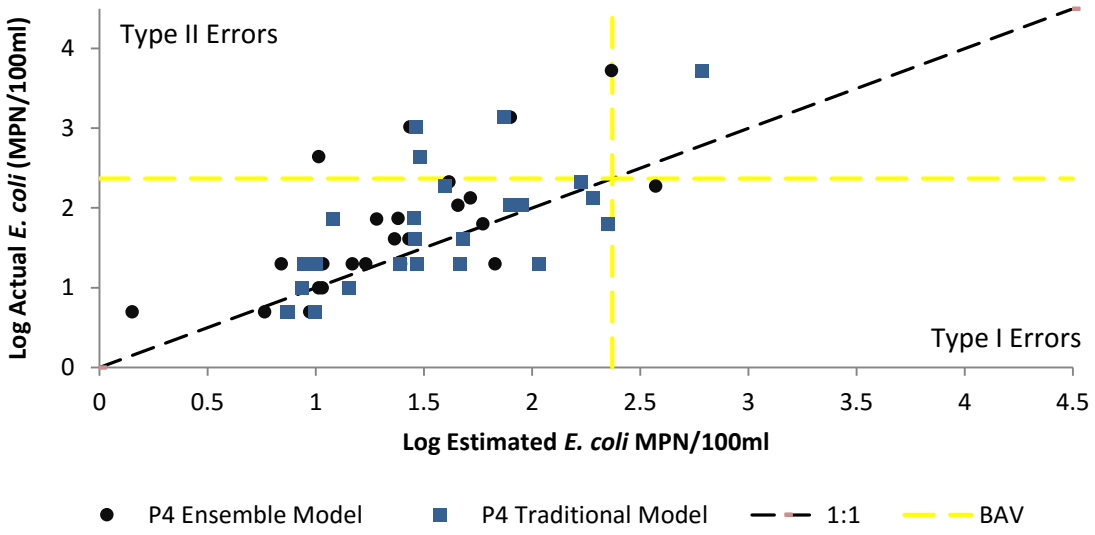


**Figure 34. Ensemble and traditional VB MLR location specific models compared to actual verification set *E. coli* data at location P4 (n=25). Data in upper right quadrant, upper left quadrant, lower left quadrant and lower right quadrant represent accurate predictions of exceedances, Type II errors, accurate predictions of non-exceedances and Type I errors, respectively.**

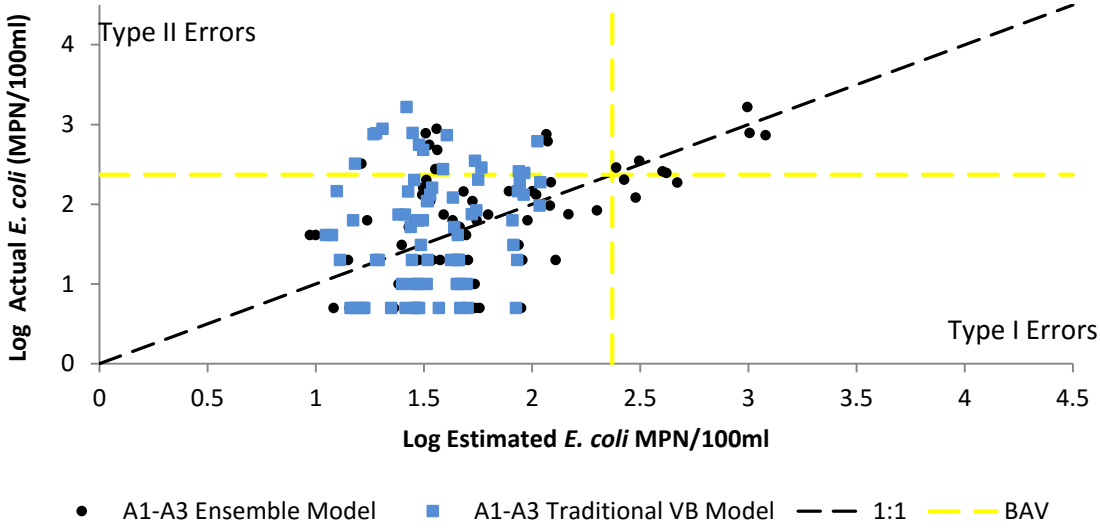


**Figure 35. Ensemble and traditional VB MLR composite models compared to actual verification set *E. coli* data at location A1-A3 (n=75). Data in upper right quadrant, upper left quadrant, lower left quadrant and lower right quadrant represent accurate predictions of exceedances, Type II errors, accurate predictions of non-exceedances and Type I errors, respectively.**

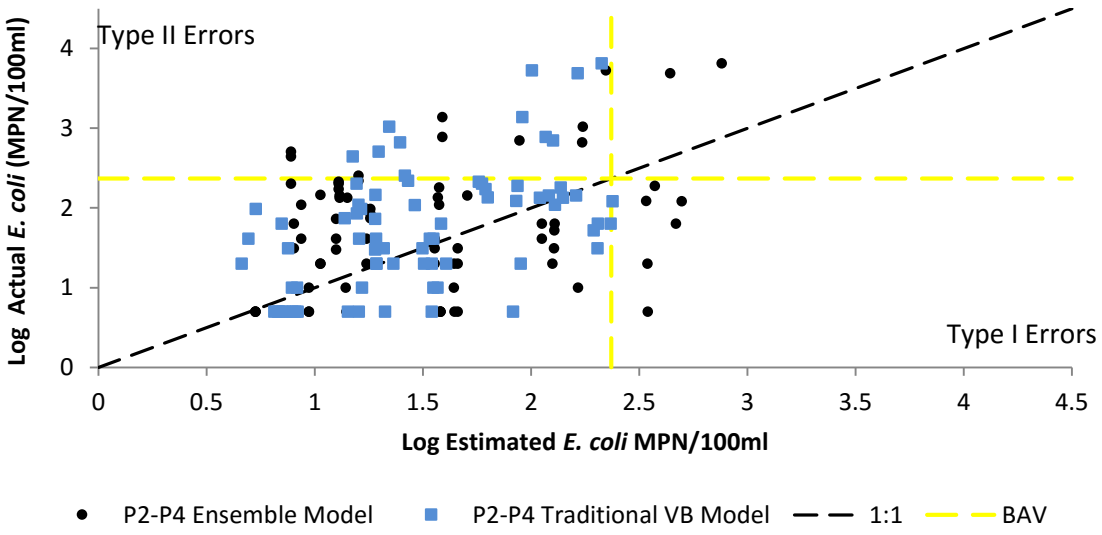


**Figure 36. Ensemble and traditional VB MLR composite models compared to actual verification set *E. coli* data at location P2-P4 (n=75). Data in upper right quadrant, upper left quadrant, lower left quadrant and lower right quadrant represent accurate predictions of exceedances, Type II errors, accurate predictions of non-exceedances and Type I errors, respectively.**

**Table 12. Summary data of model performance for location specific models using verification data set. *Bolded* values indicate which model type had the more optimal performance for the selected statistic (values equal between model types not bolded). Mixing events defined as dates with mixing ratio ≥ 0.01.**

| Performance and comparison between traditional VB MLR and Ensemble location specific predictive models | | | | | | | | |
|---|---|---|---|---|---|---|---|---|
| Traditional VB Predictive Models | | | | | | | | |
| Location | A3 | A2 | A1 | P1 | P2 | P3 | P4 | Overall |
| n | *25* | 25 | 25 | 25 | 25 | *25* | 25 | 175 |
| $R^2$ | ***0.268*** | 0.347 | 0.390 | 0.286 | 0.466 | ***0.399*** | 0.466 | 0.350 |
| RMSE | ***0.640*** | 0.600 | 0.568 | 0.621 | ***0.549*** | ***0.623*** | ***0.599*** | ***0.601*** |
| *E. coli* Exceedances | 7 | 5 | 3 | 5 | 3 | 4 | 4 | 31 |
| Sensitivity | 0.143 | 0.400 | 0.000 | 0.000 | 0.333 | 0.250 | ***0.250*** | 0.194 |
| Specificity | 1.000 | ***1.000*** | ***1.000*** | 0.900 | 0.909 | ***1.000*** | ***1.000*** | ***0.972*** |
| Mixing Events (n) | 15 | 13 | 16 | 12 | 9 | 6 | 8 | 79 |
| Ensemble Predictive Models | | | | | | | | |
| Location | A3 | A2 | A1 | P1 | P2 | P3 | P4 | Overall |
| n | *25* | 25 | 25 | 25 | 25 | *25* | 25 | 175 |
| $R^2$ | 0.234 | ***0.374*** | ***0.609*** | ***0.597*** | ***0.475*** | 0.180 | ***0.478*** | ***0.368*** |
| RMSE | 0.681 | ***0.592*** | ***0.481*** | ***0.475*** | 0.595 | 0.736 | 0.666 | 0.611 |
| *E. coli* Exceedances | 7 | 5 | 3 | 5 | 3 | 4 | 4 | 31 |
| Sensitivity | ***0.429*** | 0.400 | ***0.667*** | ***0.600*** | ***0.667*** | 0.250 | 0.000 | ***0.419*** |
| Specificity | 1.000 | 0.950 | *0.909* | 0.900 | 0.909 | 0.952 | 0.952 | 0.938 |
| Mixing Events (n) | 15 | 13 | 16 | 12 | 9 | 6 | 8 | 79 |

**Table 13. Summary data of model performance for composite models using verification data set. *Bolded* values indicate which model type had the more optimal performance for the selected statistic (values equal between model types not bolded).**

| Performance and comparison between composite traditional VB MLR and Ensemble predictive models | | | |
|---|---|---|---|
| Traditional VB Predictive Models | | | |
| Location | A1-A3 | P2-P4 | Overall |
| n | 75 | 75 | 150 |
| $R^2$ | 0.024 | **0.273** | 0.143 |
| RMSE | 0.731 | **0.708** | ***1.018*** |
| *E. coli* Exceedances | 15 | 11 | 26 |
| Sensitivity | 0.000 | 0.000 | 0.000 |
| Specificity | **1.000** | ***0.984*** | ***0.992*** |
| Mixing Events (n) (Mixing Ratio ≥ 0.01) | 44 | 23 | 67 |
| Ensemble Predictive Models | | | |
| Location | A1-A3 | P2-P4 | Overall |
| n | 75 | 75 | 150 |
| $R^2$ | **0.295** | *0.096* | ***0.155*** |
| RMSE | **0.602** | 0.833 | 1.027 |
| *E. coli* Exceedances | 15 | 11 | 26 |
| Sensitivity | **0.467** | **0.182** | ***0.324*** |
| Specificity | 0.950 | 0.906 | 0.928 |
| Mixing Events (n) (Mixing Ratio ≥ 0.01) | 44 | 23 | 67 |

$R^2$ and RMSE values between modeled and actual log normalized *E. coli* concentrations for traditional VB MLR models using verification set data ranged from 0.268 to 0.466 and 0.549 to 0.640 at Alford and Pennoyer Parks respectively. $R^2$ and RMSE values between modeled and observed log normalized *E. coli* concentrations for ensemble models using verification data ranged from 0.180 to 0.609 and 0.475 to 0.736 at Alford and Pennoyer Parks respectively. Sensitivity ranged from 0.00 to 0.400 and specificity ranged from 0.900 to 1.00 for traditional VB MLR models. Sensitivity ranged from 0.00 to 0.667 and specificity ranged from 0.909 to 1.00 for ensemble models.

### 4.5.4 Comparison of Ensemble and Traditional VB MLR Models

Ensemble location specific models had higher $R^2$ values between modeled and actual *E. coli* concentrations than traditional location specific VB MLR models at five out of seven locations (A2, A1, P1, P2 and P4) and Overall (0.368 vs 0.350). Ensemble models also had a higher or equal sensitivity to traditional VB MLR models at six locations (A3, A2, A1, P1, P2 and P3) and overall (0.419 vs. 0.194).

Traditional VB MLR location specific models had a lower RMSE between actual and modeled *E. coli* concentrations than ensemble location specific models at four locations (A3, P2, P3 and P4) and overall (0.601 vs. 0.611). Traditional VB MLR locations specific models also had greater or equal specificity compared to ensemble locations specific models at all locations and overall (0.972 vs. 0.938).

Overall, composite models had lower $R^2$ values, higher RMSE, lower sensitivity, and similar sensitivity compared to location specific models. For example, traditional composite models for locations A1-A3 and ensemble composite models for locations P2-P4 had $R^2$ values of less than 0.1. Additionally, traditional ensemble models had sensitivity equal to zero. Similar to location specific models, composite ensemble models had higher $R^2$ values, RMSE and sensitivity than traditional models; traditional models had lower specificity.

Difference between model performances are examined on two verification set dates, 7/19/2015 and 5/30/2013 (Figures 37 and 38). On both dates, ensemble models (locations specific and composite models) were able to estimate *E. coli* concentrations exceeding BAV at locations A1-A3 by modeling *E. coli* contributions from the Pike River. Traditional VB models did

not consistently indicate exceedances on these dates. However, neither modeling technique reliably predicted exceedances of BAVs at Pennoyer Park sampling locations on 7/19/2015. Additionally, the ensemble based modeling technique falsely predicted an exceedance at location A2 (location specific and composite) and P3 (Composite model only) on 5/30/2013.

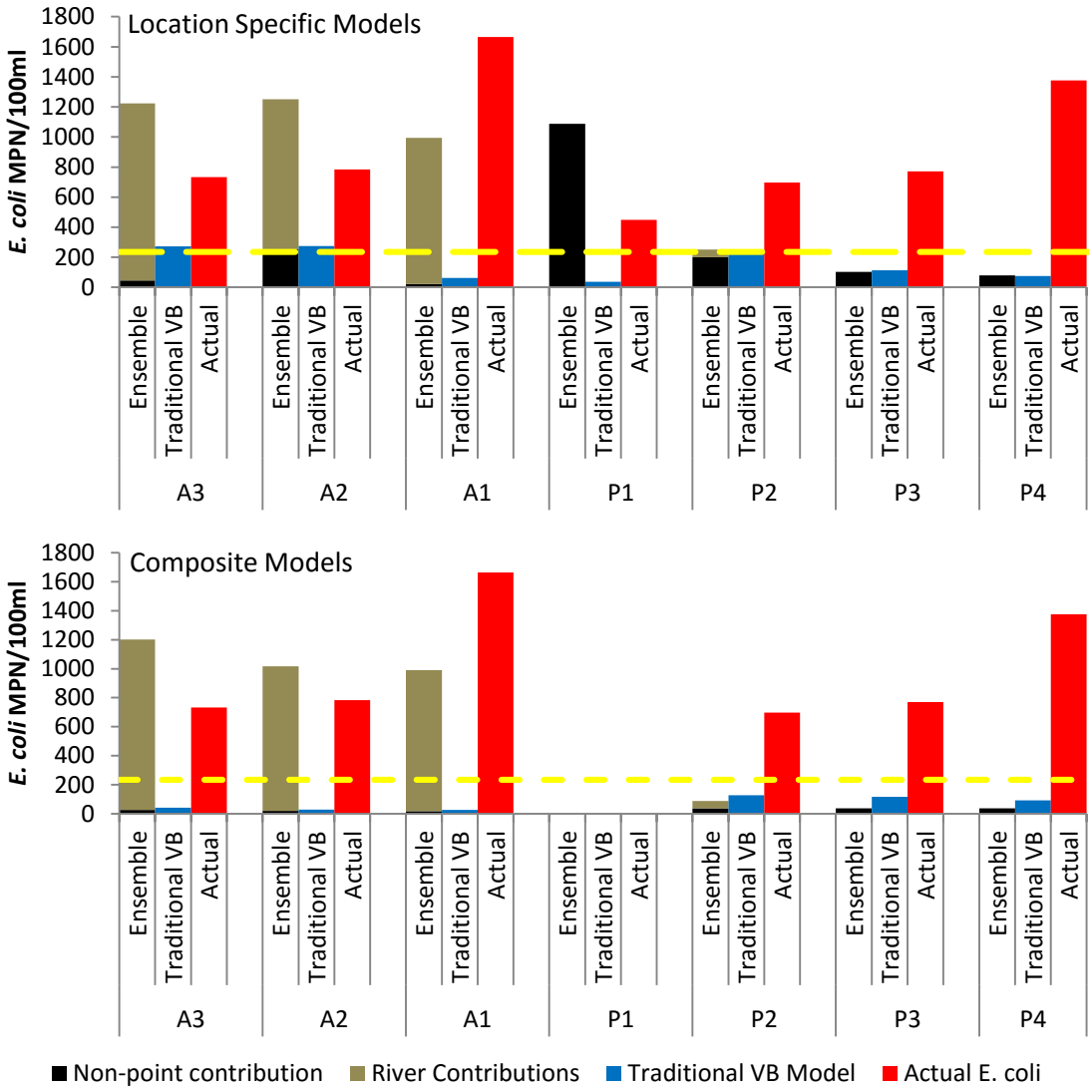


**Figure 37. Comparison between actual *E. coli* concentrations and model predictions on 7/19/2015. Yellow line represents *E. coli* BAV. Ensemble models are show as the sum of the river estimated contribution (W x $C_{PR}$) and non-point contribution ([1-W] x $C_{PC}$).**

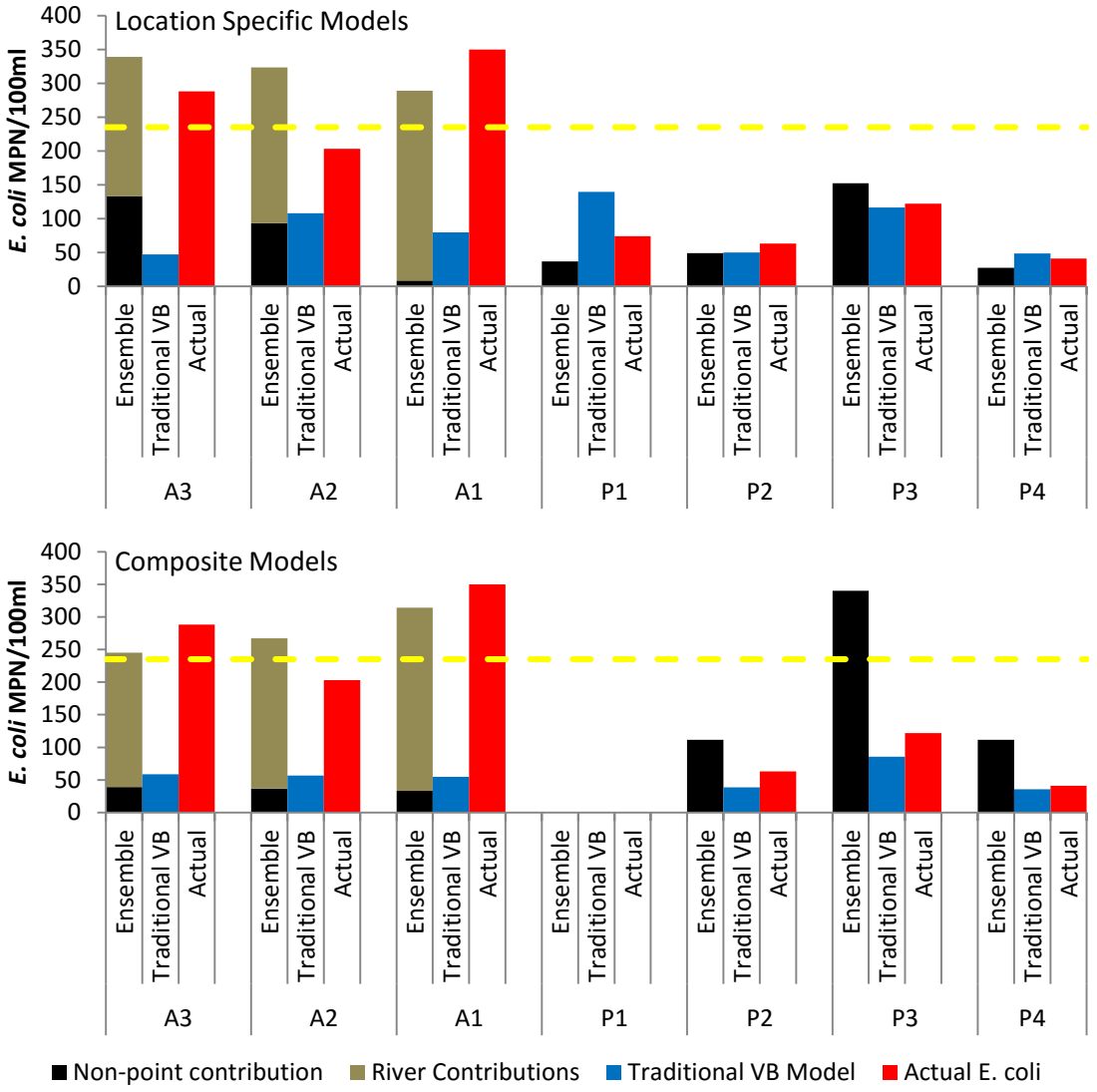


**Figure 38. Comparison between actual *E. coli* concentrations and model predictions on 5/30/2015. Yellow line represents *E. coli* BAV. Ensemble models are show as the sum of the river estimated contribution (W x $C_{PR}$) and non-point contribution ([1-W] x $C_{PC}$).**

In general, the difference in model performance between traditional VB MLR and ensemble models measured by $R^2$ values and RMSE were small, i.e. models had similar performance. The main differences in performance between location specific ensemble and traditional VB models were related to sensitivity and specificity. Ensemble models had a higher sensitivity, but lower specificity.

4.5.5 Model Residuals

Model residuals (actual *E. coli* concentrations minus modeled values) were compared to estimated *E. coli* contributions from the Pike River (actual *E. coli* concentration of the river multiplied by mixing ratio) at each sampling location using the verification data set. There were statistically significant positive correlations between location specific traditional VB MLR model residuals and estimated *E. coli* contributions from the Pike River at locations A3, A2 and A1 (Spearman's Rank correlation, $p<0.05$). There were no statistically significant correlations between model residuals and estimated Pike River *E. coli* contributions for location specific ensemble models ($p>0.05$). There were no correlations between model residuals and estimated Pike River *E. coli* concentrations for Pennoyer Park composite models ($p>0.05$); however, there were positive correlations between model residuals for both ensemble and traditional VB composite models ($p<0.05$). Positive correlations between traditional VB MLR model residuals and estimated *E. coli* contributions from the Pike River indicates traditional VB MLR models failed to account for Pike River *E. coli* contributions. The performance of traditional VB MLR models could be improved by incorporating contributions from the Pike River.

4.5.6 Traditional VB MLR Models with Contributions From the Pike River

Mixing ratios and modeled Pike River *E. coli* concentrations were incorporated into traditional VB MLR models using equation 4 and compared to the verification data set (Table 14-15). Traditional VB models incorporating modeled Pike River *E. coli* concentrations had improved $R^2$ values and lower RMSE for six out of seven location specific models (All locations

except P3) compared to traditional VB MLR models. Similarly, composite models had improved performance measured by $R^2$, RMSE and sensitivity by incorporating modeled Pike River *E. coli* concentrations. Overall, traditional VB models incorporating contributions from the Pike River had high $R^2$ values (location specific: 0.395 vs. 0.350; composite 0.297 vs. 0.143) and lower RMSE (location specific: 0.575 vs. 0.601; composite: 1.027 vs. 0.630). Additionally, all models had higher or equal sensitivities. However, specificity was decreased for five out of seven location specific models (A2, A1, P2, P3 and P4). In comparison to ensemble models, location specific models which incorporated river mixing had higher overall $R^2$ values between modeled and actual *E. coli* concentrations (0.395 vs. 0.368) and lower RMSE (0.575 vs. 0.611).

**Table 14. Summary data for traditional VB location specific models performance incorporation modeled Pike River *E. coli* concentrations using verification data set. *Bolded* values indicate where models out performed traditional VB models (values equal between models not bolded).**

| Location Specific Traditional VB MLR model with modeled Pike River *E. coli* concentrations | | | | | | | | |
|---|---|---|---|---|---|---|---|---|
| Location | A3 | A2 | A1 | P1 | P2 | P3 | P4 | Overall |
| n | 25 | 25 | 25 | 25 | 25 | 25 | 25 | 175 |
| $R^2$ | **0.320** | **0.370** | **0.607** | **0.298** | **0.537** | 0.361 | **0.475** | **0.395** |
| RMSE | **0.598** | **0.595** | **0.483** | **0.617** | **0.501** | 0.638 | **0.576** | **0.575** |
| Sensitivity | **0.429** | 0.400 | **0.667** | 0.000 | **0.667** | 0.250 | 0.250 | **0.355** |
| Specificity | 1.000 | 0.900 | 0.909 | 0.900 | 0.864 | 0.952 | 0.952 | 0.924 |

**Table 15. Summary data for traditional VB composite model performance incorporation modeled Pike River *E. coli* concentrations using verification data set. *Bolded* values indicate where models out performed traditional VB models (values equal between models not bolded).**

| Composite Traditional VB MLR model with modeled Pike River *E. coli* concentrations | | | |
|---|---|---|---|
| Location | A1-A3 | P2-P4 | Overall |
| n | 75 | 75 | 150 |
| $R^2$ | **0.318** | **0.321** | **0.297** |
| RMSE | **0.591** | **0.668** | **0.630** |
| Sensitivity | **0.467** | **0.273** | **0.385** |
| Specificity | 0.950 | 0.953 | 0.952 |

# 5. Discussion

There are two disadvantages to the current use of FIB to gauge recreational water quality: 1) difficulties identifying sources of impairment and conveyance mechanisms resulting in exceedances of water quality standards and 2) the ability to gauge water quality on time scales that are protective of human health. MST techniques have been developed to determine the host origin of FIB. However, the results may not be informative enough to identify the portal of entry if there are multiple conveyance methods which introduce the source of FIB. Near real time analytical techniques have been created. However, high costs and lack of technical expertise prohibit the implementation at many locations. Therefore, statistical based modeling is often used to predict water quality in real time. However, this technique fails to identify the mechanism responsible for elevated FIB.

This study evaluated data elements found within BSS forms to determine their influence on the mixing of the Pike River to coastal waters. Applying this information can make MST more discriminative and aid in the identification of conveyance mechanisms responsible for elevated FIB concentrations. Further, it was investigated whether mixing between river and coastal locations was predictive of river FIB contributions to coastal locations and evaluated applications for predictive models.

Data confirmed that Pike River discharge generally had elevated *E. coli* concentrations and that when it was conveyed to adjacent beaches it served to deteriorate water quality. This was consistent with Koski and Kinzelman (2013). The river also had consistently higher specific conductivity levels than coastal locations, indicating that the mixing of the river into Lake

Michigan coastal waters would imprint elevated specific conductivity levels (which were used to quantify mixing ratios). Similarly, other studies have noted elevated bulk tracer levels in rivers (total dissolved solids and conductivity) compared to coastal locations within the Great Lakes (Visocky, 1977; Harvey, 1995). Therefore, techniques used in this study to quantify the mixing of the Pike River into coastal waters may be valid at other locations.

## 5.1 Accuracy and Precision of Mixing Ratio Calculations

Mixing calculations assume constant specific conductivity levels across the study area on each date except for changes caused by river mixing. However, specific conductivity values were higher near the mouth of the river on days when discharge was blocked by a sandbar. The elevated levels near the mouth are likely related to the river becoming a losing stream as it enters the sandy areas near the beach. This results in a greater horizontal gradient to the water table in the areas near the river, increasing groundwater exfiltration to the lake. As groundwater has a higher specific conductivity values than the lake, the increased groundwater exfiltration results in elevated coastal levels in the vicinity of the Pike River. Similarly, stormwater outfalls and/or infiltration basins located at Alford and Pennoyer Park may cause disturbances to the groundwater table and induce non-uniform exfiltration when flowing, i.e. following precipitation events. Localized (non-uniform) groundwater exfiltration increases specific conductivity levels at coastal locations, which calculations treat as river mixing, therefore, creating accuracy errors.

Mixing calculations also assume a large difference in tracer levels/concentrations between the source and receiving body. In this study it was found that the specific conductivity level of the river decreased following precipitation events. Trends of decreasing specific

conductivity levels in rivers following precipitation have been noted in other Great Lakes studies (Haack et al, 2003). Because of this phenomenon, the ability to make precise measurements was decreased following precipitation due to the lesser difference in source and background specific conductivity levels. This was somewhat troublesome as Pike River *E. coli* concentration increases with discharge volume i.e. following precipitation events. During this study, the maximum observed *E. coli* concentration in the river was 24,192 MPN/100 ml. Under these conditions, a mixing ratio of less than one percent, the lower bounds of quantification, would result in coastal *E. coli* concentrations above the BAV. Therefore, the ability to measure mixing ratios is decreased at times when precise measurements are required.

Precision and accuracy errors may be reduced by measuring multiple tracers, as recommended by Schemel et al (2006), or using tracers that are unique to the source being evaluated and are less likely to be found within groundwater.

## 5.2 Factors Influencing the Direction and Magnitude of Mixing

The analysis of mixing ratio data determined factors associated with the blending of river discharge into coastal water. These factors included spatial variation, longshore current direction, wind direction and volume of river discharge. Collectively, these variables are currently captured through the BSS process at many beaches. Therefore, data is widely available and is currently being used. While studies have concluded environmental factors can affect the distribution of fecal contamination from point sources, none are known to directly quantify the degree of mixing of the source into recreational surface waters (Nevers et al, 2007).

### 5.2.1 Spatial Variability

In this study it was found that the frequency and magnitude of mixing was greater at sampling locations to the south of the Pike River compared to the north. Factors that explain the directionally of river mixing were not predictive of this result (i.e. longshore current and wind direction). Other factors, not examined within this study, may also explain the directionality of river coastal water mixing favoring southern directions. The Coriolis Effect, which is most pronounced in large scale systems, induces a clockwise rotation to river plumes in the northern hemisphere (Garvine, 1995; Mestres et al, 2007). This would result in more frequent mixing to the south of the Pike River. However, the Coriolis Effect tends to be small, but not insignificant, for systems of the size studied and plume dynamics are often controlled by prevailing winds (Mestres et al, 2007).

In addition to the Coriolis Effect, local coastal infrastructure may influence the dominant direction of mixing. A jetty supports the mouth of the Kenosha Harbor 2.2 km to the south of the Piker River. This jetty extends 200 meters into the lake and may disrupt the strength of longshore currents directed to the north. Demirbilek et al (2009) noted in lab experiments that jetties can turn the direction of the longshore current seaward by 90 degrees, therefore disturbing the longshore currents on opposite sides of a jetty. The current study did not measure flow velocities in the field to verify this hypothesis.

Additionally, there are no engineered structures supporting the mouth of the Pike River. This causes the angle at which the river discharges into the lake to vary rather than being strictly perpendicular. It is possible that the river discharged at an angle directing the flow to

the south more frequently than to the north. The southern angle of the discharge may be strong enough to allow momentum to overcome the net longshore current direction, causing mixing to occur more frequently to the south of the river. Future field studies should evaluate coastal structures and determine their impact on the directionally and magnitude of point source mixing.

This study found the magnitude and frequency of mixing events decreased with increasing distance from the river's mouth with two exceptions. The frequency of mixing events was greater at locations 400 meters north and 650 meters south of the river than closer locations on their same respective sides (by proximity, south or north of the mouth). Stormwater outfalls and/or infiltration basins were located adjacent to these locations. The stormwater outfalls and/or infiltration basins may have caused local groundwater mounding following precipitation events, resulting in non-uniform groundwater exfiltration at these locations. Therefore, the apparent increase in the frequency and magnitude of mixing at locations further from the river's mouth is more likely due to errors in the calculation of the mixing ratio rather than being indicative of increased mixing further from the river. Although mixing decreased with distance from the river, mixing ratios were high enough at all locations (distances within 650 meters of the river mouth) to result in exceedances of BAVs.

### 5.2.2 Longshore Current and Wind Direction

This study evaluated two factors related to the direction of river coastal water mixing, longshore current and wind direction. These factors are interrelated i.e. a consistent wind will cause the longshore current to flow in a similar direction. In this study it was found that river

mixing at distances of 130 meters and more from the river's mouth generally followed the dominant longshore current direction. However, mixing was not influenced by in the same manner at sites in close proximity to the river's mouth. For this river/coastal system, locations in close proximity to the river's mouth (20 meters) may representative the near field area where mixing is controlled by the characteristics of the of the source (e.g. geometry, discharge velocity, orientation), rather than being affected by the circulation properties of the lake (Morelissen et al, 2013). The results of this study are in agreement with past research that examined longshore current directions at locations farther from the river's mouth (≥130 meters) (Ahn et al, 2005).

The dominant wind direction also had significant effects on river/coastal water mixing, e.g. higher mixing to the north of the river's mouth with southerly winds and to the south of the river's mouth with north winds. Interestingly, the size of wind vectors favorable to mixing differed between locations (north and south of the river's mouth). There were more wind directions favorable to river mixing at locations to the south of the river. This difference may be related to factors which are speculated to result in greater mixing at Pennoyer Park than Alford Park, e.g. Coriolis Effect, infrastructure to the south of the beach and the angle at which the river discharges into the lake. This study is in agreement with others who noted the effects of wind on the directionality of plume movements on small scale systems (Mestres et al, 2007; Gaston et al, 2006).

Longshore current and wind directions, collected through BSS, is predictive of the directionality of point source mixing. Thus, environmental factors determined at the time of

sample collection can be used to predict the interactions of a point source of FIB with coastal waters. Using strength of evidence approach, this may inform or discredit a potential conveyance mechanism resulting in impaired water quality. However, in close proximity to a point source, mixing may be controlled by the characteristics of the discharge (e.g. flow, geometry, etc.). These factors may not provide sufficient evidence to indicate a point source is impacting water quality.

### 5.2.3 River Discharge

In this study it was found that higher discharge volumes increased the propensity for mixing to occur to the south of the river. Smaller discharge volumes were associated with longshore currents that favored mixing to the north of the river, which may have limited the detection of significant trends at these locations. This study is agreement with past studies that have noted discharge volumes affect the size of river plumes and increase the area impacted (Mestres et al, 2007; Garvine, 1995, Gaston et al, 2006). It was also found that mixing increased to the south of the river's mouth (20 meters) with unfavorable lake dynamics (northern longshore current) with large discharge volumes. Large discharge volumes may promote bilateral pluming, causing areas to be impacted even with unfavorable longshore current directions (Mestres et al, 2007).

*E. coli* concentrations frequently exceed the BAV at beaches following precipitation events. This is often attributed to surface runoff, containing elevated levels of FIB (Clary et al, 2008). This study indicated that high discharge volumes, following precipitation, increased the propensity for point sources of FIB to mix with coastal waters in addition to elevated *E. coli*

concentrations following precipitation. Together, these factors (surface runoff and mixing) explain increases in water quality exceedances following precipitation events.

## 5.3 End Member Mixing Models

Coastal outfalls and rivers often have large variance in *E. coli* concentrations (Clary et al, 2009; Nevers et al, 2007). In order for coastal locations to be effected by these sources, high concentrations of FIB must coincide with mixing. This study evaluated whether the degree of mixing between the Pike River and Lake Michigan coastal waters, along with the *E. coli* concentrations of Pike River, could determine *E. coli* contributions to coastal waters using an end member mixing model. *E. coli* contributions to coastal waters were estimated as the product of measured river *E. coli* concentrations and coastal mixing ratios. The only other known study to employ this technique to estimate environmental *E. coli* concentrations was McLellan et al (2007). However, McLellan et al (2007) measured open water *E. coli* concentrations to determine bacteria disappearance in sewage overflow plumes rather than using this technique as a source tracking tool to determine point source contributions to beaches.

This study found that a two component end member mixing model was able to accurately estimate coastal *E. coli* concentrations when the dominant source of *E. coli* was likely related to the river, but only at distances farther from the river's mouth. Models fit observed coastal *E. coli* concentrations at distances of 130 to 400 meters from the river's mouth and regressions approximated a 1:1 slope indicating limited/no bacteria die off in transit. End member models only included terms describing dilution, not bacteria die off. Therefore, this

study indicated dilution is the dominant disappearance mechanism for *E. coli* in open coastal waters at sites distal from the river's mouth.

Although model fit was lower at 400 m from the river's mouth than at closer distances, it is unclear if this was due to the model being less effective at these distances or if errors associated with non-uniform groundwater exfiltration near the stormwater outfall/infiltration basin caused errors in the mixing calculation, lowering model fit. Therefore, this study was unable to determine an exact distance from the Pike River where the end member models failedto predict coastal *E. coli* contributions. However, other researchers have found the detection of bacteria is minimal at distances above five kilometers due to die-off and dilution (Ahn et al, 2005; McLellan et al, 2007). Corrections may need to be applied to end member models to account for bacteria die off at locations farther from the river's mouth than those examined in this study, i.e those proposed in Carvalho et al (2007).

At sites immediately adjacent to the river's mouth (20 meters), end member mixing model fit observed coastal *E. coli* concentrations poorly. The model generally over predicted observed *E. coli* concentrations as indicated by the slope of the regression between actual and predicted values. Prior to data analysis, it was expected that limited bacterial die off, in transit to this location, would yield the best fit. The poor model fit is likely related to non-uniform groundwater exfiltration resulting in localized elevated specific conductivity levels near the mouth of the river (see section 5.1). Mixing calculations treat these elevated specific conductivity values as river mixing, resulting in the over prediction of Pike River *E. coli* contributions. River water recharging the groundwater system and later exfiltrating into

coastal waters near the mouth of the river was unlikely to contribute a significant amount of FIB as groundwater was found to generally have a low *E. coli* concentration at the study site and similar Lake Michigan locations (Skalbeck et al, 2010; Silva, 2013). Future studies should evaluate the use of alternative tracers when evaluating locations near points of discharge (e.g. non unique sources of the tracer).

There are multiple applications associated with end member mixing model relevant to beach managers. For example, we found the Pike River was responsible for between 12 and 15 percent of exceedances of BAVs at Alford Park and between 26 and 42 percent at Pennoyer Park depending upon location. Additionally, Pike River *E. coli* contributions to coastal waters explained more of the variance of *E. coli* concentrations at locations to the south of the river (Pennoyer Park) than the north (Alford Park). *E. coli* variability and exceedances of BAVs not explained by the river maybe caused by non-point sources such as contribution from sediments, algae, or wildlife (Whitman et al, 2003; Byappanahalli et al, 2007; Englebert et al, 2008; Byappanahalli et al, 2009; Alm et al, 2003; Kinzelman et al, 2004; Beversdorf et al, 2007; Skinner et al, 2010). Determining the influence of point sources of FIB on beach water quality can help to determine outstanding sources of water quality impairment through a subtractive approach (Kinzelman et al, 2009). By quantifying the impact of a point source of bacterial contamination on coastal water quality, restoration projects will have the greatest benefit relative to cost. They can be also be prioritized and objective estimates of the value of restoration can be determined.

## 5.4 Predictive Models

Commonly used bacteria enumeration methods require 18-24 hours to provide results. The time delay between sample collection and the availability and results may expose the public to unsafe swimming conditions. Therefore, there is a need to identify water quality at beaches in real-time. Models are one cost effective solution to provide water quality information in near real-time. Programs such as Virtual Beach provide a low cost and accessible means for regression based model development. However, regression based models generated using these programs may be criticized for their failure to identify mechanistic means for elevated bacteria concentrations. Even with these failures, it has been shown the current use of the persistence model (water quality status based upon previous day's results) fails to adequately protect public health due to most water quality impairments lasting only one day (Leecaster and Weisberg, 2001; Nevers and Whitman, 2011). Regression based models are superior at identifying beach status in real-time in comparison to the persistence model at many locations (Francy et al, 2013).

In order for models to inform the public of water quality, models must be able to accurately predict exceedances and non-exceedances of bacteria standards; IE. models must have high sensitivity and specificity. Francy et al (2013) defined good model performance as sensitivity of 0.50 and above and specificity of 0.85 and above. However, in a study of 43 beaches throughout the Great Lakes, only 17 out of 42 met the criteria for sensitivity; alternatively, 50% of models met the criteria for specificity (Francy et al, 2013). Therefore, challenges in regression based predictive model development are to improve sensitivity and specificity.

This study evaluated the performance of ensemble predictive models in comparison to traditional VB MLR models. Ensemble models estimated coastal *E. coli* concentrations by linking predictive models for coastal *E. coli* concentrations in the absence of river mixing (presumably modeling non-point *E. coli* concentrations) and the Pike River. This modeling approach elucidates river and coastal water interactions which provides a partial explanation for predicted *E. coli* concentrations. Therefore, this approach provides real-time information on the conveyance mechanism resulting in exceedances of water quality standards.

Model variables and performance were consistent with past studies. For example, Nevers et al (2007) found wave height, precipitation, turbidity, wind speed/directions, water temperature, specific conductance and river discharge to be significant factors for predicting *E. coli* concentrations at locations adjacent to a river mouth. Model performance for the river was consistent with results from other studies who found river discharge to be a significant explanatory factor for bacteria concentrations (Brauewere et al 2014; David and Haggard, 2011).

This study found that integrating modeled Pike River *E. coli* contributions into coastal models (traditional VB or ensemble; location specific models or composite models) improved performance. Traditional VB models, incorporating modeled Pike River *E. coli* concentrations, had improved fit in comparison to traditional VB models for $R^2$, RMSE, and sensitivity, but with lower sensitivity. Ensemble models also had much higher sensitivity than traditional VB MLR models, but with lower specificity. Higher sensitivity indicates this modeling approach is more protective of public health than traditional VB MLR models. However, lower specificity will

have negative economic repercussions at areas which rely upon tourism due to more Type I errors (Rabinovici et al, 2004). Additionally, location specific models had better model performance than composite models as measured by $R^2$, RMSE, and sensitivity.

Traditional VB models were not able to account for Pike River *E. coli* contributions at locations to the north of the river, as evidenced by model residuals. This may have been a function of the way the data was split between training and verification sets. The verification set contained a higher fraction of mixing events compared to the training set at the northern sampling locations (Alford Park). If traditional VB predictive models generally fail to account for the influence of point sources, improved modeling techniques are required, such as the ensemble approach used in this study. Future research is needed on this subject.

# 6. Conclusions

This study sought to identify conditions favorable to the mixing of the Pike River into Lake Michigan coastal waters, identify the associated impact of the river on coastal *E. coli* concentrations and use this information to more accurately gauge water quality in real-time through predictive models. Environmental factors that appear on EPA's Great Lake Beach Sanitary Surveys were explanatory for the directionality and magnitude of mixing between these two water bodies. Adjacent beaches were impacted by river discharge based on prevailing winds and longshore current, however in some cases there was mixing close to the river mouth regardless of weather and hydrological factors. Mixing ratios and Pike River *E. coli* concentrations were able to accurately predict the concentration of *E. coli* at coastal locations greater than 20m from the river's mouth. Models predictive of *E. coli*, which used mixing ratios as a mechanistic link to join coastal and river models, achieved greater sensitivity in comparison to traditional VB MLR models. Quantifying mixing of river effluent into coastal waters validates their influence as a point source of pollution and improves the ability to accurately predict recreational water quality in real time. Evaluating the degree of mixing between coastal waters and point sources of bacterial contamination therefore has the potential to improve public health protection by providing information resulting in better beach management.

# 7. Works Cited


Ahn, J. H., Grant, S. B., Surbeck, C. Q., Digiacomo, P. M., Nezlin, N. P., and Jiang, S. (2005). Coastal water quality impact of stormwater runoff from an urban watershed in southern California. *Environmental Science and Technology, 39 (16)* , 5940-5953.

Alm, E. W., Burke, J., and Spain, A. (2003). Fecal indicator bacteria are abundant in wet sand at freshwater beaches. *Water Research, 37 (16)* , 3978-3982.

Beaches Environmental Assesment and Coastal Health Act of 2000, 114 U.S.C. § 870 (2000).

Beversdorf, L. J., Bornstein-Forst, S. M., and McLellan, S. L. (2007). The potential for beach sand to serve as a reservoir forEscherichia coli and the physical influences on cell die-off. *Journal of Applied Microbiology, 102 (5)* , 1372-1381.

Brauwere, A. D., Ouattara, N. K., and Servais, P. (2014). Modeling fecal indicator bacteria concentrations in natural surface waters: a review. *Critical Reveiws in Environmental Science and Technology, 44 (21)* , 2380-2453.

Byappanahalli, M. N., Sawdey, R., Ishii, S., Shively, D. A., Ferguson, J. A., Whitman, R. L., et al. (2009). Seasonal stability of Cladophora-associated Salmonella in Lake Michigan watersheds. *Water Research, 43 (3)* , 806-814.

Byappanahalli, M. N., Whitman, R. L., Shively, D. A., Ferguson, J. I., and Sadowsky, M. J. (2007). Population structure of Cladophora-borne E. coli in nearshore water of Lake Michigan. *Water Research, 41 (16)* , 3649-3654.

Carvalho, J. L., Feitosa, R. C., Rosman, P. C., and Roberts, P. J. (2006). A bacterial Decay Model for Coastal Outfall Plumes. *Journal of Coastal Research, Special Issue 39* , 1524-1528.

Clary, J., Jones, J., Urbonas, B. Q., Strecker, E., and Wagner, T. (2008). Can Stormwater BMPs Remove Bacteria? New Findings from the International Stormwater BMP Database. *At Press for Publication in Stormwater Magazine May/June 2008* , 1-14.

Coffey, R., Cummins, E., O'Flaherty, V., and Cormican, M. (2010). Pathogen sources estimation and scenario analysis using the soil and water assessment tool (SWAT). *Human and Ecological Risk Assessment, 16 (4)* , 913-933.

Craun, G. F., Calderon, R. L., and Craun, M. F. (2005). Outbreaks associated with recreational water in the United States. *International Journal of Environmental Health Research, 15 (4)* , 243-262.

Crowe, A. S., and Meek, G. A. (2009). Groundwater conditions beneath beaches of Lake Huron, Ontario, Canada. *Aquatic Ecosystem and Health Management, 12 (4)* , 444-455.

David, M. M., and Haggard, B. E. (2011). Development of Regression-Based Models to Predict Fecal Bacteria Numbers at Select Sites within the Illinois River Watershed, Arkansas and Oklahoma, USA. *Water Air Soil Pollution, 215* , 525-547.

Demirbilek, Z., Lin, L., Seabergh, W. C., Mase, H., and Sheng, J. (2009). Laboratory and numerical studies of hydrodynamics near jetties. *Coastal Engineering Journal, 51 (2)* , 143-175.

Dick, L. K., and Field, K. G. (2004). Rapid Estimation of Numbers of Fecal Bacteroides by Use of a Quantitative PCR Assay for 16S rRNA Genes. *Applied and Environmental Microbiology, 70 (9)* , 5695-5697.

Dufour, A. P. (1984). *Health Effects Criteria for Fresh Recreational Waters.* Washington, DC: United States Environmental Protection Agency .

Englebert, E. T., Mcdermott, C., and Kleinheinz, G. T. (2008). Effects of the nuisance algae, Cladophora, on Escherichia coli at recreation beaches in Wisconsin. *Science of the Total Environment, 404 (1)* , 10-17.

Environment Canada and United States Environmental Protection Agency (SOLEC). (2009). *State of the Great Lakes 2009.* Available at: (http://www.epa.gov/solec/sogl2009/sogl2009complete.pdf).

Field, K. (2008). Microbial source tracking: its utility and limitations toward the protection of recreational waters in the Great Lakes basin. *Great Lakes Science Advisory Board Priorities 2005-2007* , 59-65.

Francy, D. S., Amie, B. M., Carvin, R. B., Corsi, S. R., Fuller, L. M., Harrison, J. H., et al. (2013). *Developing and Implementing Predictive Models for Estimating Recreational Water Quality at Great Lake Beaches: Scientific Investigations Report 2013-5166.* Reston, Virginia: United States Geological Survey.

Frick, W. E., Ge, Z., and Zepp, R. G. (2008). Nowcasting and forecasting concentrations of biological contaminants at beaches: a feasibility and case study. *Environmental Science and Technology, 42 (13)* , 4818-4824.

Fujioka, R. S., Hashimoto, H. H., Siwak, E. B., and Young, R. H. (1981). Effect of sunlight on survival of indicator bacteria in seawater. *Appl Environ Microbiol, 41 (3)* , 690-696.

Garcia-Armisen, T., Thoucenin, B., and Servais, P. (2006). Modelling faecal coliforms dynamics in the Seine Estuary, France. *Water Science and Technology, 54 (3)* , 177-184.

Garvine, R. W. (1995). A dynamical system for classifying buoyant coastal discharges. *Continental Shelf Research, 15 (13)* , 1585-1596.

Gaston, T. F., Schlacher, T. A., and Connolly, R. M. (2006). Flood discharges of a small river into open coastal waters: Plume traits and material fate. *Estuarine, Coastal and Shelf Science, 69* , 4-9.

Ge, Z., Nevers, M. B., Schwab, D. J., and Whitman, R. L. (2010). Coastal loading and transport of Escherichia coli at an embayed beach in Lake Michigan. *Environmental Science and Technology, 44 (17)* , 6731-6737.

Haack, S. K., Fogarty, L. R., and Wright, C. (2003). Escherichia coli and Enterococci at Beaches in the Grand Traverse Bay, Lake Michigan: Sources, Characteristics, and Environmental Pathways. *Environmental Science and Technology, 37 (15)* , 3275-3282.

Harvey, F. E. (1995). *Evaluation and development of methods for hydrogeologic studies in deep lakes: Applications in the Hamilton Harbour, Western Lake Ontario, Ph.D. thesis.* Waterloo, Ontario, Canada: Department of Earth Science, University of Waterloo.

Harvey, F. E., Lee, D. R., Rudolph, D. L., and Frape, S. K. (1997). Locating groundwater discharge in large lakes using bottom sediment electrical conductivity mapping. *Water Resources Research, (33) 11* , 2609-2615.

Hellweger, F. L. (2007). Ensemble modeling of E. coli in the Charles River, Boston, Massachusetts, USA. *Water Science and Technology, 56 (6)* , 39-46.

Houston, J. R. (2008). The economic value of beaches -- A 2008 update. *Shore and Beach, 76 (3)* , 22-26.

IDEXX. (2013). *Colilert-18 Procedure.* Retrieved December 1st, 2014, from IDEXX: https://www.idexx.com/resource-library/water/colilert-18-procedure-en.pdf

Ishii, S., Ksoll, W. B., Hicks, R. E., and Sadowsky, M. J. (2006). Presence and growth of naturalized Escherichia coli in temperate soils from Lake Superior watersheds. *American Society for Microbiology 72 (1)* , 612–621.

Jamieson, R. C., Joy, D. M., Lee, H., Kostaschuk, R., and Gordon, R. J. (2005). Resuspension of sediment-associated Escherichia coli in a natural stream. *Journal of Environmental Quality, 34 (2)* , 581-589.

Kinzelman, J. L., and Mclellan, S. L. (2009). Success of science-based best management practices in reducing swimming bans--a case study from Racine, Wisconsin, USA. *Aquatic Ecosystem Health and Management, 12 (2)* , 187-196.

Kinzelman, J., McLellan, S. L., Daniels, A. D., Cashin, S., Singh, A., Gradus, S., et al. (2004). Non-point source pollution: Determination of replication versus persistence of Escherichia coli in surface water and sediments with correlation of levels to readily measurable environmental parameters. *Journal of Water and Health, 2 (2)* , 103-114.

Koski, A. J., and Kinzelman, J. L. (2013). *Recreational Water Quality Along Kenosha's Fresh Coast - GLRI Beach Sanitary Survey Project - Data report 2010-2012.* Racine, WI: City of Racine.

Kovatch, C. (2006). Proceedings of the USEPA National Beaches Conference. Niagara Falls, NY, October 11-13th, 2006.

Leecaster, M. K., and Weisberg, S. B. (2001). Effect of sampling frequency on shoreline microbiology assessments. *Marine Pollution Bulletin, 42 (11)* , 1150-1154.

Matsubayashi, U., T, V. G., and Takag, F. (1993). Hydrograph separation and flow analysis by specific electrical conductance of water. *Journal of Hydrology, 152 (1-4)* , 179-199.

McLellan, S. L., Hollis, E. J., Depas, M. M., Van Dyke, M., Harris, J., and Scopel, C. O. (2007). Distribution and Fate of Escherichia coli in Lake Michigan following Contamination with Urban Stormwater and Combined Sewer Overflows. *Journal of Great Lakes Research, 33 (3)* , 566-580.

Mestres, M., Sanchez-Arcilla, A., and Sierra, J. P. (2007). Modeled Dynamics of a Small-scale River Plume under Different Forcing Conditions. *Journal of Coastal Research, 47* , 84-96.

Morelissen, R., Kaaij, T., and Bleninger, T. (2013). Dynamic coupling of near field and far field models for simulating effluent discharges. *Water Science and Technology, 67 (10)* , 2210-2220.

Nevers, M. B., and Whitman, R. L. (2011). Efficacy of monitoring and empirical predictive modeling at improving public health protection at Chicago beaches. *Water Research, 45 (4)* , 1659-1668.

Nevers, M. B., and Whitman, R. L. (2005). Nowcast modeling of Escherichia coli concentrations at multiple urban beaches of southern Lake Michigan. *Water Research, 39 (20)* , 5250–5260.

Nevers, M. B., Whitman, R. L., Frick, W. E., and Ge, Z. (2007). Interaction and influence of two creeks on Escherichia coli concentrations of nearby beaches: Exploration of predictability and mechanisms. *Journal of Environmental Quality, (36) 5* , 1338-1345.

Rabinovici, S. J., Bernknopf, R. L., Wein, A. M., Coursey, D. L., and Whitman, R. L. (2004). Economic and health risk trade-offs of swim closures at a Lake Michigan Beach. *Environmental Science and Technology, 38 (10)* , 2737-2745.

Schemel, L. E., Cox, M. H., Runkel, R. L., and Kimball, B. A. (2006). Multiple injected and natural conservative tracers quantify mixing in a stream confluence affected by acid mine drainage near Silverton, Colorado. *Hydrological Processes, 20 (13)* , 2727-2743.

Schillinger, J. E., and Gannon, J. J. (1985). Bacterial adsorption and suspended particles in urban stormwater. *Water Pollution Control Federation, 57 (5)* , 384-389.

Schueler, T. and Holland, H. (Eds.). (2000). Microbes and urban watersheds: ways to kill 'em, Article 67. In *The Practise of Watershed Protection, 3 (1)* (pp. 566-574). Ellicott City, MD: Center for Watershed Protection.

Seyfried, P. L., Tobin, R. S., Brown, N. E., and Ness, P. F. (1985). A prospective study of swimming-related illness: I. swimming-associated health risk. *American Journal of Public Health, 75 (9)* , 1068-1070.

Shannon, K. E., Lee, D. Y., Trevors, J. T., and Beaudette, L. A. (2007). Application of real-time quantitative PCR for the detection of selected pathogens during municipal wastewater treatment. *Science of the Total Environment, 328 (1)* , 121-129.

Silva, M. R. (2013). *An Integrative Investigation of Sources, Fate, and Transport of Bacteria in Milwaukee Coastal Beaches.* Milwaukee, WI: University of Wisconsin Milwaukee School of Engineering.

Skalbeck, J. D., Kinzelman, J. L., and Mayer, G. C. (2010). Fecal indicator organism density in beach sands: Impact of sediment grain size, uniformity, and hydrologic factors on surface water loading. *Journal of Great Lakes Research, 36 (4)* , 217-218.

Skinner, J. F., Guzman, J., and Kappeler, J. (2010). Regrowth of entrococci and fecal coliform in biofilm. *Stormwater, July/August* , Available Online: http://www.stormh2o.com/july-august-2010/regrowth-enterococci-fecalcoliform.aspx.

*Standard Methods for the Examination of Water and Wastewater, 21st Edition.* In Section 9223 B (2005).

Thompson, P. D. (1977). How to Improve Accuracy by Combining Independent Forecasts. *Monthly Weather Review, 105* , 228-229.

United States Environmental Protection Agency (US EPA). (1986). *Ambient Water Quality for Bacteria.* Washington, D.C.: United States Environmental Protection Agency.

United States Environmental Protection Agency (US EPA). (2014, August 7th). *Beach Sanitary Surveys*. Retrieved December 1st, 2014, from United States Environmental Protection Agency: http://www2.epa.gov/beach-tech/beach-sanitary-surveys

United States Environmental Protection Agency (US EPA). (2011, June 5th). *National Summary of Impaired Waters and TMDL Information*. Retrieved June 5TH, 2011, from Watershed Assessment, Tracking and Environmental Results: http://iaspub.epa.gov/waters10/attains_nation_cy.control?p_report_type=T

United States Environmental Protection Agency (US EPA). (2012). *Recreational Water Quality Criteria.* Available online at: http://water.epa.gov/scitech/swguidance/standards/criteria/health/recreation/upload/RWQC2012.pdf. Washington, DC: Office of Water.

United States Environmental Protection Agency (US EPA). (2013). *Virtual Beach 3.0.* Athens, GA: Center for Exposure Assessment Modeling.

United States Geological Survey (USGS). (2007). *Chemical and hydrologic data from the Cement Creek and Upper Animas River confluence and mixing zone, Silverton, Colorado, September 1997 - Open Report 2007-1048.* Reston, Virginia: US Department of the Interior/ US Geological Survey.

United States Geological Survey (USGS). (2013). *Developing and implementing predictive models for estimating recreational water quality at Great Lake beaches.* Reston, Virginia: United States Department of the Interior and United States Geological Survey.

Visocky, A. P. (1977). *Hydrologic study of Illinois Beach State Park.* Urbana, IL: Illinois State Water Survey.

Whitman, R. L., and Nevers, M. B. (2003). Foreshore sand as a source of Escherichia Coli in nearshore water of a Lake Michigan Beach. *Applied and Environmental Microbiology, 69 (9)* , 5555-5562.

Whitman, R. L., Shively, D. A., Pawlik, H., Nevers, M. B., and Byappanahalli, M. N. (2003). Occurrence of Escherichia coli and Enterococci in Cladophora (Chlorophyta) in nearshore water and beach sand of Lake Michigan. *Applied and Environmental Microbiology, 69 (8)* , 4714–4719.

Wu, J., Rees, P., Storrer, S., Alderisio, K., and Dorner, S. (2009). Fate and transport modeling of potential pathogens: The contribution from sediments. *Journal of the American Water Resources Association, 45 (1)* , 35-44.

## Appendix A: Correlations Between *E. coli* and Specific Conductivity

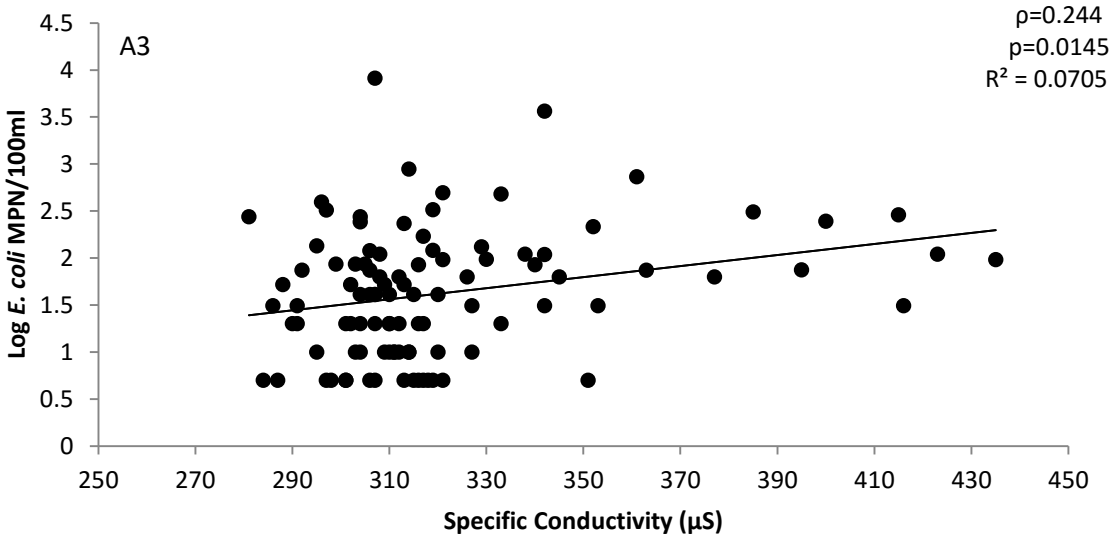


Correlation between specific conductivity (µS) and *E. coli* (MPN/100 ml) at location A3 (n=100). See section 4.4.2 for correlation between estimated river *E. coli* contributions to coastal waters and actual coastal *E. coli* concentrations.

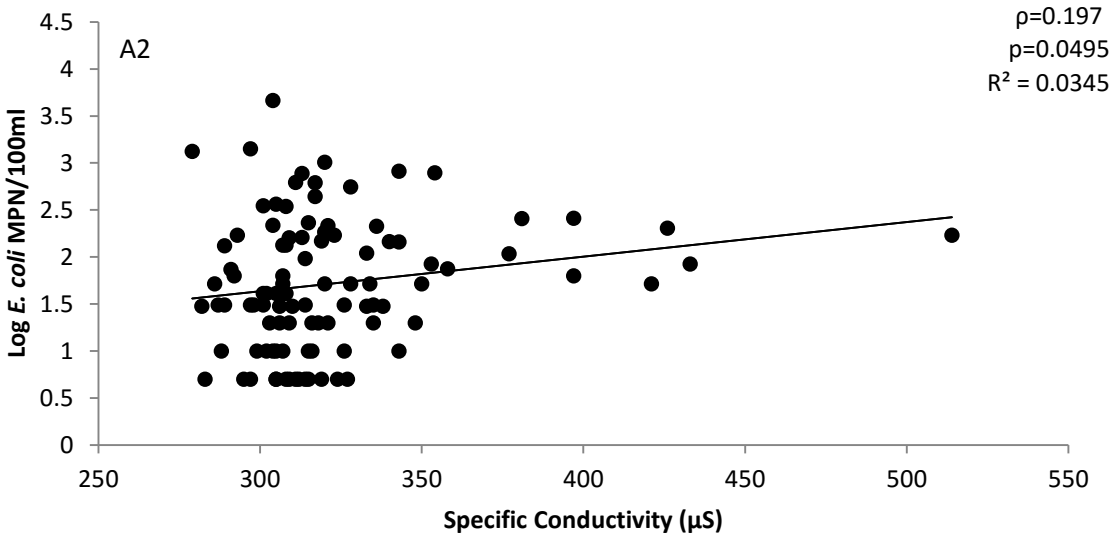


Correlation between specific conductivity (µS) and *E. coli* (MPN/100 ml) at location A2 (n=100). See section 4.4.2 for correlation between estimated river *E. coli* contributions to coastal waters and actual coastal *E. coli* concentrations.

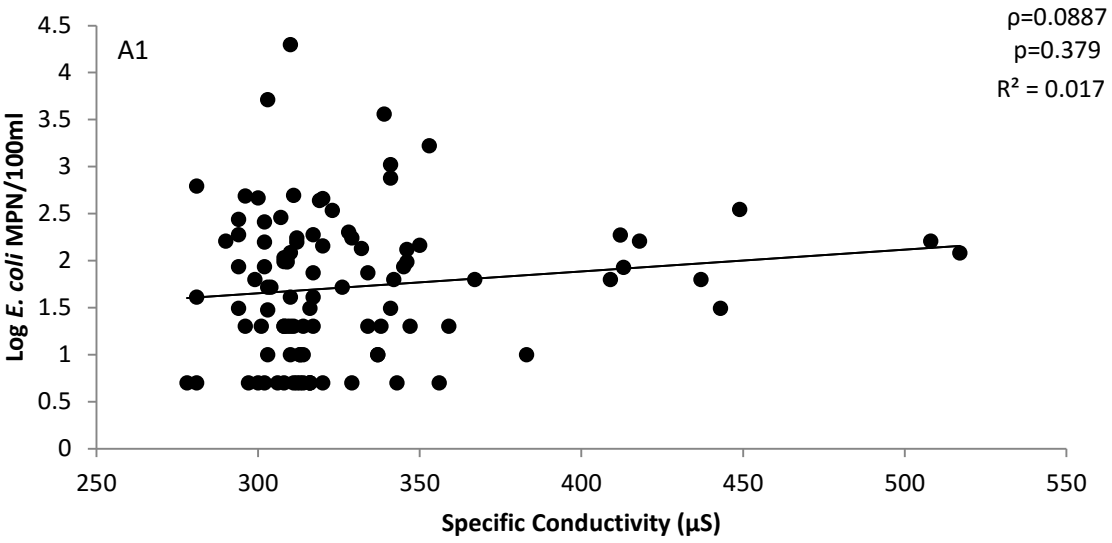


Correlation between specific conductivity (µS) and *E. coli* (MPN/100 ml) at location A1 (n=100). See section 4.4.2 for correlation between estimated river *E. coli* contributions to coastal waters and actual coastal *E. coli* concentrations.

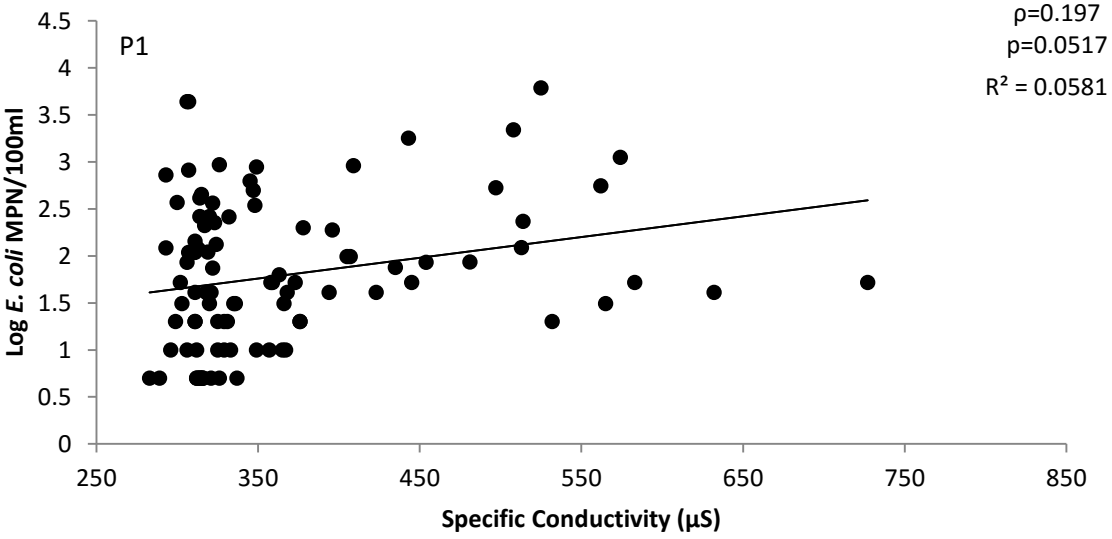


Correlation between specific conductivity (µS) and *E. coli* (MPN/100 ml) at location P1 (n=98). See section 4.4.2 for correlation between estimated river *E. coli* contributions to coastal waters and actual coastal *E. coli* concentrations.

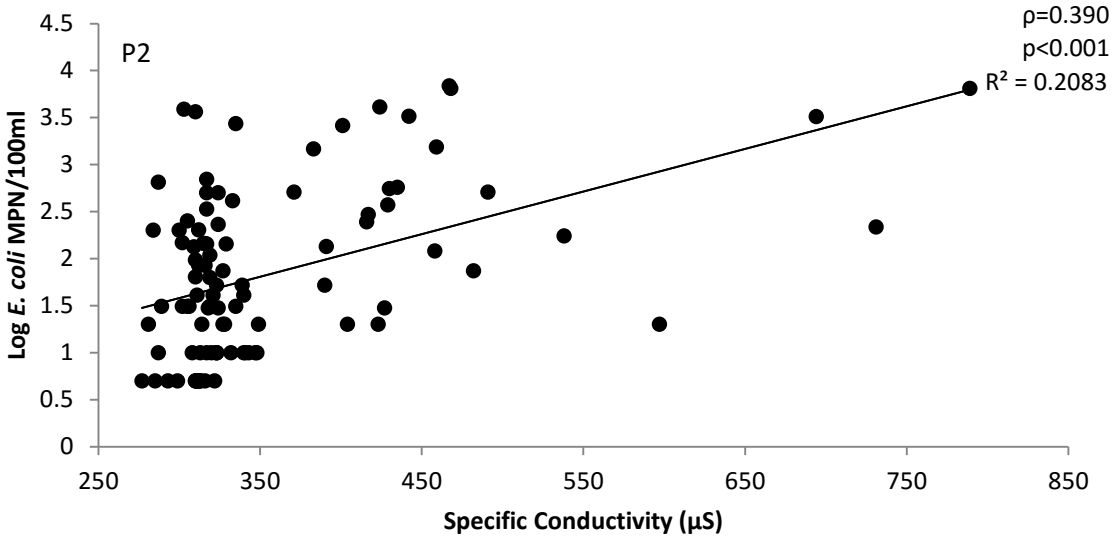


Correlation between specific conductivity (µS) and *E. coli* (MPN/100 ml) at location P2 (n=100). See section 4.4.2 for correlation between estimated river *E. coli* contributions to coastal waters and actual coastal *E. coli* concentrations.

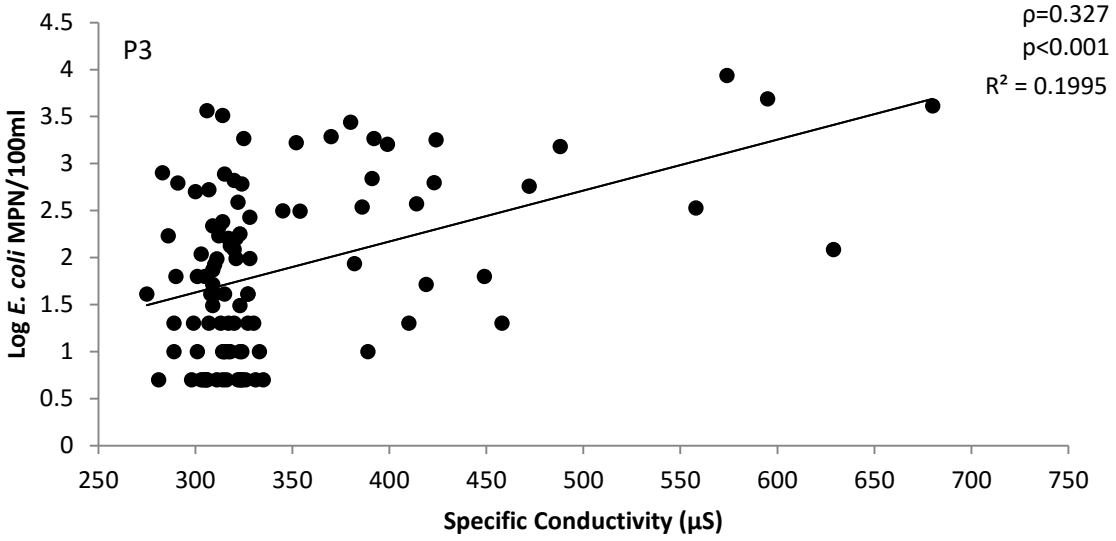


Correlation between specific conductivity (µS) and *E. coli* (MPN/100 ml) at location P3 (n=100). See section 4.4.2 for correlation between estimated river *E. coli* contributions to coastal waters and actual coastal *E. coli* concentrations.

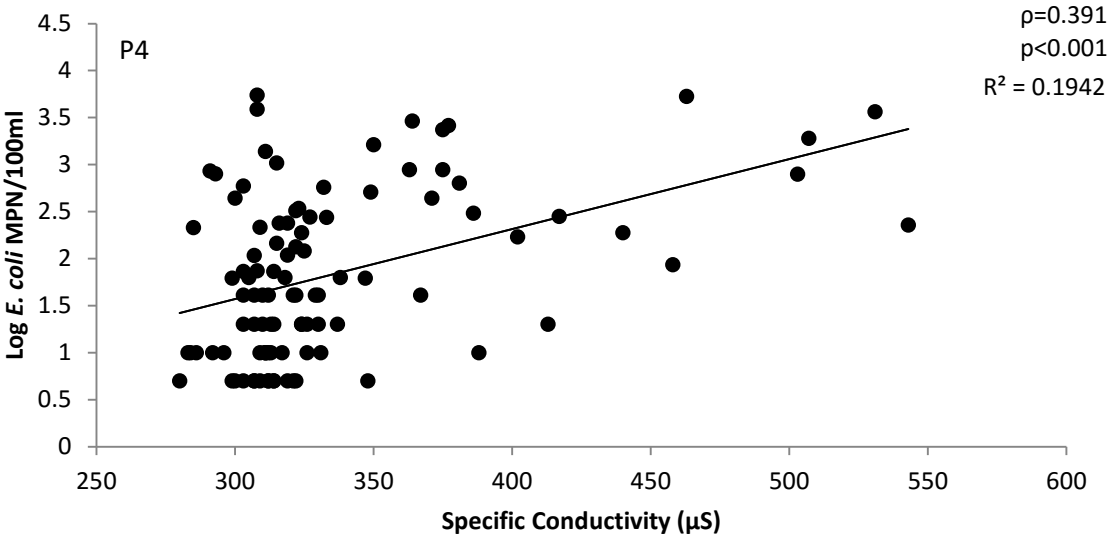


Correlation between specific conductivity (µS) and *E. coli* (MPN/100 ml) at location P4 (n=100). See section 4.4.2 for correlation between estimated river *E. coli* contributions to coastal waters and actual coastal *E. coli* concentrations.

## APPENDIX B: Predictive Model Visualizations and Statistics

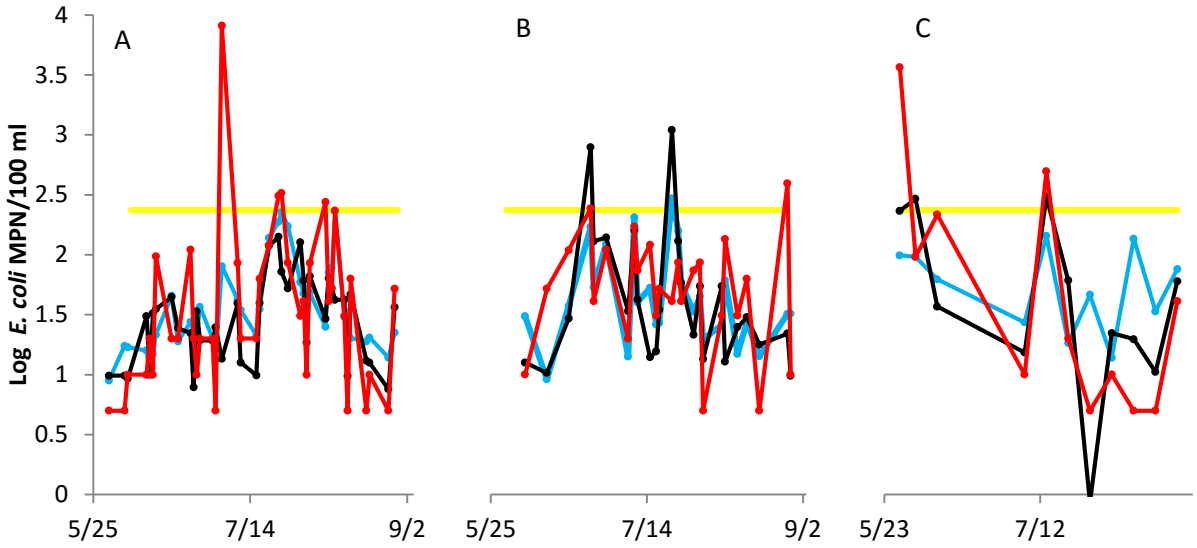


Comparison between actual *E. coli* concentrations (red) (MPN/100ml), ensemble model results (black) and traditional Virtual Beach (blue) model results for training set data at location A3 (n=75). Yellow line represents beach action value. A, B, and C represents data from years 2012, 2013 and 2014, respectively. Note: ensemble models are compared to all training set data, not only the subset of training data used for the model build.

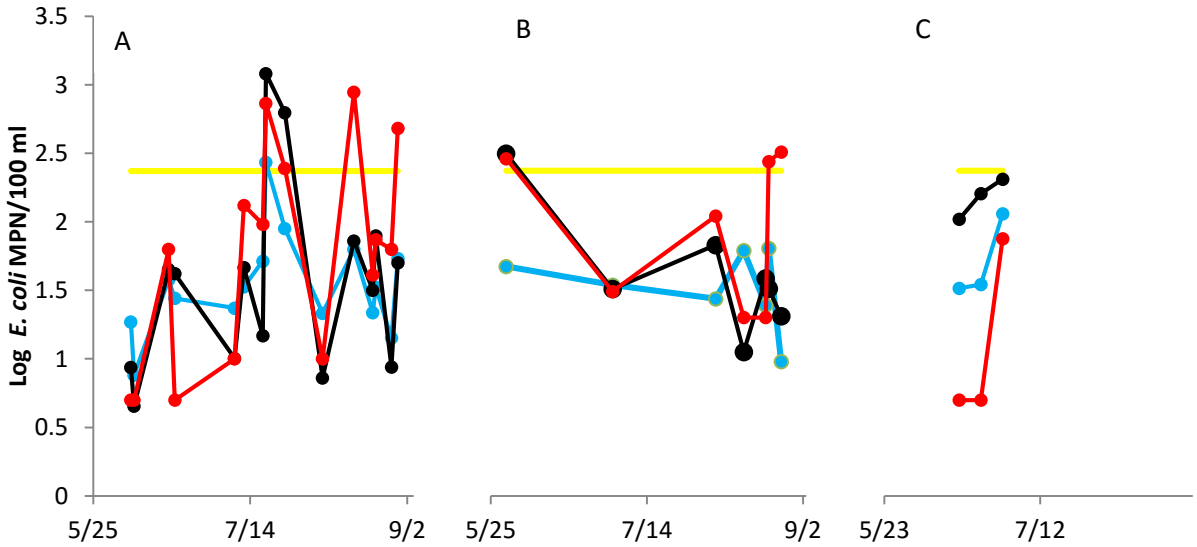


Comparison between actual *E. coli* concentrations (red) (MPN/100ml), ensemble model results (black) and traditional Virtual Beach (blue) model results for verification set data at location A3 (n=25). Yellow line represents beach action value. A, B, and C represents data from years 2012, 2013 and 2014, respectively.

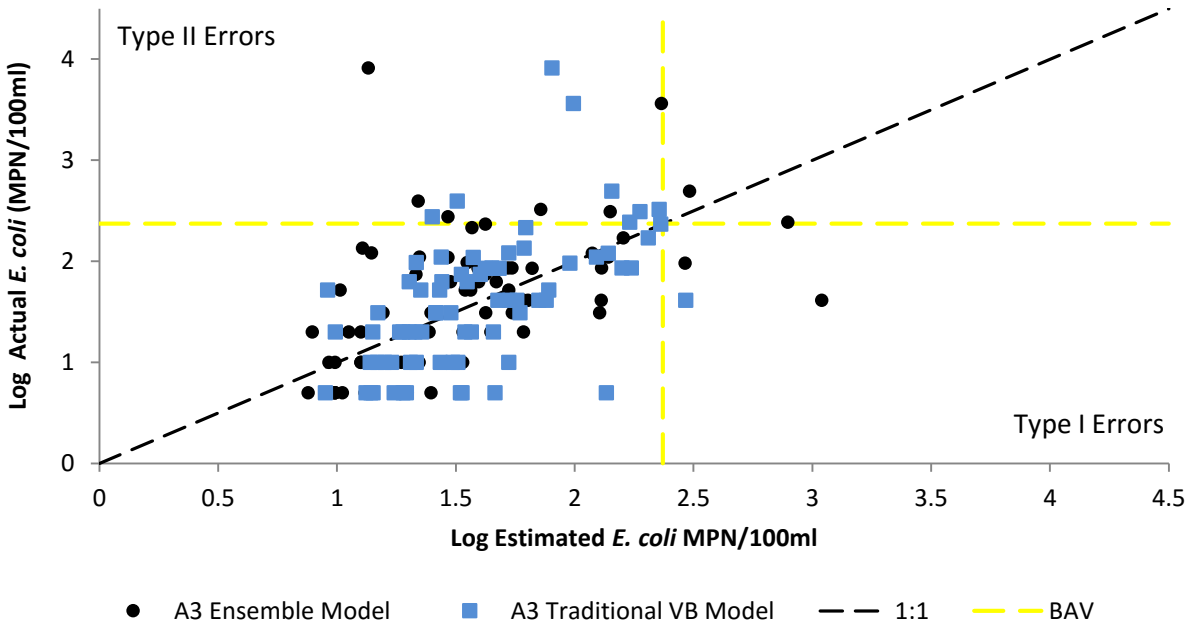


Actual *E. coli* concentrations (training set data, n=75) compared to traditional Virtual Beach and ensemble model results at location A3. See section 4.5.3 for comparisons between verification set. Note: ensemble models are compared to all training set data, not only the subset of training data used for the model build.

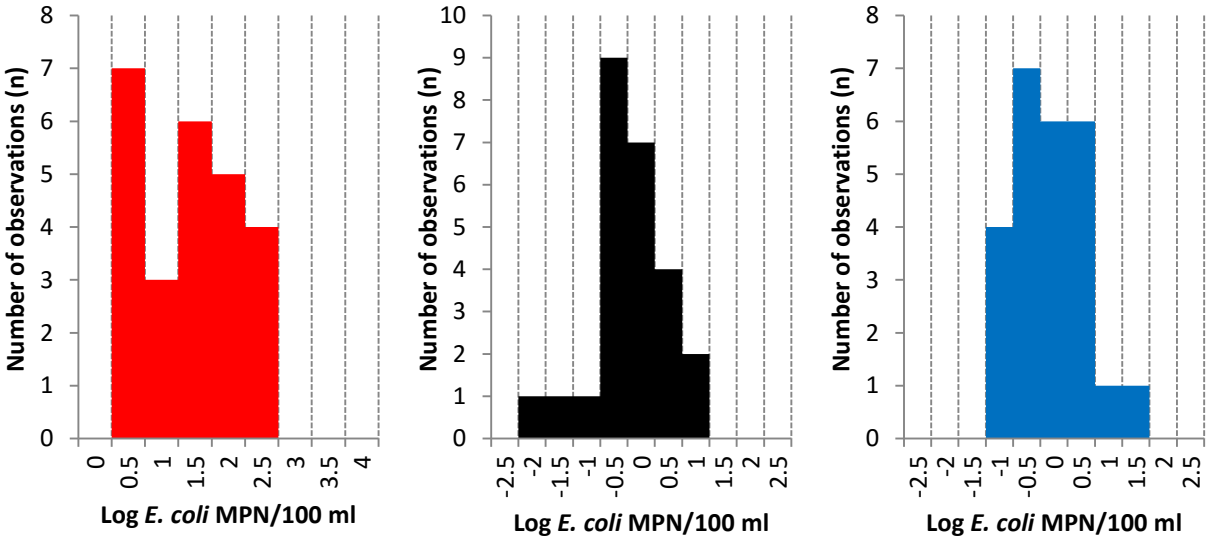


Histograms of actual *E. coli* concentrations (red), ensemble model residuals (black) and traditional Virtual Beach model residuals (blue) at location A3 for verification set data (n=25). Model residuals defined as actual *E. coli* concentration minus modeled concentrations.

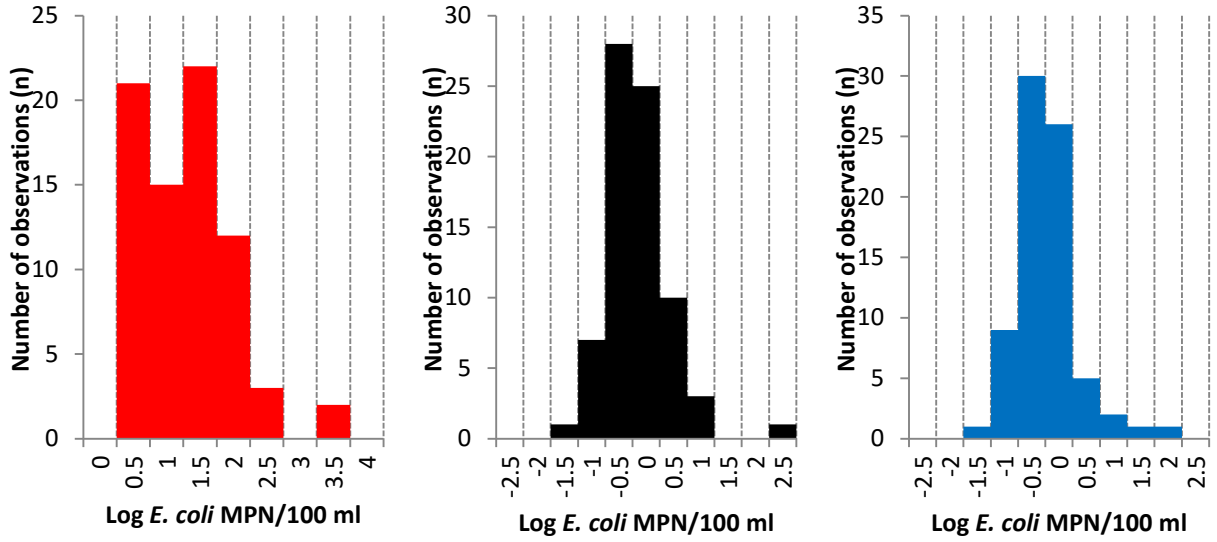


Histograms of actual *E. coli* concentrations (red), ensemble model residuals (black) and traditional Virtual Beach model residuals (blue) at location A3 for training set data (n=75). Model residuals defined as actual *E. coli* concentration minus modeled concentrations. Note: ensemble models are compared to all training set data, not only the subset of training data used for the model build.

| Location A3 | Ensemble Model | | Traditional VB Model | |
|---|---|---|---|---|
| | Training | Verification | Training | Verification |
| n | 75 | 25 | 75 | 25 |
| Average *E. coli* (MPN/100 ml) | 1.516 | 1.647 | 1.592 | 1.551 |
| Standard Deviation | 0.492 | 0.609 | 0.373 | 0.332 |
| Average Residual | 0.076 | 0.072 | 0.000 | 0.168 |
| Type I Errors (n) | 2 | 0 | 1 | 0 |
| Type II Errors (n) | 6 | 4 | 8 | 6 |
| Pearson's r | 0.519 | 0.483 | 0.569 | 0.518 |
| $R^2$ | 0.270 | 0.234 | 0.324 | 0.268 |
| RMSE | 0.582 | 0.681 | 0.536 | 0.640 |
| Specificity | 0.970 | 1.000 | 0.985 | 1.000 |
| Sensitivity | 0.250 | 0.429 | 0.028 | 0.100 |

Model statistics at location A3. Note: ensemble models are compared to all training set data, not only the subset of training data used for the model build.

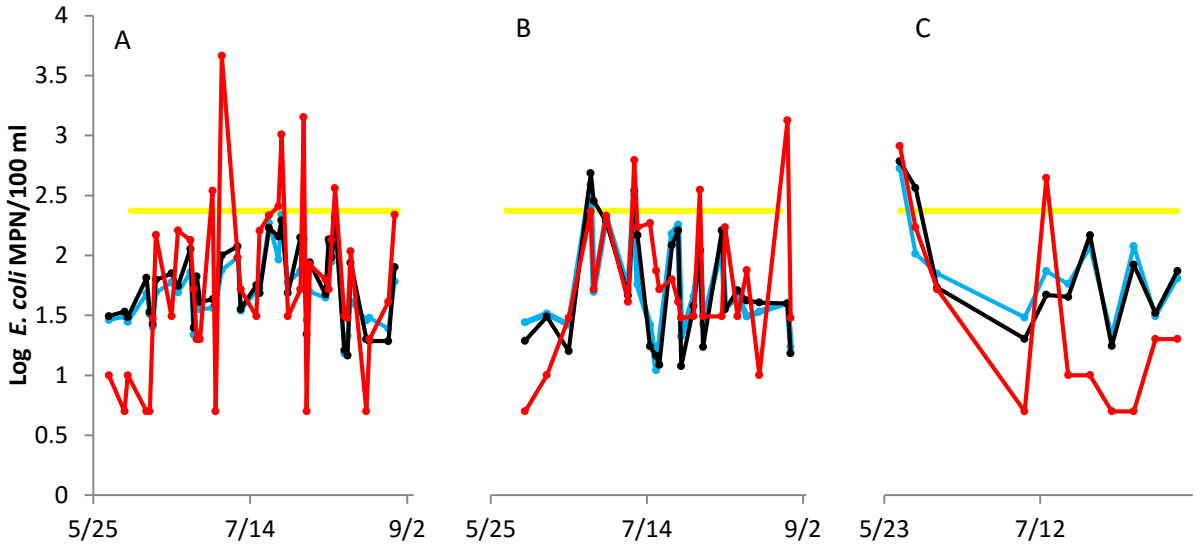


Comparison between actual *E. coli* concentrations (red) (MPN/100ml), ensemble model results (black) and traditional Virtual Beach (blue) model results for training set data at location A2 (n=75). Yellow line represents beach action value. A, B, and C represents data from years 2012, 2013 and 2014, respectively. Note: ensemble models are compared to all training set data, not only the subset of training data used for the model build.

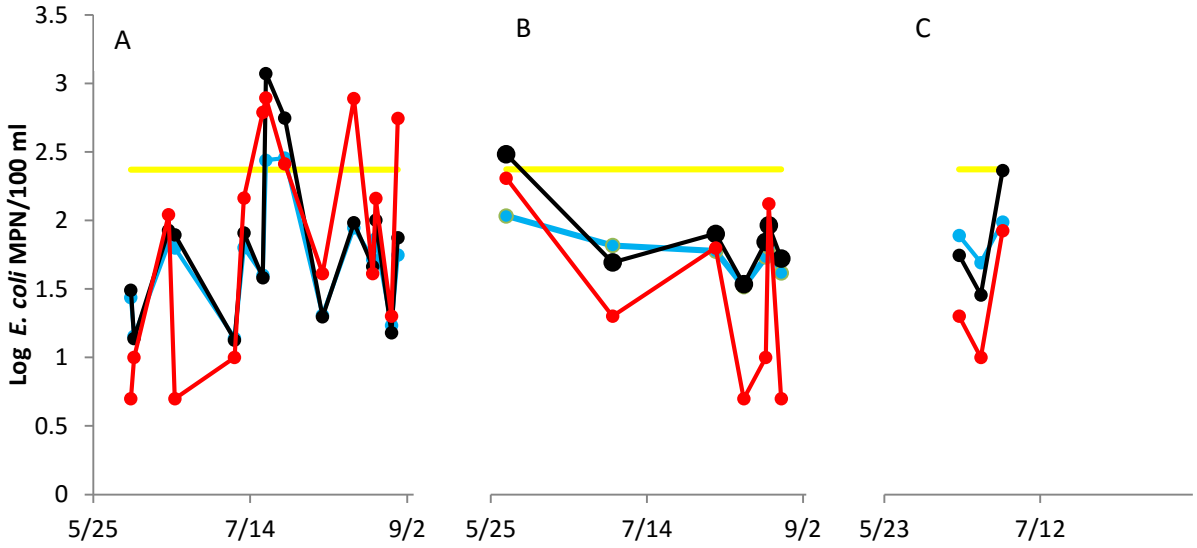


Comparison between actual *E. coli* concentrations (red) (MPN/100ml), ensemble model results (black) and traditional Virtual Beach (blue) model results for verification set data at location A2 (n=25). Yellow line represents beach action value. A, B, and C represents data from years 2012, 2013 and 2014, respectively.

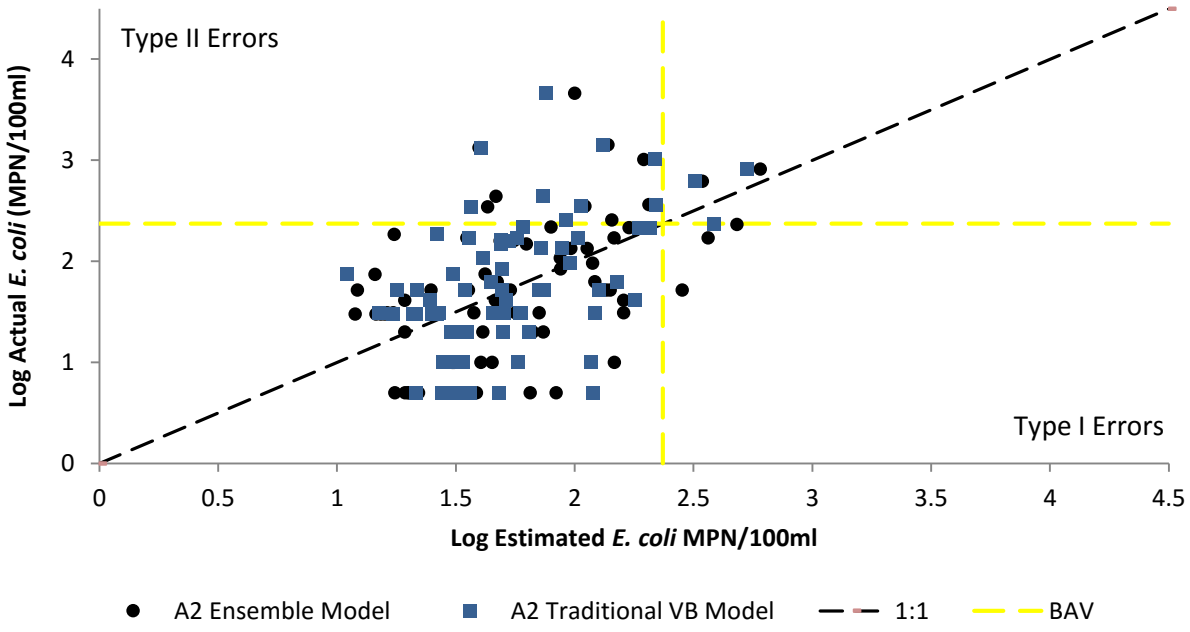


Actual *E. coli* concentrations (training set data, n=75) compared to traditional Virtual Beach and ensemble model results at location A2. See section 4.5.3 for comparisons between verification set.

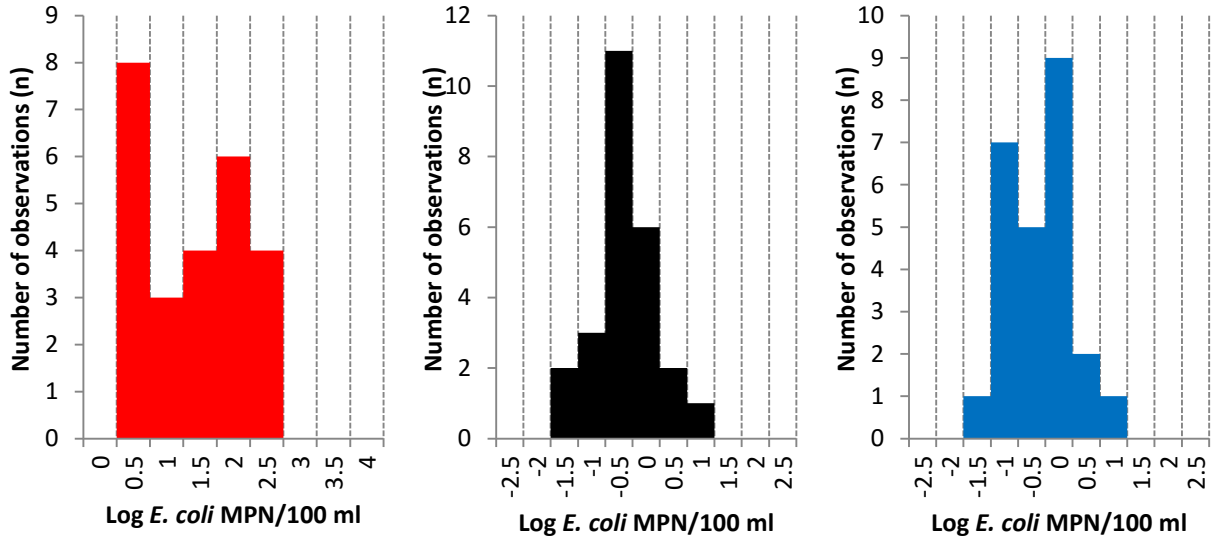


Histograms of actual *E. coli* concentrations (red), ensemble model residuals (black) and traditional Virtual Beach model residuals (blue) at location A2 for verification set data (n=25). Model residuals defined as actual *E. coli* concentration minus modeled concentrations.

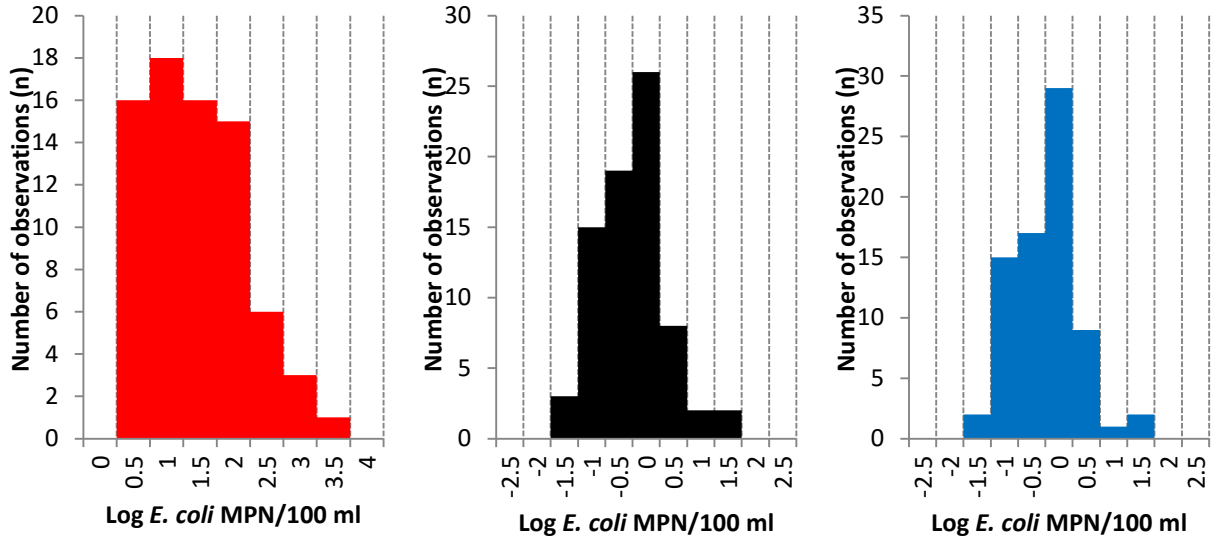


Histograms of actual *E. coli* concentrations (red), ensemble model residuals (black) and traditional Virtual Beach model residuals (blue) at location A2 for training set data (n=75). Model residuals defined as actual *E. coli* concentration minus modeled concentrations. Note: ensemble models are compared to all training set data, not only the subset of training data used for the model build.

| Location A2 | A2 Ensemble Model | | Traditional VB Model | |
|---|---|---|---|---|
| | Training | Verification | Training | Verification |
| n | 75 | 25 | 75 | 25 |
| Average E. coli (MPN/100 ml) | 1.751 | 1.824 | 1.726 | 1.734 |
| Standard Deviation | 0.407 | 0.472 | 0.343 | 0.328 |
| Average Residual | -0.025 | -0.137 | 0.000 | -0.047 |
| Type I Errors (n) | 3 | 1 | 1 | 0 |
| Type II Errors (n) | 9 | 3 | 9 | 3 |
| Pearson's r | 0.513 | 0.611 | 0.502 | 0.589 |
| $R^2$ | 0.263 | 0.374 | 0.252 | 0.347 |
| RMSE | 0.585 | 0.592 | 0.586 | 0.600 |
| Specificity | 0.953 | 0.950 | 0.984 | 1.000 |
| Sensitivity | 0.182 | 0.400 | 0.250 | 0.286 |

Model statistics at location A2. Note: ensemble models are compared to all training set data, not only the subset of training data used for the model build.

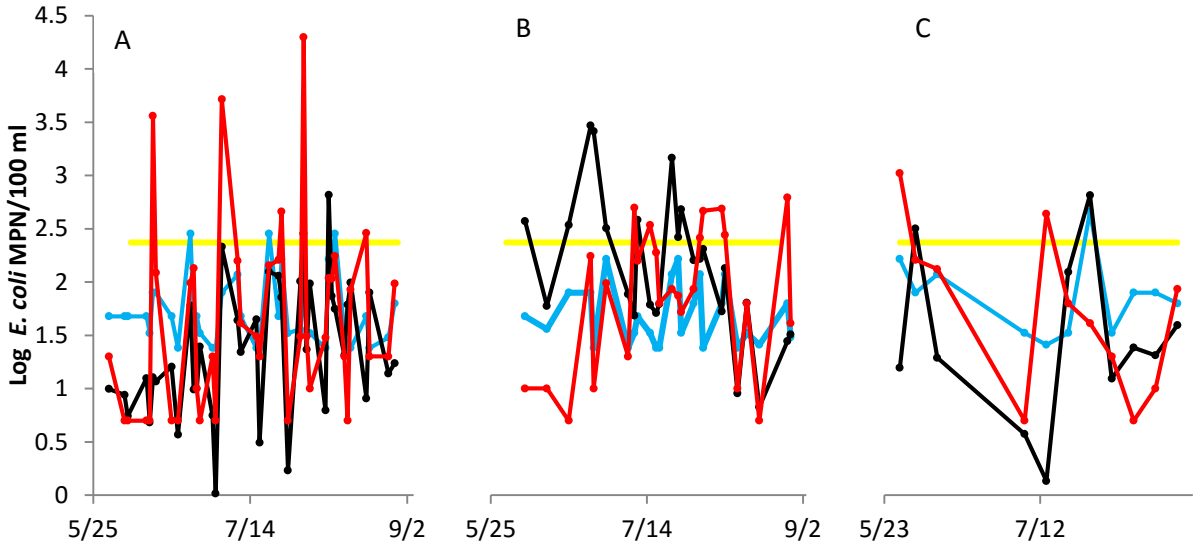


Comparison between actual *E. coli* concentrations (red) (MPN/100ml), ensemble model results (black) and traditional Virtual Beach (blue) model results for training set data at location A1 (n=75). Yellow line represents beach action value. A, B, and C represents data from years 2012, 2013 and 2014, respectively. Note: ensemble models are compared to all training set data, not only the subset of training data used for the model build.

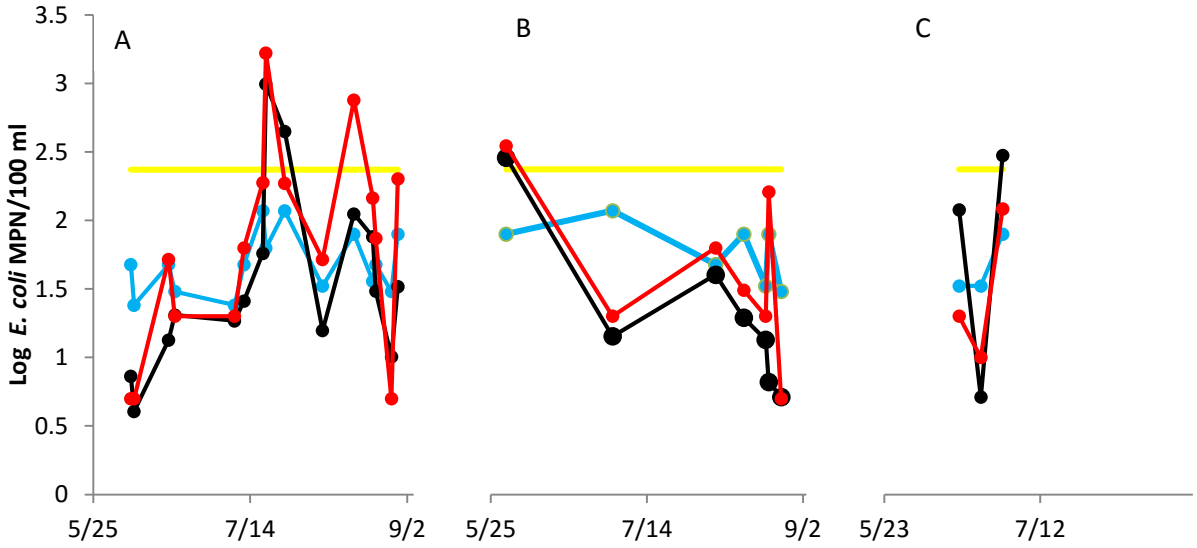


Comparison between actual *E. coli* concentrations (red) (MPN/100ml), ensemble model results (black) and traditional Virtual Beach (blue) model results for verification set data at location A1 (n=25). Yellow line represents beach action value. A, B, and C represents data from years 2012, 2013 and 2014, respectively.

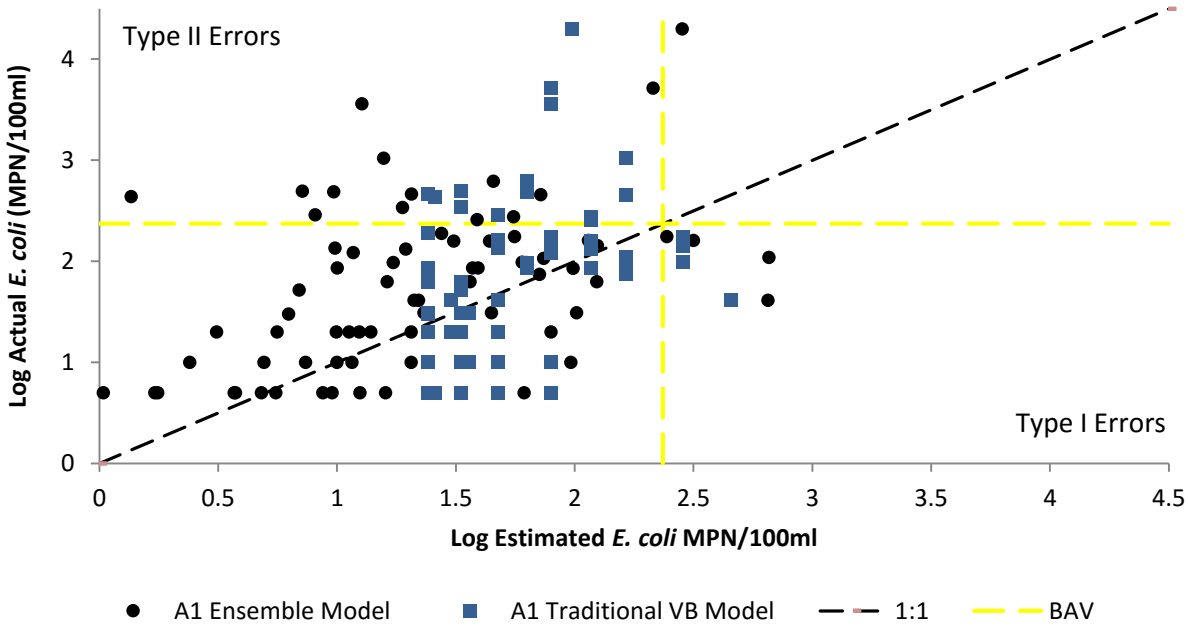


Actual *E. coli* concentrations (training set data, n=75) compared to traditional Virtual Beach and ensemble model results at location A1. See section 4.5.3 for comparisons between verification set. Note: ensemble models are compared to all training set data, not only the subset of training data used for the model build.

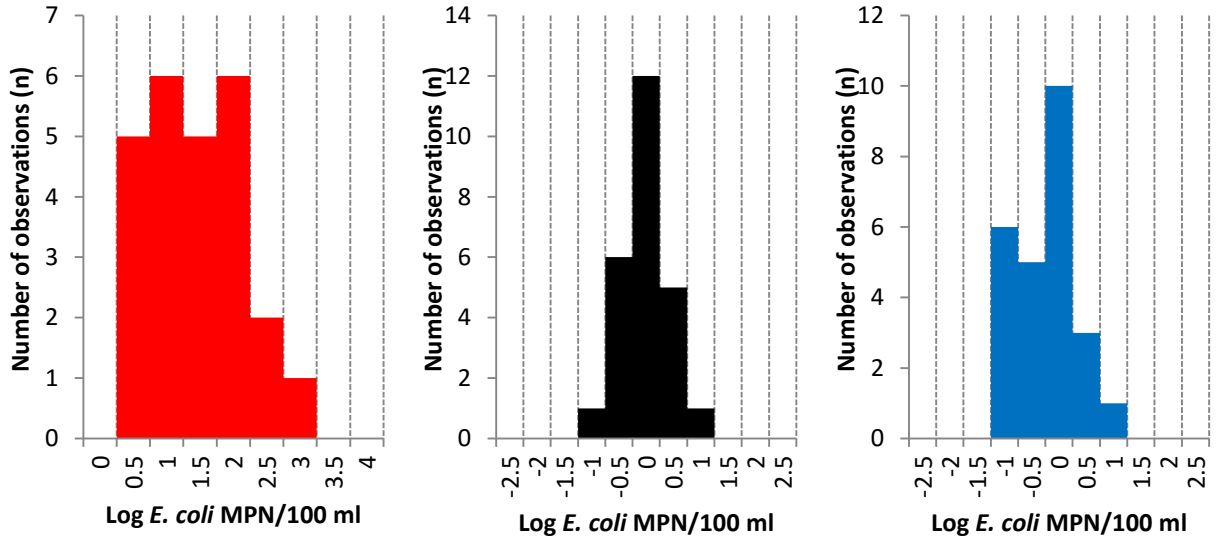


Histograms of actual *E. coli* concentrations (red), ensemble model residuals (black) and traditional Virtual Beach model residuals (blue) at location A1 for verification set data (n=25). Model residuals defined as actual *E. coli* concentration minus modeled concentrations.

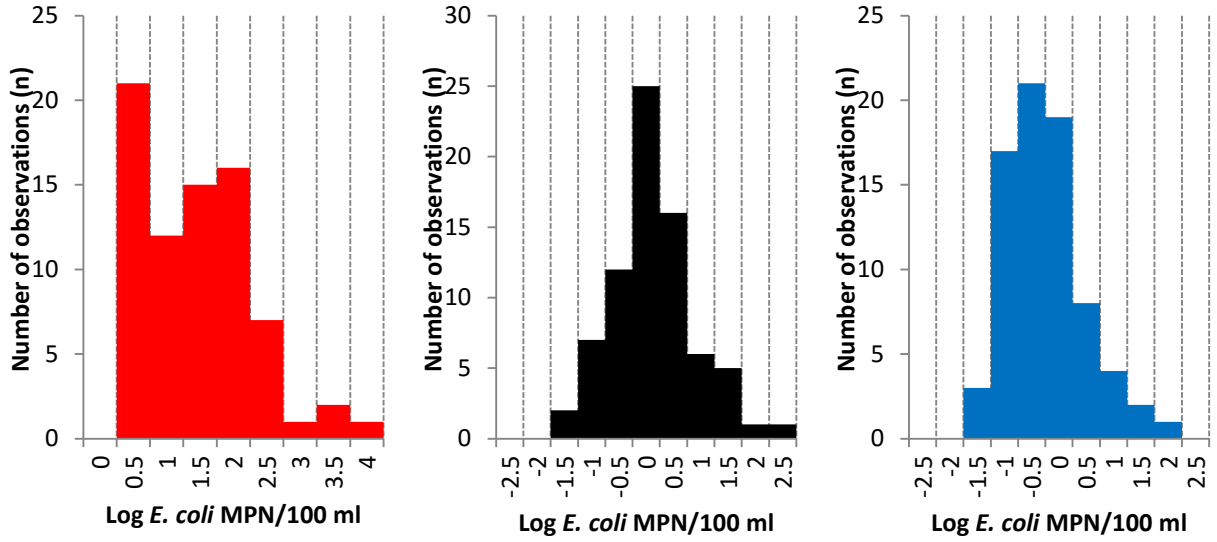


Histograms of actual *E. coli* concentrations (red), ensemble model residuals (black) and traditional Virtual Beach model residuals (blue) at location A1 for training set data (n=75). Model residuals defined as actual *E. coli* concentration minus modeled concentrations. Note: ensemble models are compared to all training set data, not only the subset of training data used for the model build.

| Location A1 | Ensemble Model | | Traditional VB Model | |
|---|---|---|---|---|
| | Training | Verification | Training | Verification |
| n | 75 | 25 | 75 | 25 |
| Average E. coli (MPN/100 ml) | 1.340 | 1.502 | 1.725 | 1.706 |
| Standard Deviation | 0.606 | 0.647 | 0.320 | 0.220 |
| Average Residual | 0.385 | 0.204 | 0.000 | 0.000 |
| Type I Errors (n) | 4 | 2 | 4 | 0 |
| Type II Errors (n) | 13 | 1 | 14 | 3 |
| Pearson's r | 0.436 | 0.781 | 0.403 | 0.624 |
| $R^2$ | 0.190 | 0.609 | 0.162 | 0.390 |
| RMSE | 0.847 | 0.481 | 0.721 | 0.568 |
| Specificity | 0.934 | 0.909 | 0.934 | 1.000 |
| Sensitivity | 0.071 | 0.667 | 0.091 | 0.000 |

Model statistics at location A1. Note: ensemble models are compared to all training set data, not only the subset of training data used for the model build.

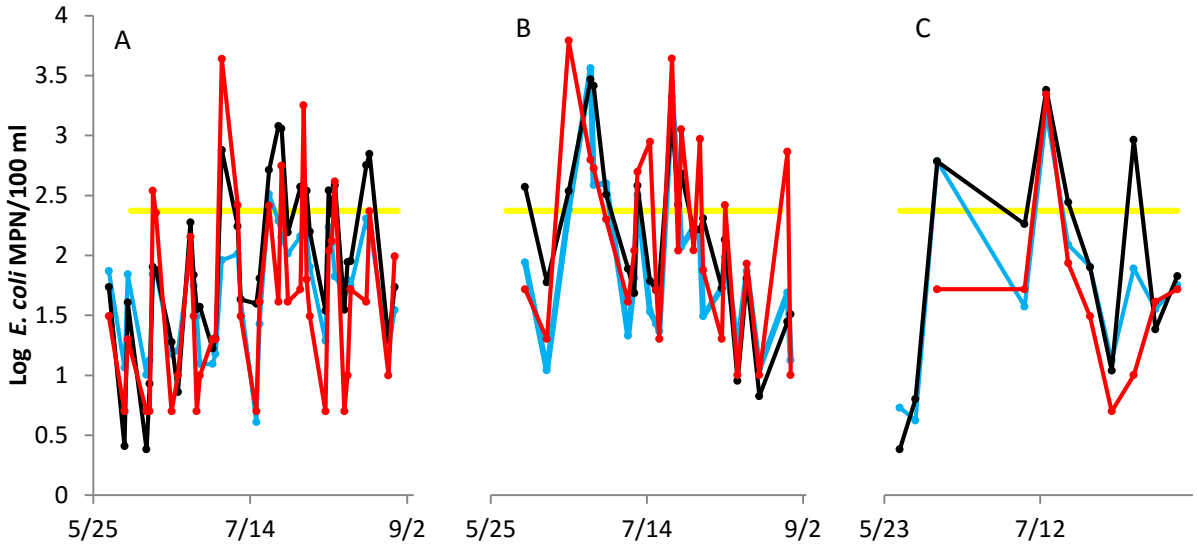


Comparison between actual *E. coli* concentrations (red) (MPN/100ml), ensemble model results (black) and traditional Virtual Beach (blue) model results for training set data at location P1 (n=73). Yellow line represents beach action value. A, B, and C represents data from years 2012, 2013 and 2014, respectively. Note: ensemble models are compared to all training set data, not only the subset of training data used for the model build.

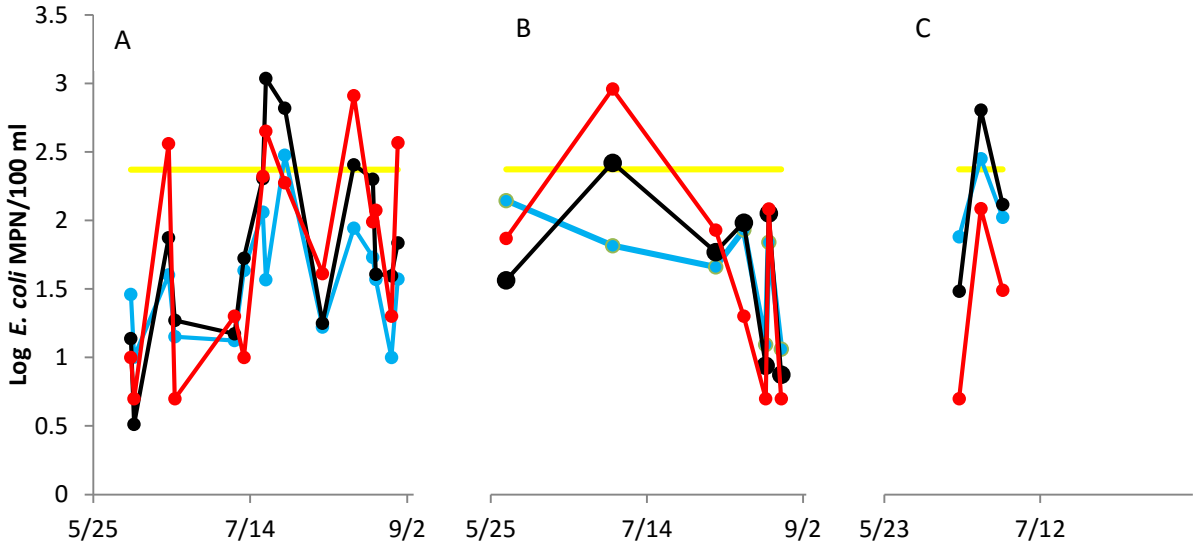


Comparison between actual *E. coli* concentrations (red) (MPN/100ml), ensemble model results (black) and traditional Virtual Beach (blue) model results for verification set data at location P1 (n=25). Yellow line represents beach action value. A, B, and C represents data from years 2012, 2013 and 2014, respectively.

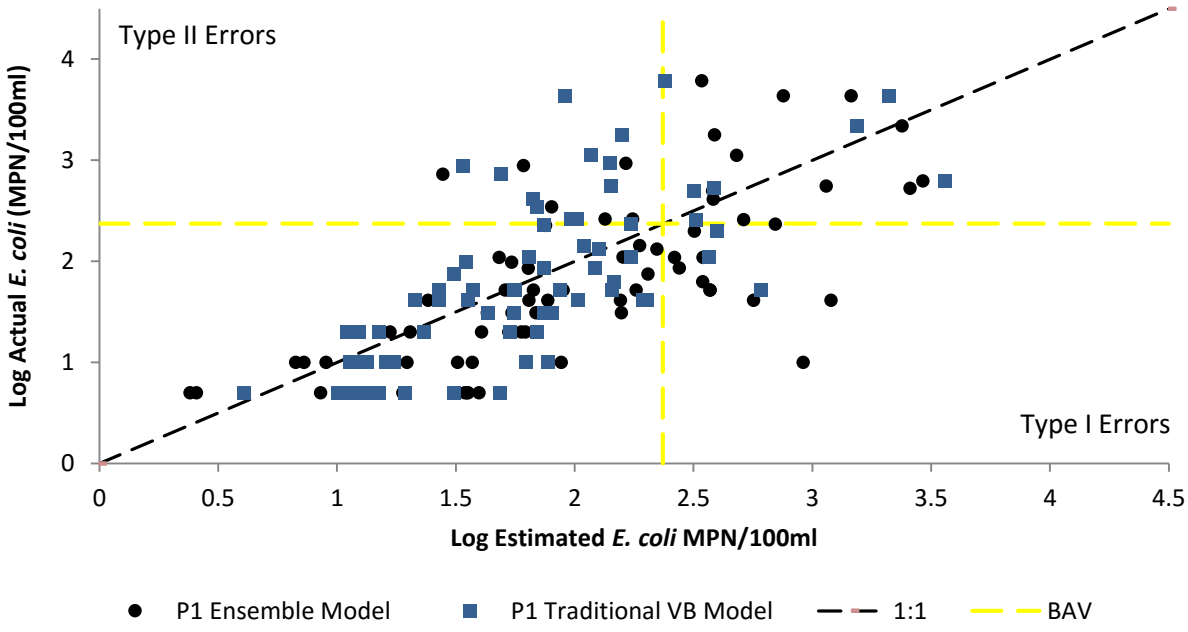


Actual *E. coli* concentrations (training set data, n=73) compared to traditional Virtual Beach and ensemble model results at location P1. See section 4.5.3 for comparisons between verification set. Note: ensemble models are compared to all training set data, not only the subset of training data used for the model build.

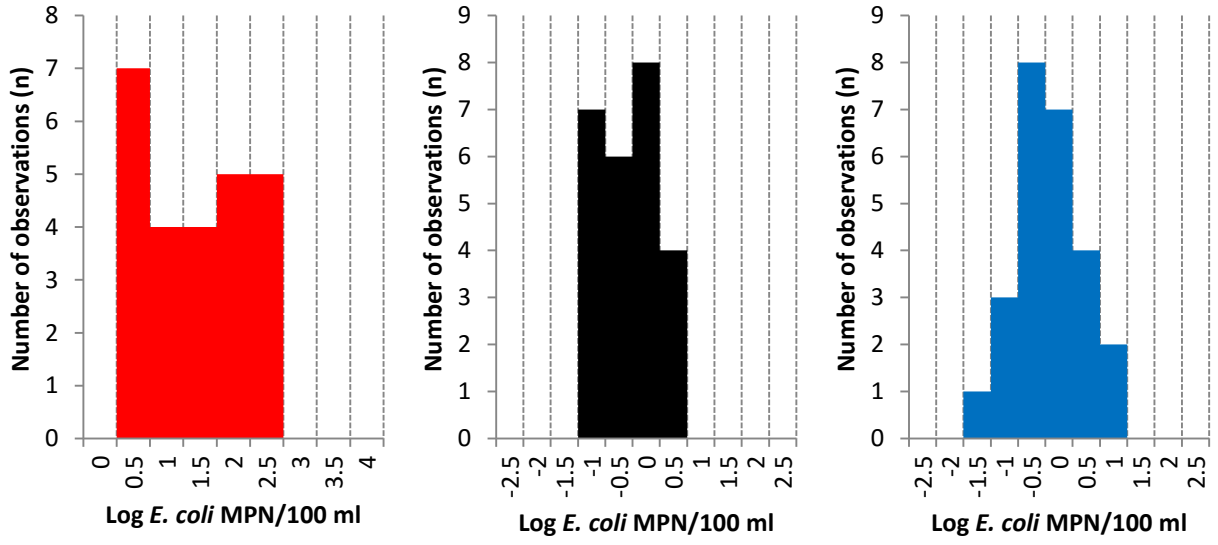


Histograms of actual *E. coli* concentrations (red), ensemble model residuals (black) and traditional Virtual Beach model residuals (blue) at location P1 for verification set data (n=25). Model residuals defined as actual *E. coli* concentration minus modeled concentrations.

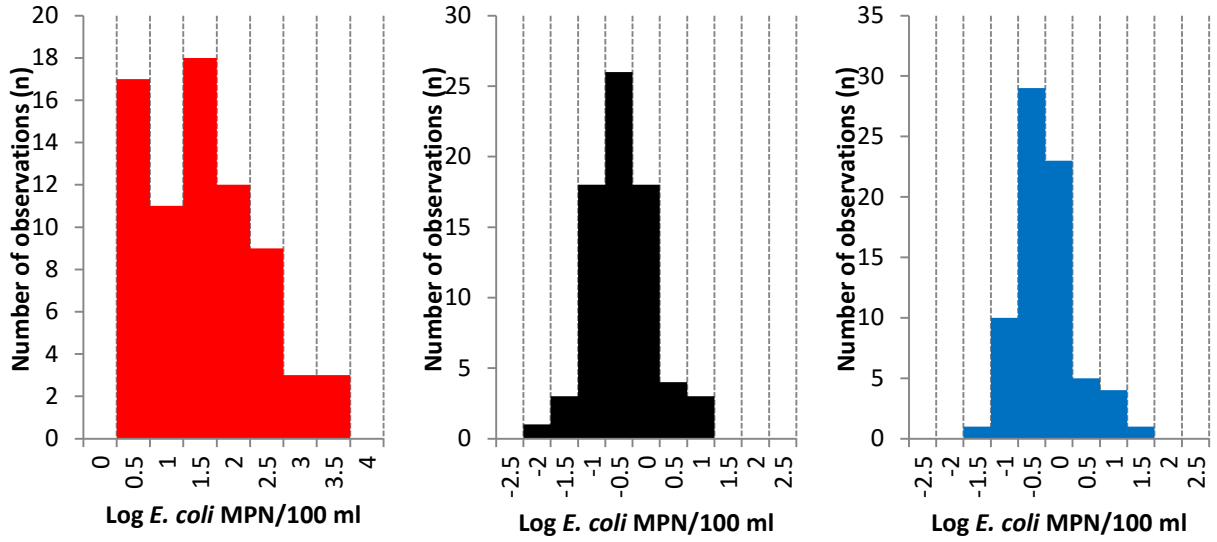


Histograms of actual *E. coli* concentrations (red), ensemble model residuals (black) and traditional Virtual Beach model residuals (blue) at location P1 for training set data (n=73). Model residuals defined as actual *E. coli* concentration minus modeled concentrations. Note: ensemble models are compared to all training set data, not only the subset of training data used for the model build.

| Location P1 | Ensemble Model | | Traditional VB Model | |
|---|---|---|---|---|
| | Training | Verification | Training | Verification |
| n | 73 | 25 | 73 | 25 |
| Average E. coli (MPN/100 ml) | 2.027 | 1.794 | 1.823 | 1.641 |
| Standard Deviation | 0.687 | 0.644 | 0.566 | 0.429 |
| Average Residual | -0.199 | -0.083 | 0.000 | 0.070 |
| Type I Errors (n) | 12 | 2 | 3 | 2 |
| Type II Errors (n) | 6 | 2 | 11 | 5 |
| Pearson's r | 0.692 | 0.772 | 0.707 | 0.535 |
| $R^2$ | 0.479 | 0.597 | 0.500 | 0.286 |
| RMSE | 0.614 | 0.475 | 0.554 | 0.621 |
| Specificity | 0.782 | 0.900 | 0.945 | 0.900 |
| Sensitivity | 0.667 | 0.600 | 0.071 | 0.000 |

Model statistics at location P1. Note: ensemble models are compared to all training set data, not only the subset of training data used for the model build.

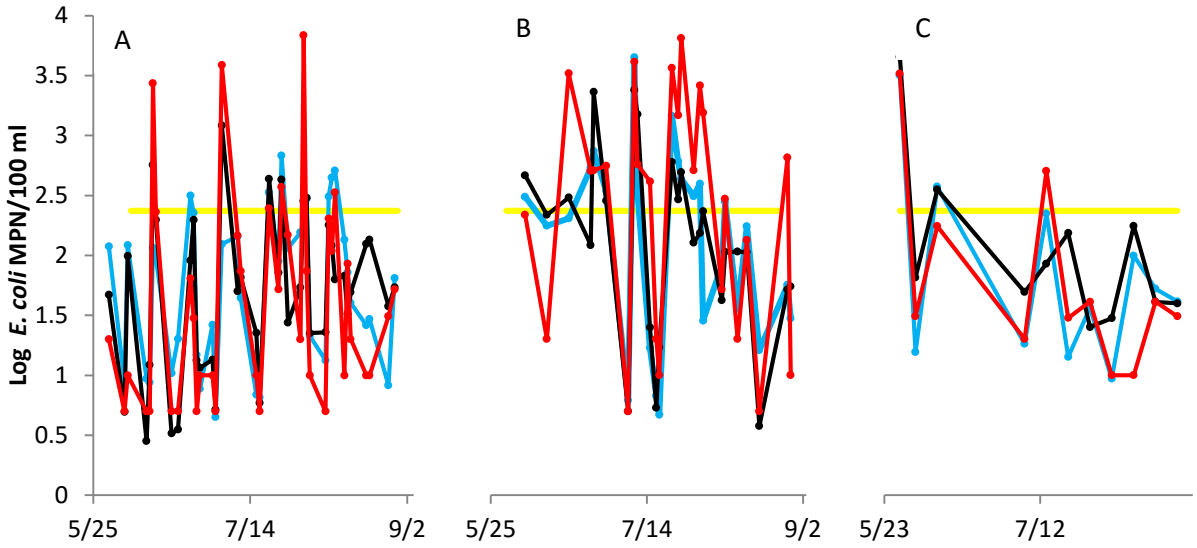


Comparison between actual *E. coli* concentrations (red) (MPN/100ml), ensemble model results (black) and traditional Virtual Beach (blue) model results for training set data at location P2 (n=75). Yellow line represents beach action value. A, B, and C represents data from years 2012, 2013 and 2014, respectively. Note: ensemble models are compared to all training set data, not only the subset of training data used for the model build.

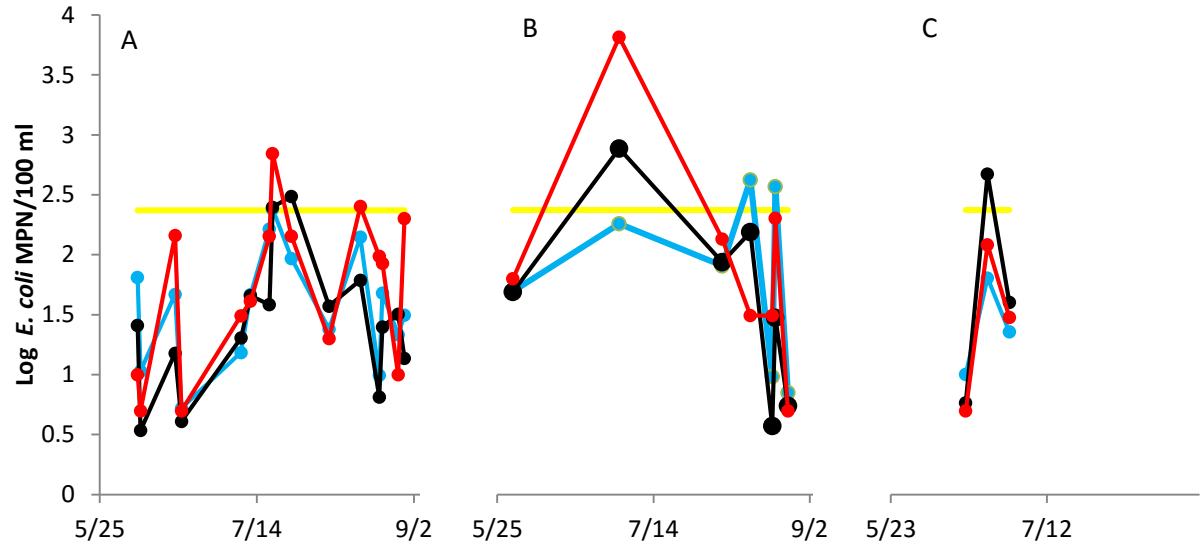


Comparison between actual *E. coli* concentrations (red) (MPN/100ml), ensemble model results (black) and traditional Virtual Beach (blue) model results for verification set data at location P2 (n=25). Yellow line represents beach action value. A, B, and C represents data from years 2012, 2013 and 2014, respectively.

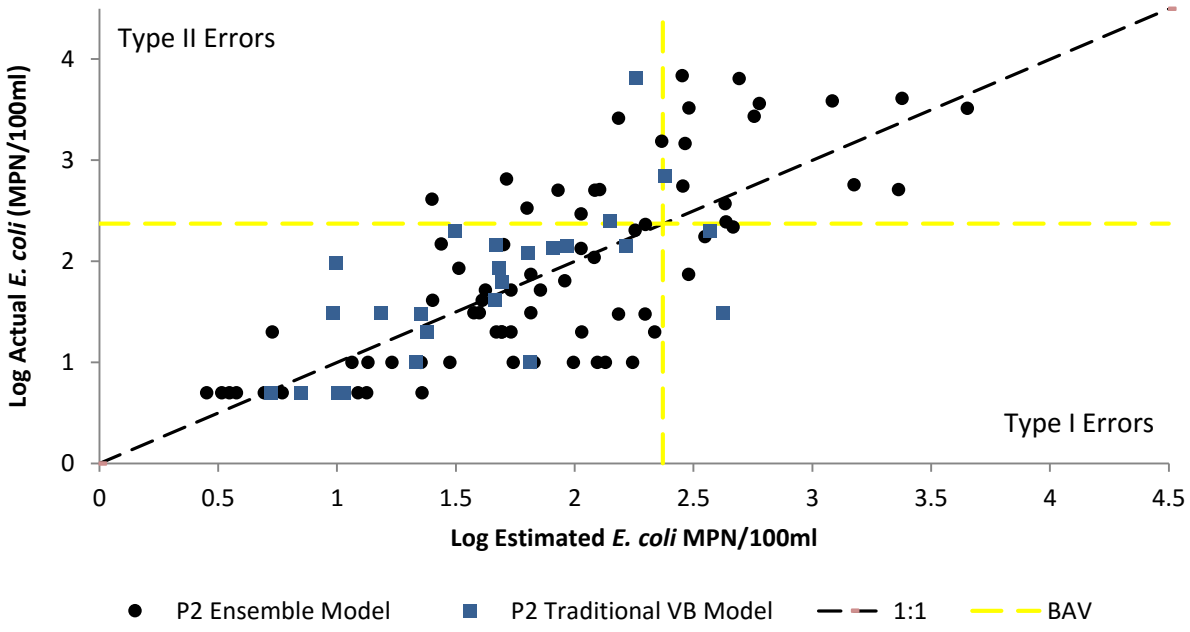


Actual *E. coli* concentrations (training set data, n=75) compared to traditional Virtual Beach and ensemble model results at location P2. See section 4.5.3 for comparisons between verification set. Note: ensemble models are compared to all training set data, not only the subset of training data used for the model build.

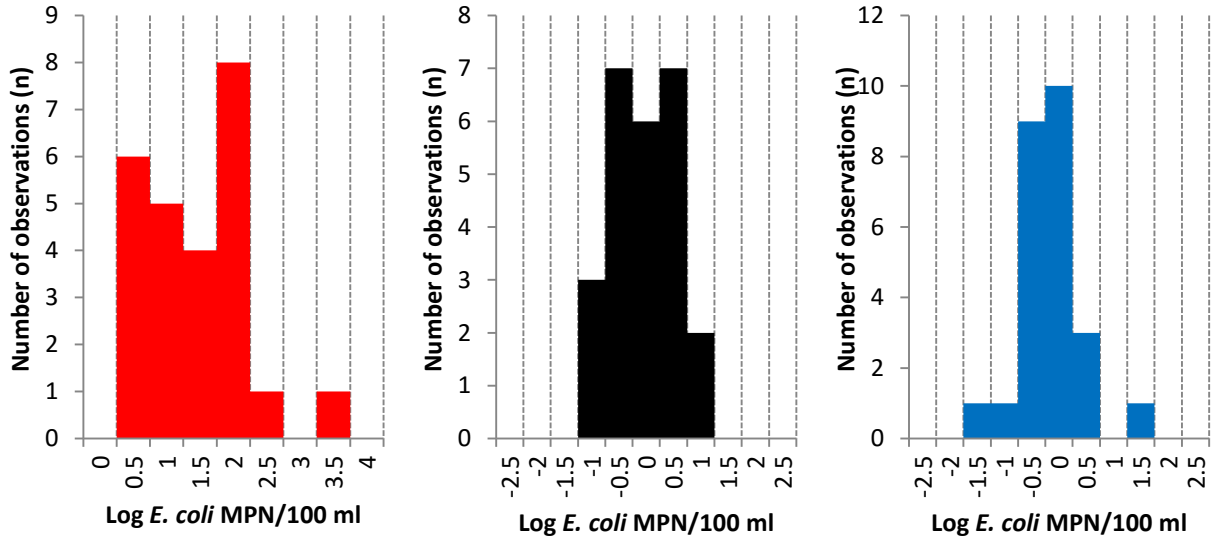


Histograms of actual *E. coli* concentrations (red), ensemble model residuals (black) and traditional Virtual Beach model residuals (blue) at location P2 for verification set data (n=25). Model residuals defined as actual *E. coli* concentration minus modeled concentrations.

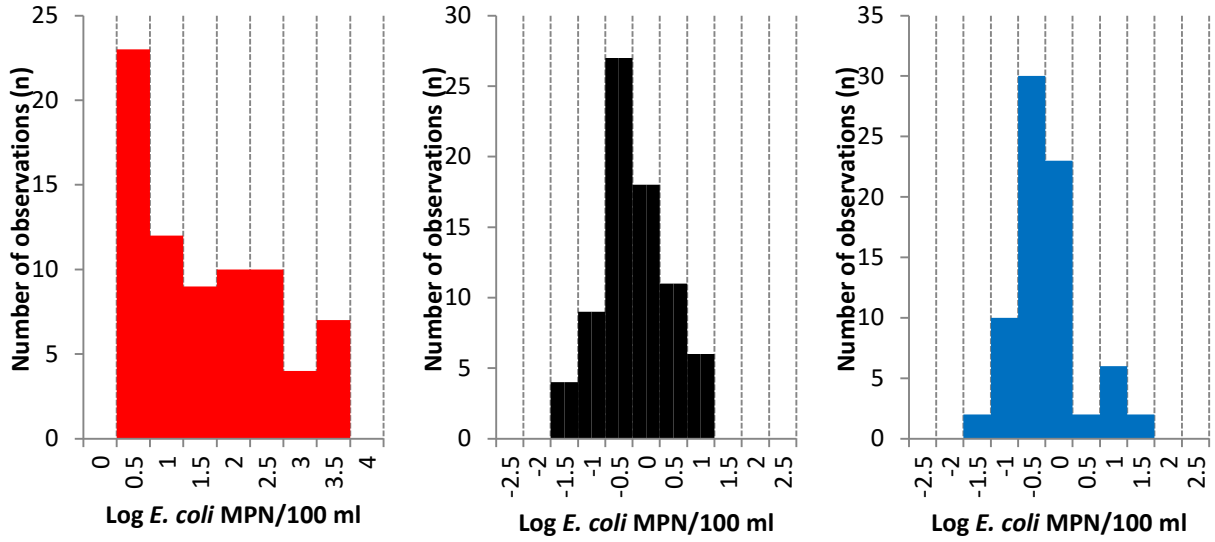


Histograms of actual *E. coli* concentrations (red), ensemble model residuals (black) and traditional Virtual Beach model residuals (blue) at location P2 for training set data (n=75). Model residuals defined as actual *E. coli* concentration minus modeled concentrations. Note: ensemble models are compared to all training set data, not only the subset of training data used for the model build.

| Location P2 | Ensemble Model | | Traditional VB Model | |
|---|---|---|---|---|
| | Training | Verification | Training | Verification |
| n | 75 | 25 | 75 | 25 |
| Average E. coli (MPN/100 ml) | 1.869 | 1.516 | 1.868 | 1.629 |
| Standard Deviation | 0.714 | 0.657 | 0.711 | 0.546 |
| Average Residual | 0.001 | 0.233 | 0.001 | 0.120 |
| Type I Errors (n) | 3 | 2 | 6 | 2 |
| Type II Errors (n) | 9 | 1 | 8 | 2 |
| Pearson's r | 0.768 | 0.689 | 0.751 | 0.682 |
| $R^2$ | 0.590 | 0.475 | 0.564 | 0.466 |
| RMSE | 0.600 | 0.595 | 0.619 | 0.549 |
| Specificity | 0.942 | 0.909 | 0.885 | 0.909 |
| Sensitivity | 0.609 | 0.667 | 0.556 | 0.200 |

Model statistics at location P2. Note: ensemble models are compared to all training set data, not only the subset of training data used for the model build.

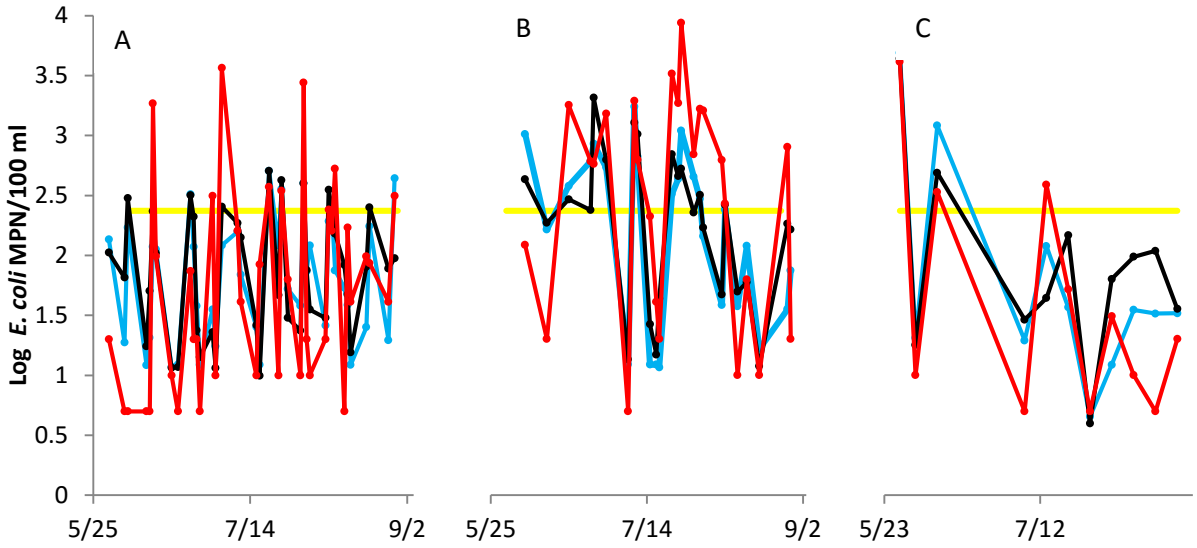


Comparison between actual *E. coli* concentrations (red) (MPN/100ml), ensemble model results (black) and traditional Virtual Beach (blue) model results for training set data at location P3 (n=75). Yellow line represents beach action value. A, B, and C represents data from years 2012, 2013 and 2014, respectively. Note: ensemble models are compared to all training set data, not only the subset of training data used for the model build.

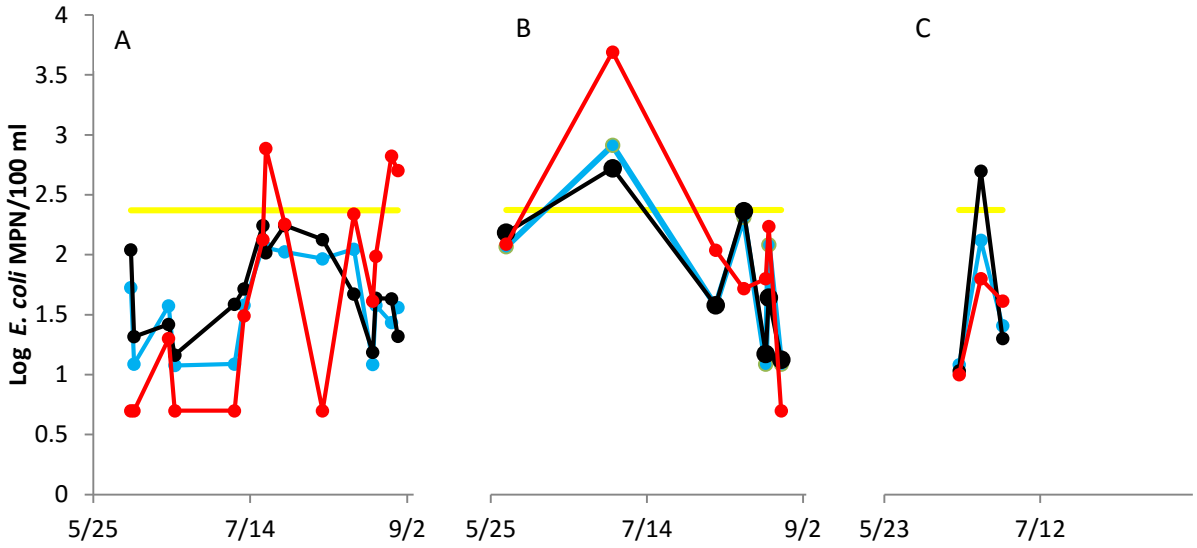


Comparison between actual *E. coli* concentrations (red) (MPN/100ml), ensemble model results (black) and traditional Virtual Beach (blue) model results for verification set data at location P3 (n=25). Yellow line represents beach action value. A, B, and C represents data from years 2012, 2013 and 2014, respectively.

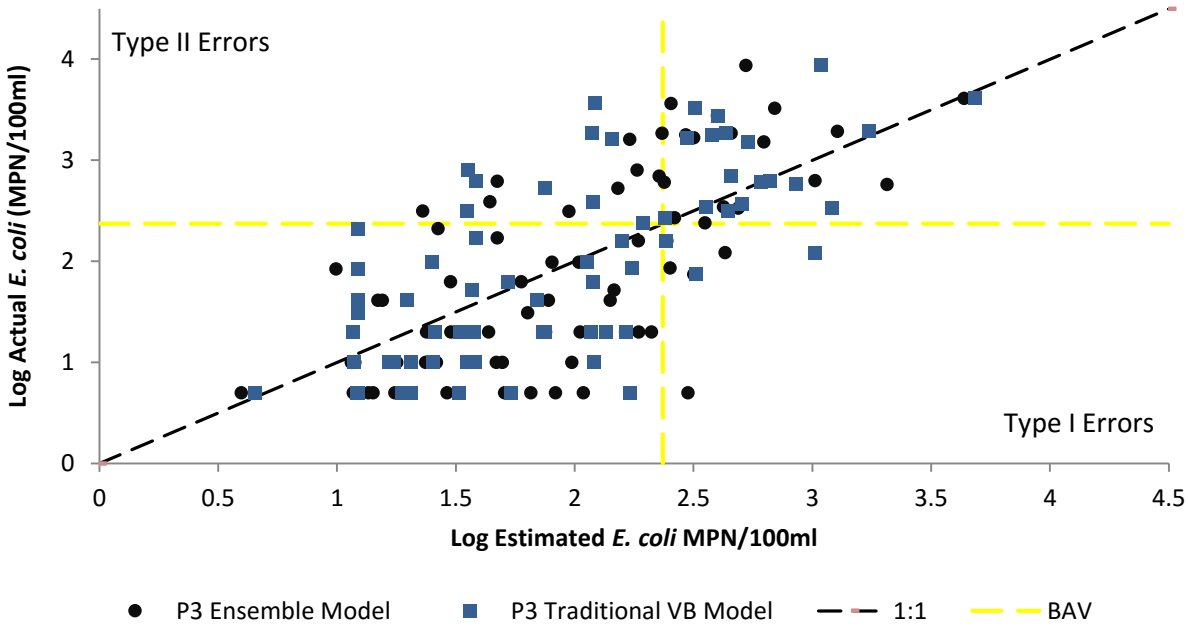


Actual *E. coli* concentrations (training set data, n=75) compared to traditional Virtual Beach and ensemble model results at location P3. See section 4.5.3 for comparisons between verification set. Note: ensemble models are compared to all training set data, not only the subset of training data used for the model build.

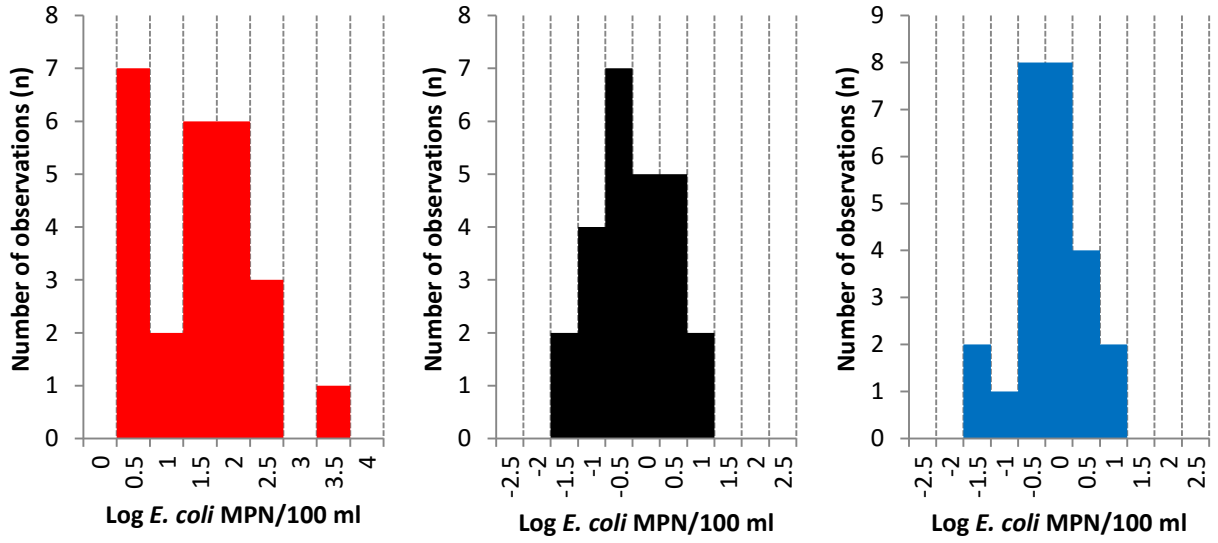


Histograms of actual *E. coli* concentrations (red), ensemble model residuals (black) and traditional Virtual Beach model residuals (blue) at location P3 for verification set data (n=25). Model residuals defined as actual *E. coli* concentration minus modeled concentrations.

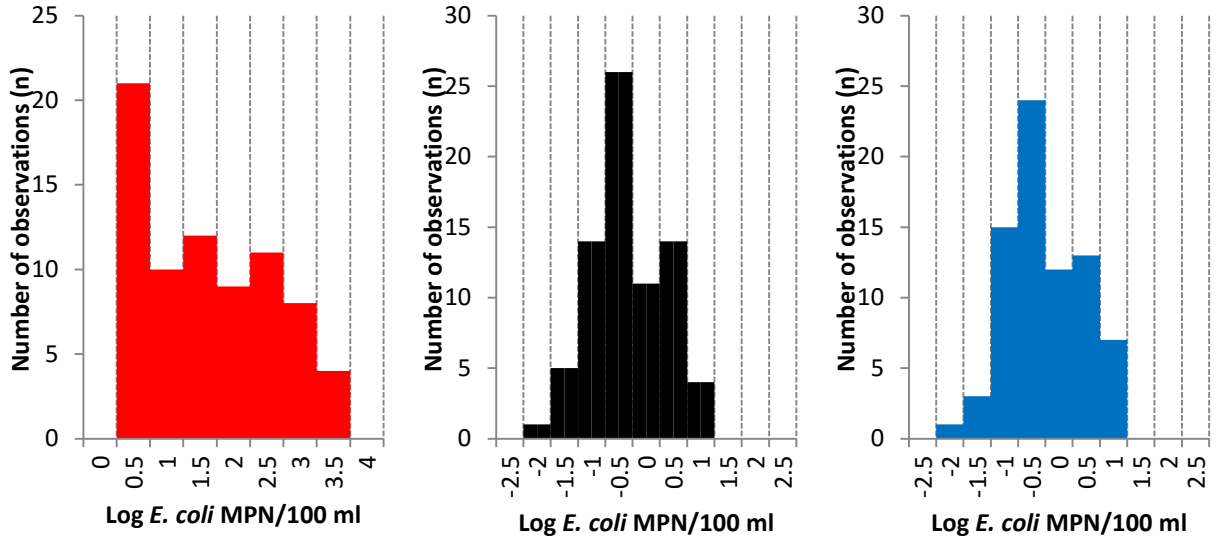


Histograms of actual *E. coli* concentrations (red), ensemble model residuals (black) and traditional Virtual Beach model residuals (blue) at location P3 for training set data (n=75). Model residuals defined as actual *E. coli* concentration minus modeled concentrations. Note: ensemble models are compared to all training set data, not only the subset of training data used for the model build.

| Location P3 | Ensemble Model | | Traditional VB Model | |
|---|---|---|---|---|
| | Training | Verification | Training | Verification |
| n | 75 | 25 | 75 | 25 |
| Average E. coli (MPN/100 ml) | 1.984 | 1.725 | 1.917 | 1.667 |
| Standard Deviation | 0.618 | 0.494 | 0.659 | 0.488 |
| Average Residual | -0.067 | 0.022 | 0.000 | 0.081 |
| Type I Errors (n) | 5 | 1 | 3 | 0 |
| Type II Errors (n) | 9 | 3 | 9 | 3 |
| Pearson's r | 0.698 | 0.424 | 0.707 | 0.631 |
| $R^2$ | 0.488 | 0.180 | 0.499 | 0.399 |
| RMSE | 0.667 | 0.736 | 0.655 | 0.623 |
| Specificity | 0.896 | 0.952 | 0.938 | 1.000 |
| Sensitivity | 0.667 | 0.250 | 0.696 | 0.333 |

Model statistics at location P3. Note: ensemble models are compared to all training set data, not only the subset of training data used for the model build.

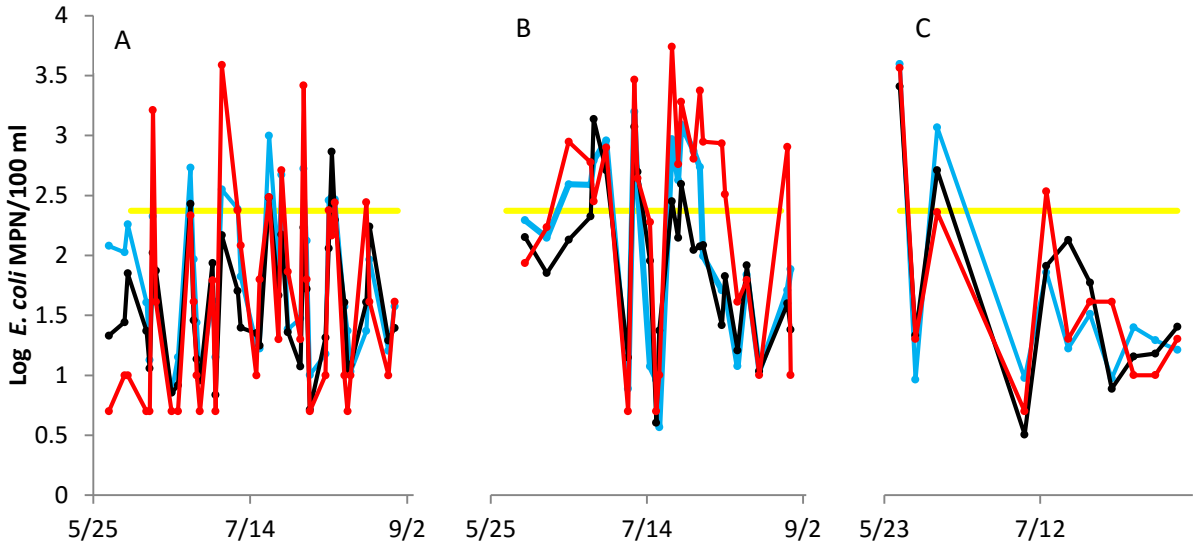


Comparison between actual *E. coli* concentrations (red) (MPN/100ml), ensemble model results (black) and traditional Virtual Beach (blue) model results for training set data at location P4 (n=75). Yellow line represents beach action value. A, B, and C represents data from years 2012, 2013 and 2014, respectively. Note: ensemble models are compared to all training set data, not only the subset of training data used for the model build.

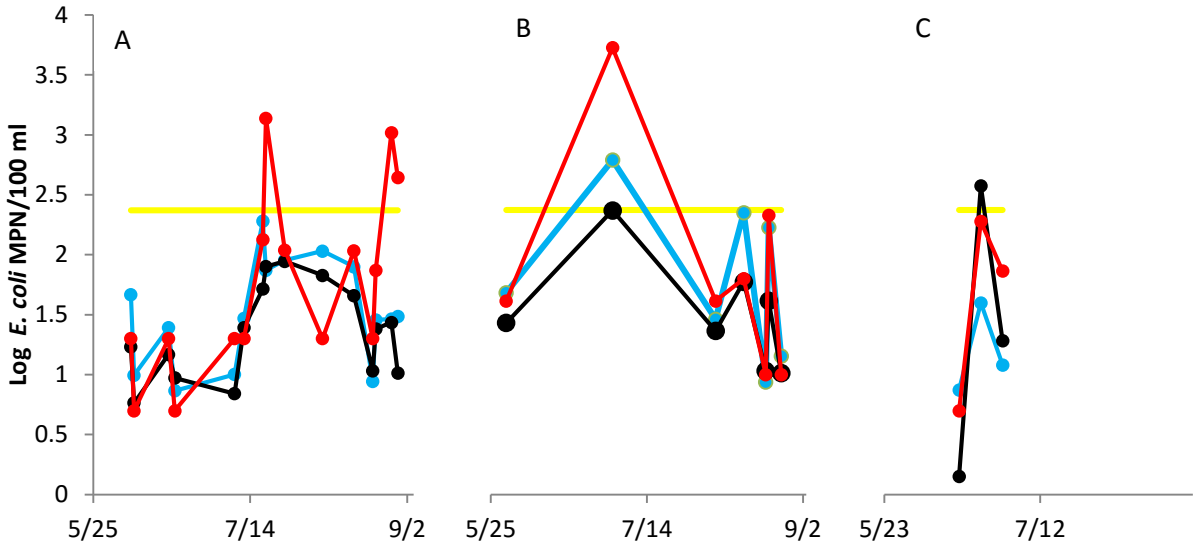


Comparison between actual *E. coli* concentrations (red) (MPN/100ml), ensemble model results (black) and traditional Virtual Beach (blue) model results for verification set data at location P4 (n=25). Yellow line represents beach action value. A, B, and C represents data from years 2012, 2013 and 2014, respectively.

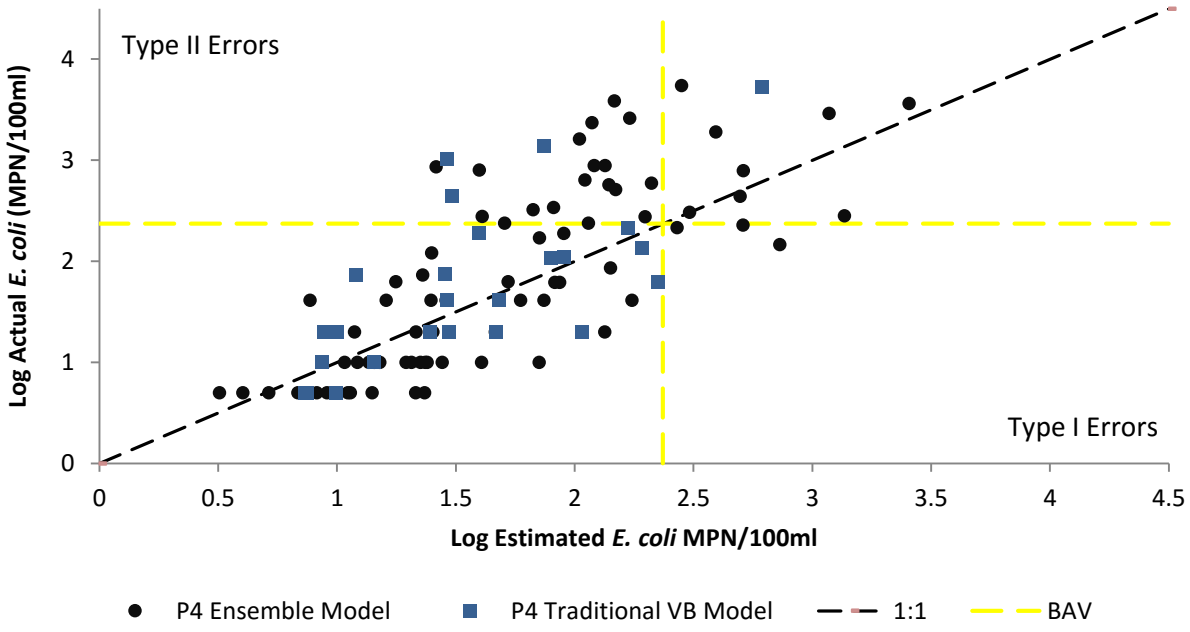


Actual *E. coli* concentrations (training set data, n=75) compared to traditional Virtual Beach and ensemble model results at location P4. See section 4.5.3 for comparisons between verification set. Note: ensemble models are compared to all training set data, not only the subset of training data used for the model build.

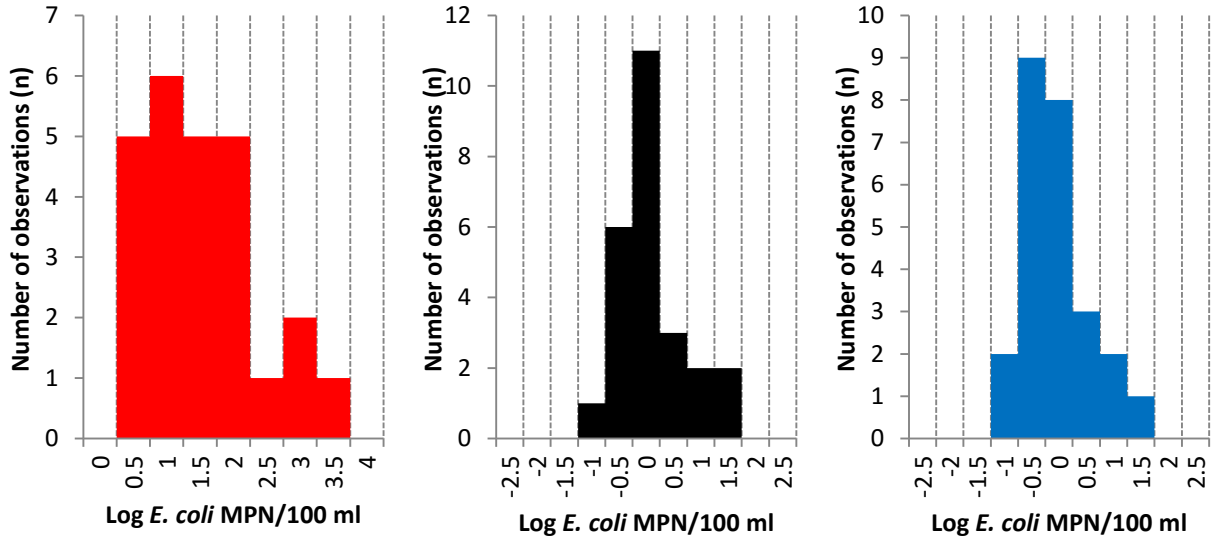


Histograms of actual *E. coli* concentrations (red), ensemble model residuals (black) and traditional Virtual Beach model residuals (blue) at location P4 for verification set data (n=25). Model residuals defined as actual *E. coli* concentration minus modeled concentrations.

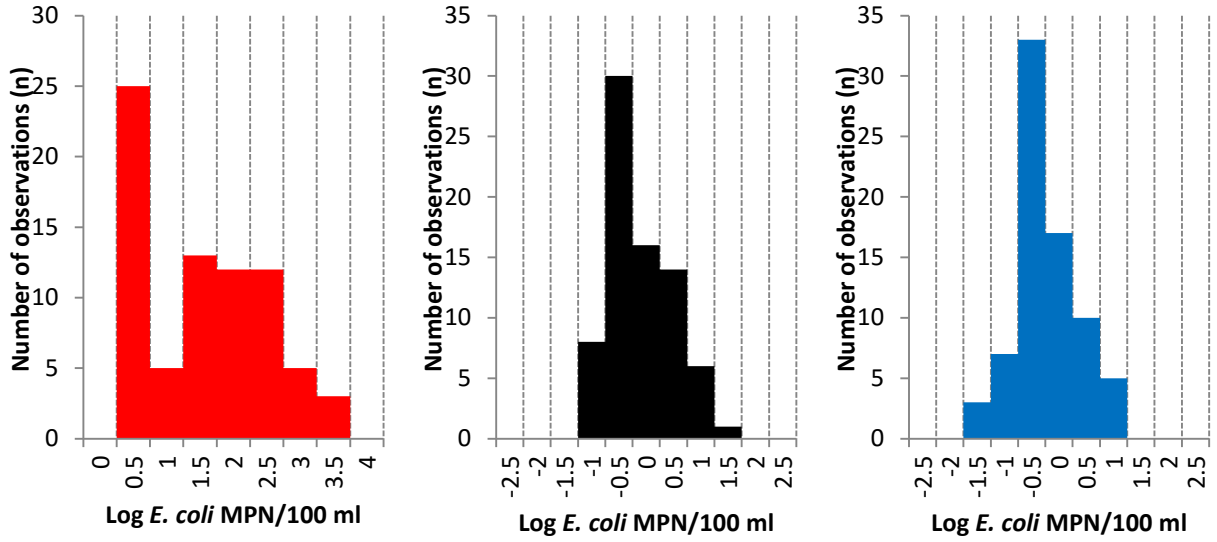


Histograms of actual *E. coli* concentrations (red), ensemble model residuals (black) and traditional Virtual Beach model residuals (blue) at location P4 for training set data (n=75). Model residuals defined as actual *E. coli* concentration minus modeled concentrations. Note: ensemble models are compared to all training set data, not only the subset of training data used for the model build.

| | Ensemble Model | | Traditional VB Model | |
|---|---|---|---|---|
| Location P4 | Training | Verification | Training | Verification |
| n | 75 | 25 | 75 | 25 |
| Average E. coli (MPN/100 ml) | 1.718 | 1.395 | 1.856 | 1.557 |
| Standard Deviation | 0.631 | 0.521 | 0.719 | 0.522 |
| Average Residual | 0.138 | 0.364 | 0.000 | 0.203 |
| Type I Errors (n) | 3 | 1 | 3 | 0 |
| Type II Errors (n) | 18 | 4 | 7 | 3 |
| Pearson's r | 0.782 | 0.691 | 0.787 | 0.682 |
| $R^2$ | 0.611 | 0.478 | 0.620 | 0.466 |
| RMSE | 0.588 | 0.666 | 0.559 | 0.599 |
| Specificity | 0.939 | 0.952 | 0.939 | 1.000 |
| Sensitivity | 0.308 | 0.000 | 0.704 | 0.250 |

Model statistics at location P4. Note: ensemble models are compared to all training set data, not only the subset of training data used for the model build.

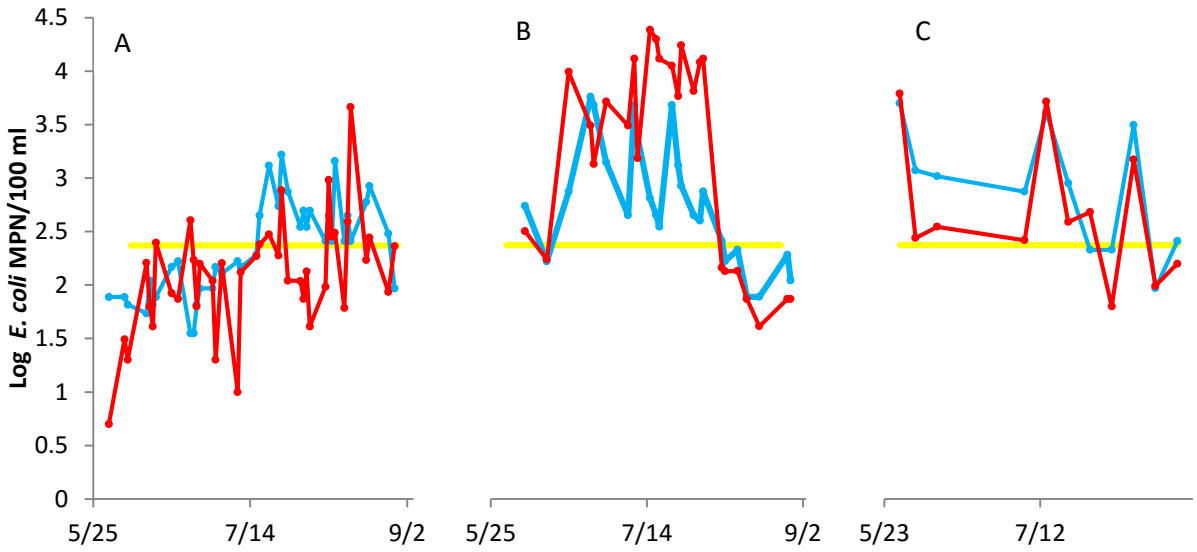


Comparison between actual *E. coli* concentrations (red) (MPN/100ml) and traditional Virtual Beach (blue) model results for training set data at the Pike River sample location (n=75). Yellow line represents beach action value. A, B, and C represents data from years 2012, 2013 and 2014, respectively.

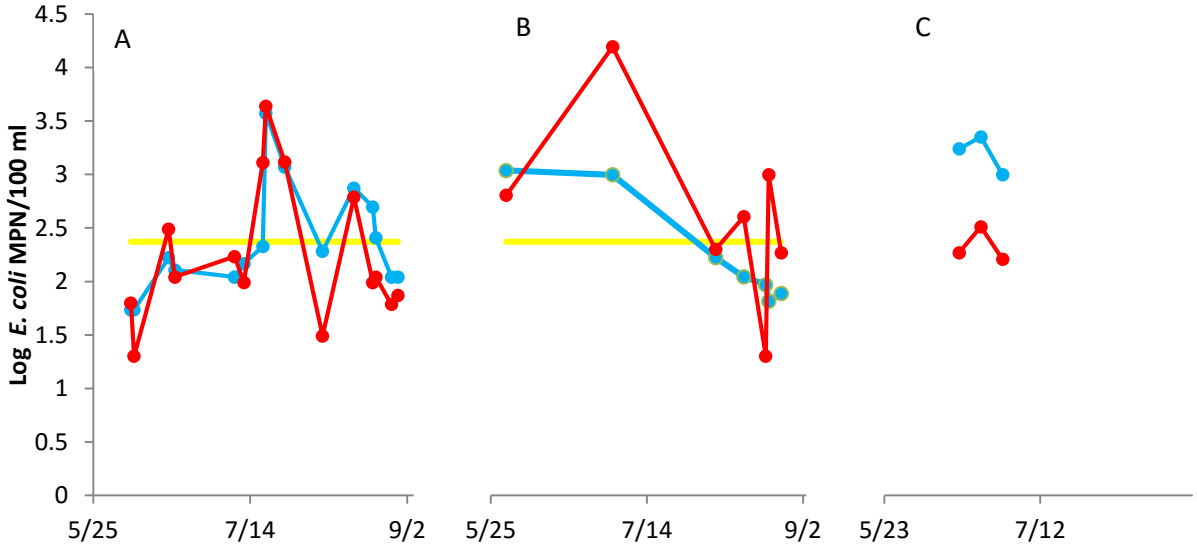


Comparison between actual *E. coli* concentrations (red) (MPN/100ml) and traditional Virtual Beach (blue) model results for verification set data at Pike River sample location (n=25). Yellow line represents beach action value. A, B, and C represents data from years 2012, 2013 and 2014, respectively.

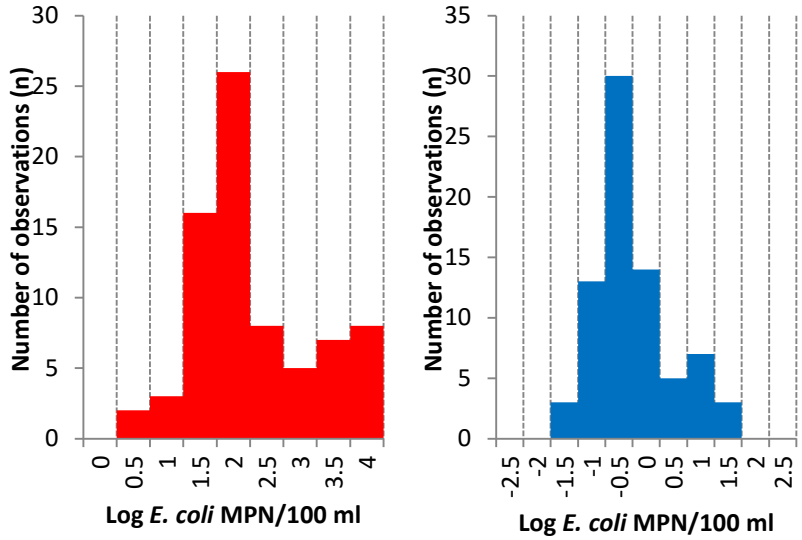


Histograms of actual *E. coli* concentrations (red) and traditional Virtual Beach model residuals (blue) for the Pike River for training set data (n=75). Model residuals defined as actual *E. coli* concentration minus modeled concentrations.

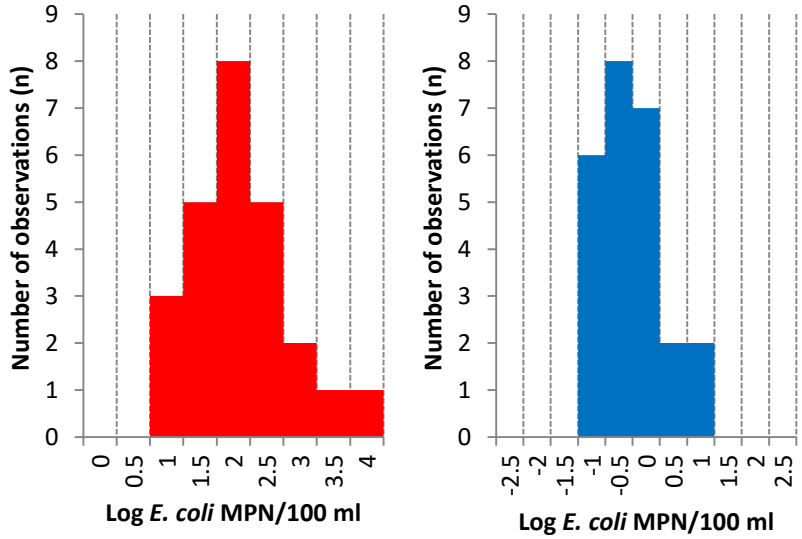


Histograms of actual *E. coli* concentrations (red) and traditional Virtual Beach model residuals (blue) for the Pike River for verification set data (n=25). Model residuals defined as actual *E. coli* concentration minus modeled concentrations.

| Pike River Model | Training | Verification |
|---|---|---|
| n | 75 | 25 |
| Average E. coli (MPN/100 ml) | 2.552 | 2.435 |
| Standard Deviation | 0.553 | 0.549 |
| Average Residual | 0.000 | -0.070 |
| Type I Errors (n) | 12 | 4 |
| Type II Errors (n) | 3 | 4 |
| Pearson's r | 0.633 | 0.572 |
| $R^2$ | 0.401 | 0.327 |
| RMSE | 0.672 | 0.579 |
| Specificity | 0.692 | 0.733 |
| Sensitivity | 0.917 | 0.600 |

Model statistics for the Pike River.

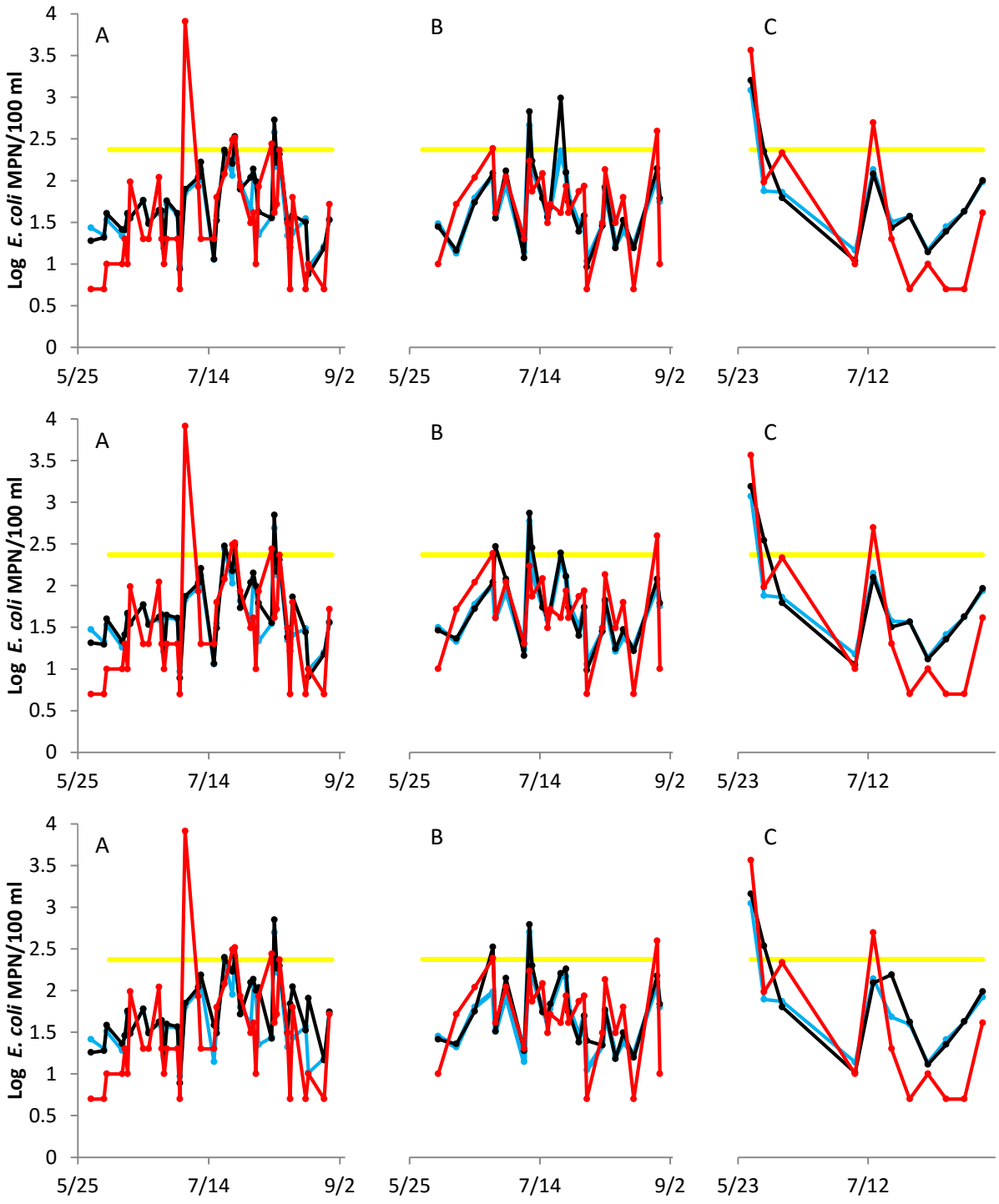


Comparison between actual *E. coli* concentrations (red) (MPN/100ml), ensemble model results (black) and traditional Virtual Beach (blue) model results for training set data using the composite model at locations A3 (top), A2 (middle) and A1 (bottom). Yellow line represents beach action value. A, B, and C represents data from years 2012, 2013 and 2014, respectively. Note: ensemble models are compared to all training set data, not only the subset of training data used for the model build.

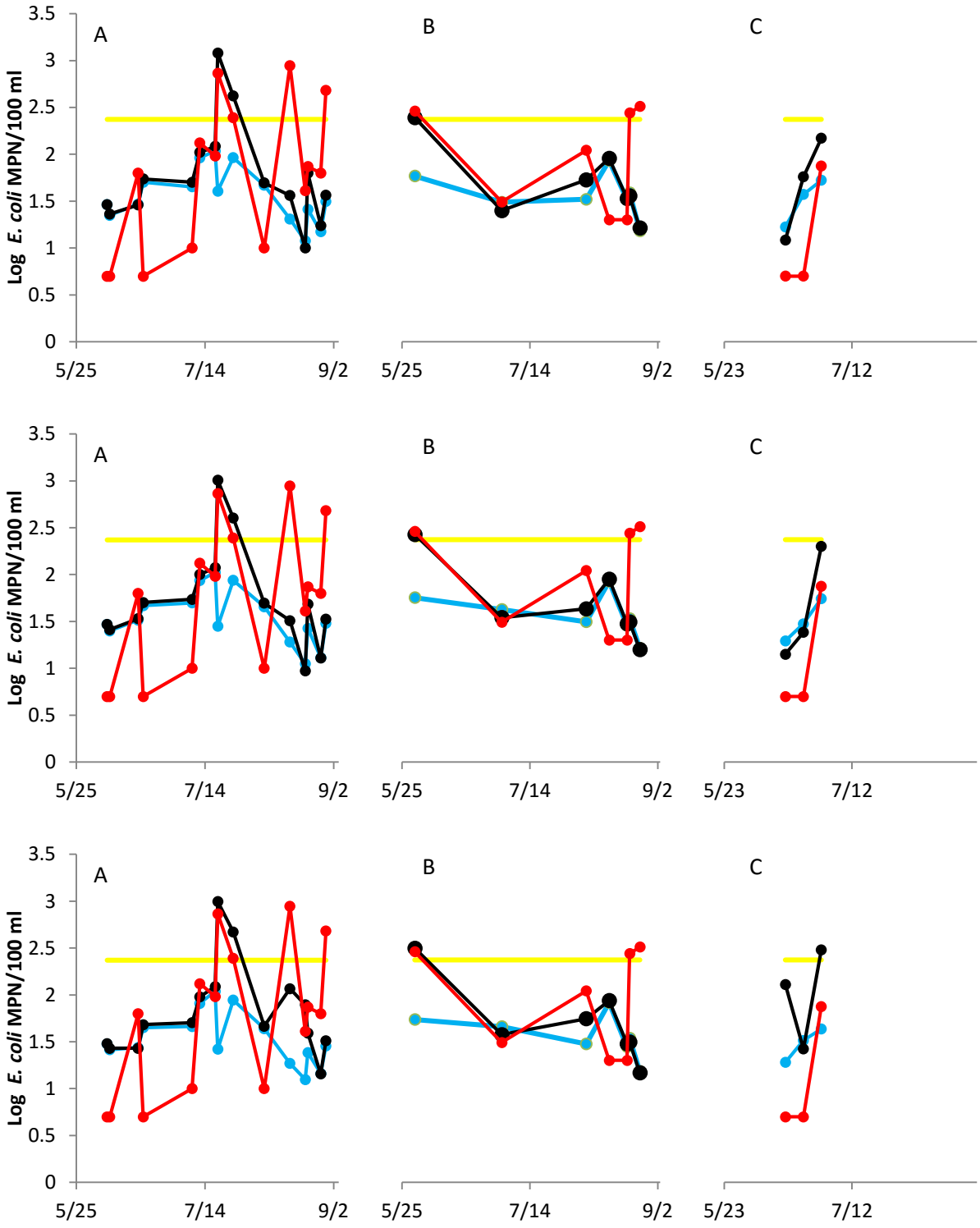


Comparison between actual *E. coli* concentrations (red) (MPN/100ml), ensemble model results (black) and traditional Virtual Beach (blue) model results for verification set data using the composite model at locations A3 (top), A2 (middle) and A1 (bottom). Yellow line represents beach action value. A, B, and C represents data from years 2012, 2013 and 2014, respectively.

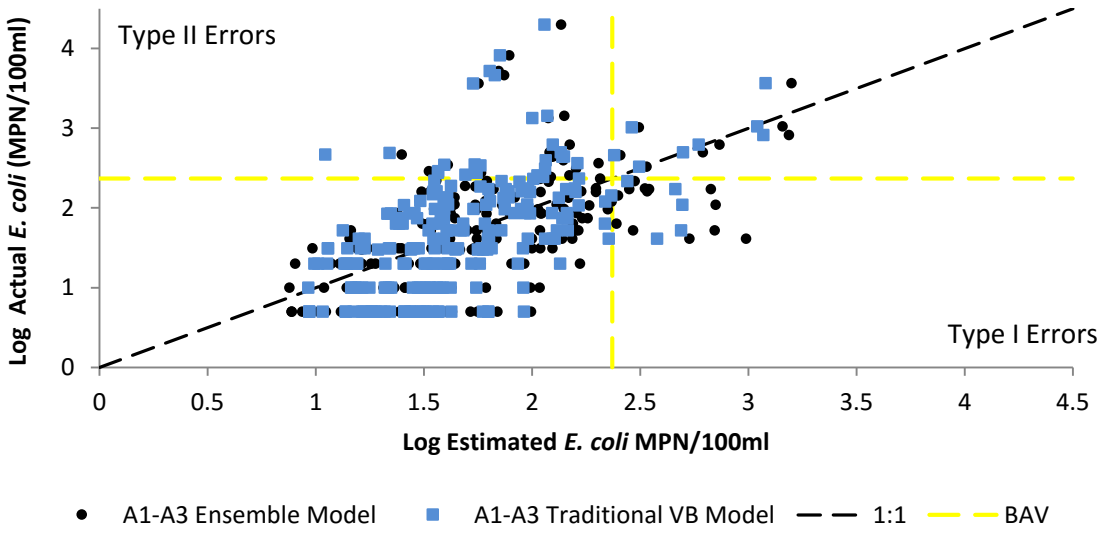


Actual *E. coli* concentrations (training set data, n=225) compared to traditional Virtual Beach and ensemble model results for composite A1-A3 model. See section 4.5.3 for comparisons between verification set. Note: ensemble models are compared to all training set data, not only the subset of training data used for the model build.

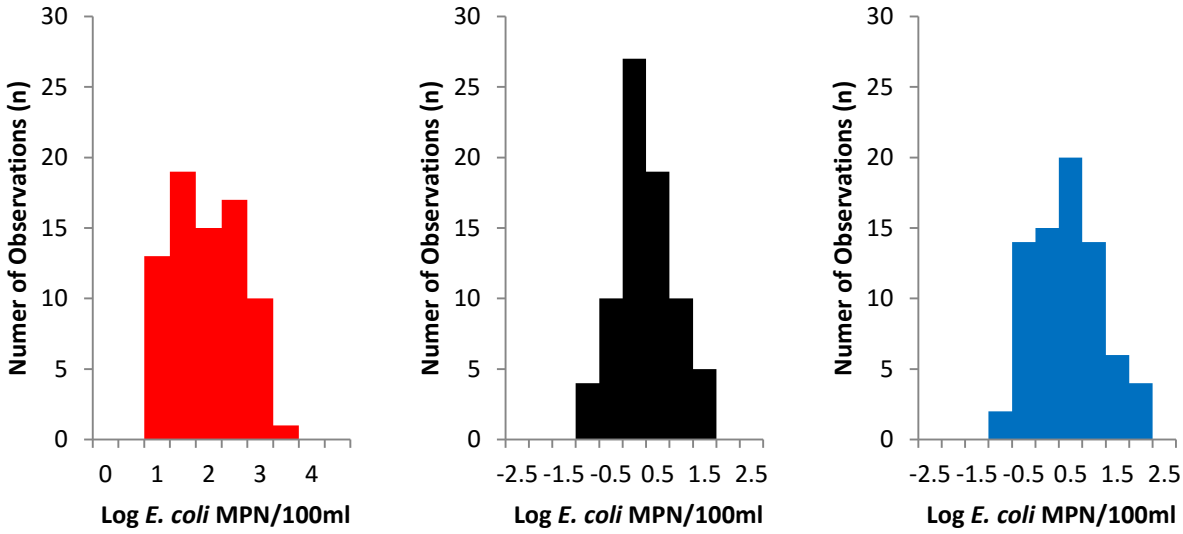


Histograms of actual *E. coli* concentrations (red), ensemble model residuals (black) and traditional Virtual Beach model residuals (blue) for A1-A3 combined model for verification set data (n=75). Model residuals defined as actual *E. coli* concentration minus modeled concentrations.

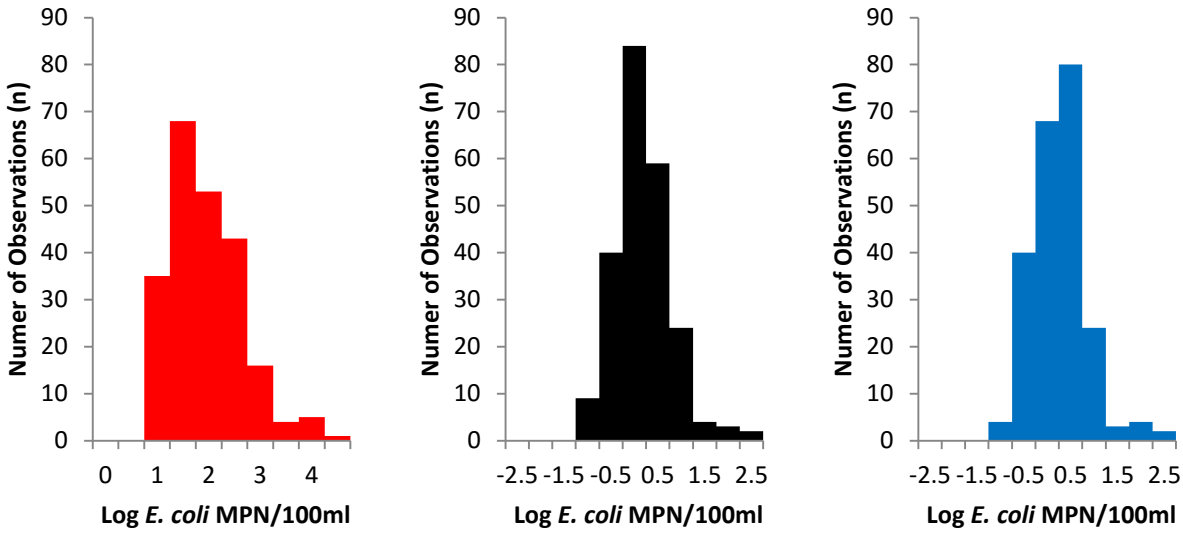


Histograms of actual *E. coli* concentrations (red), ensemble model residuals (black) and traditional Virtual Beach model residuals (blue) for A1-A3 combined model for training set data (n=225). Model residuals defined as actual *E. coli* concentration minus modeled concentrations. Note: ensemble models are compared to all training set data, not only the subset of training data used for the model build.

| Location A3-A1 Composite | Ensemble Model | | Traditional VB Model | |
|---|---|---|---|---|
| | Training | Verification | Training | Verification |
| n | 225 | 75 | 225 | 75 |
| Average *E. coli* (MPN/100 ml) | 1.807 | 1.747 | 1.732 | 1.544 |
| Standard Deviation | 0.493 | 0.471 | 0.441 | 0.251 |
| Average Residual | -0.061 | -0.043 | 0.000 | 0.160 |
| Type I Errors (n) | 13 | 3 | 5 | 0 |
| Type II Errors (n) | 25 | 8 | 25 | 15 |
| Pearson's r | 0.579 | 0.544 | 0.582 | 0.155 |
| $R^2$ | 0.335 | 0.295 | 0.339 | 0.024 |
| RMSE | 0.585 | 0.602 | 0.578 | 0.731 |
| Specificity | 0.932 | 0.950 | 0.974 | 1.000 |
| Sensitivity | 0.242 | 0.467 | 0.242 | 0.000 |

Summary statistics for A1-A3 composite model. Note: ensemble models are compared to all training set data, not only the subset of training data used for the model build.

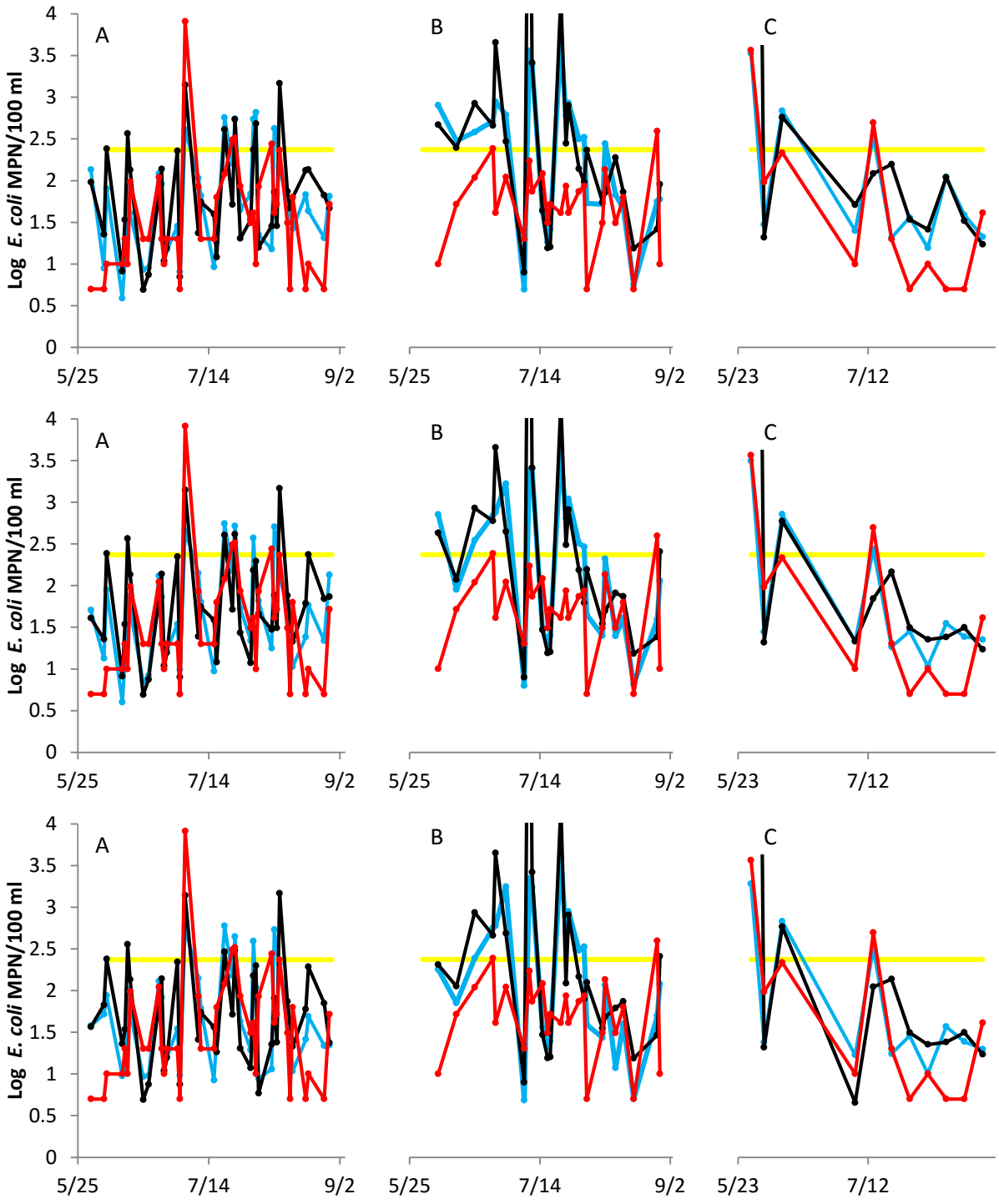


Comparison between actual *E. coli* concentrations (red) (MPN/100ml), ensemble model results (black) and traditional Virtual Beach (blue) model results for training set data using the composite model at locations P2 (top), P3 (middle) and P4 (bottom). Yellow line represents beach action value. A, B, and C represents data from years 2012, 2013 and 2014, respectively. Note: ensemble models are compared to all training set data, not only the subset of training data used for the model build.

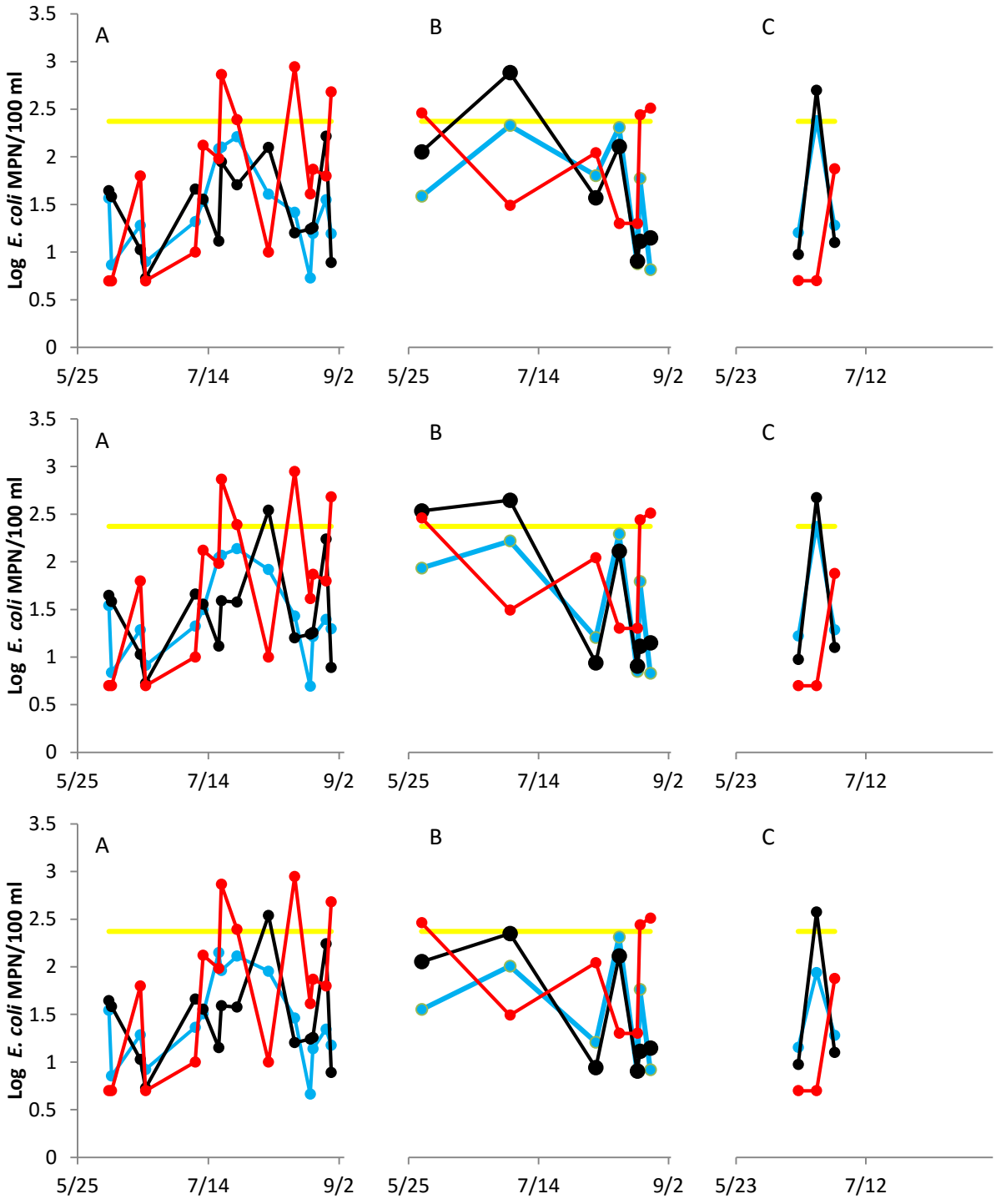


Comparison between actual *E. coli* concentrations (red) (MPN/100ml), ensemble model results (black) and traditional Virtual Beach (blue) model results for verification set data using the composite model at locations P2 (top), P3 (middle) and P4 (bottom). Yellow line represents beach action value. A, B, and C represents data from years 2012, 2013 and 2014, respectively.

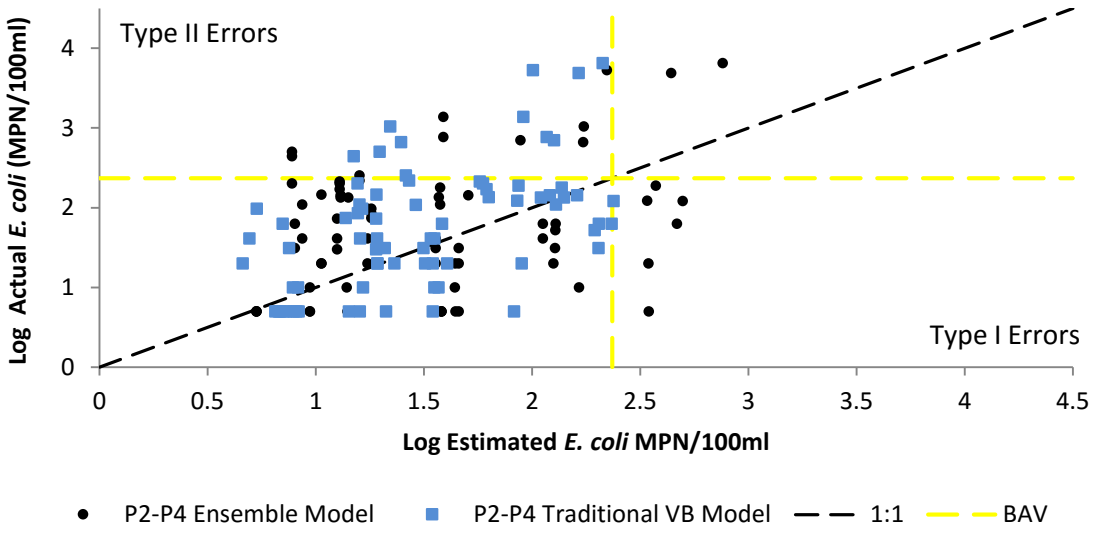


Actual *E. coli* concentrations (training set data, n=225) compared to traditional Virtual Beach and ensemble model results for composite P2-P4 model. See section 4.5.3 for comparisons between verification set. Note: ensemble models are compared to all training set data, not only the subset of training data used for the model build.

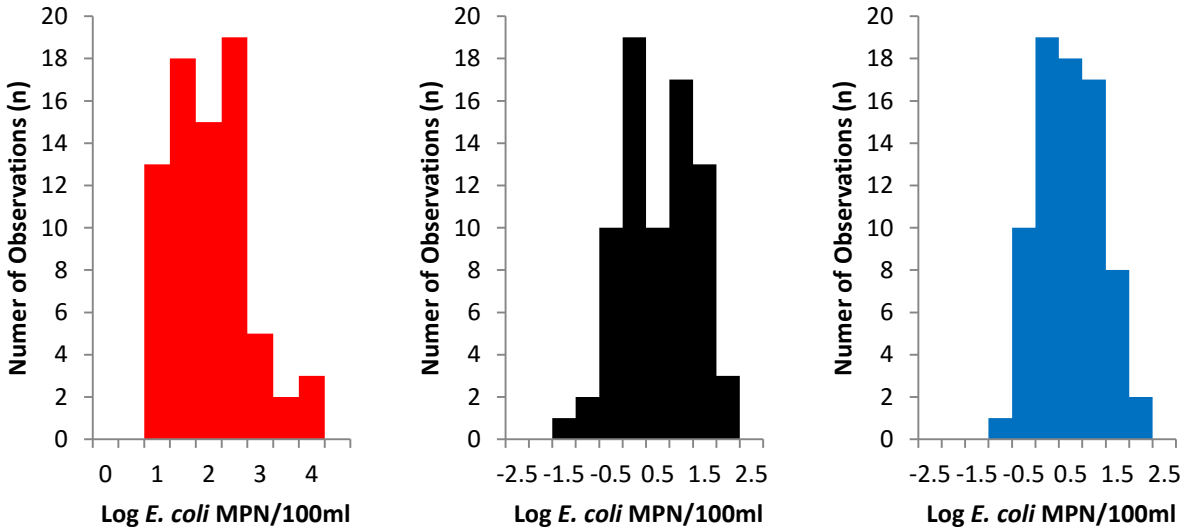


Histograms of actual *E. coli* concentrations (red), ensemble model residuals (black) and traditional Virtual Beach model residuals (blue) for P2-P4 combined model for verification set

data (n=75). Model residuals defined as actual *E. coli* concentration minus modeled concentrations.

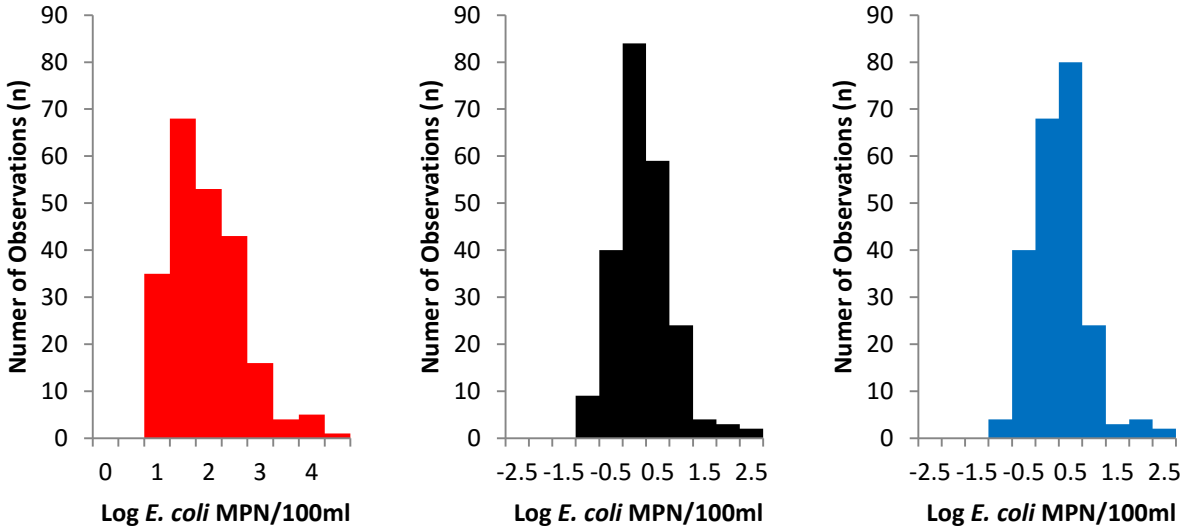


Histograms of actual *E. coli* concentrations (red), ensemble model residuals (black) and traditional Virtual Beach model residuals (blue) for P2-P4 combined model for training set data (n=75). Model residuals defined as actual *E. coli* concentration minus modeled concentrations. Note: six outliers (not shown) were associated with ensemble model and had residuals of approximately -4 (n=3) and -13 (n=3). Note: ensemble models are compared to all training set data, not only the subset of training data used for the model build.

| | Ensemble Model | | Traditional VB Model | |
|---|---|---|---|---|
| Location P2-P4 Composite | Training | Verification | Training | Verification |
| n | 225 | 75 | 225 | 75 |
| Average E. coli (MPN/100 ml) | 2.178 | 1.514 | 1.881 | 1.493 |
| Standard Deviation | 2.032 | 0.566 | 0.727 | 0.484 |
| Average Residual | -0.297 | 0.238 | 0.000 | 0.259 |
| Type I Errors (n) | 12 | 6 | 10 | 1 |
| Type II Errors (n) | 31 | 9 | 21 | 11 |
| Pearson's r | 0.474 | 0.310 | 0.785 | 0.522 |
| $R^2$ | 0.225 | 0.096 | 0.616 | 0.273 |
| RMSE | 1.810 | 0.833 | 0.572 | 0.708 |
| Specificity | 0.919 | 0.906 | 0.933 | 0.984 |
| Sensitivity | 0.592 | 0.182 | 0.724 | 0.000 |

Summary statistics for P2-P4 composite model. Note: ensemble models are compared to all training set data, not only the subset of training data used for the model build.